



Contribution to the theory of higher order sliding mode control and the control of underactuated mechanical systems

Mohamed Harmouche

► To cite this version:

Mohamed Harmouche. Contribution to the theory of higher order sliding mode control and the control of underactuated mechanical systems. Other. Université de Technologie de Belfort-Montbéliard, 2013. English. NNT : 2013BELF0214 . tel-01503945

HAL Id: tel-01503945

<https://theses.hal.science/tel-01503945>

Submitted on 7 Apr 2017

HAL is a multi-disciplinary open access archive for the deposit and dissemination of scientific research documents, whether they are published or not. The documents may come from teaching and research institutions in France or abroad, or from public or private research centers.

L'archive ouverte pluridisciplinaire **HAL**, est destinée au dépôt et à la diffusion de documents scientifiques de niveau recherche, publiés ou non, émanant des établissements d'enseignement et de recherche français ou étrangers, des laboratoires publics ou privés.

SPIM

Thèse de Doctorat



école doctorale sciences pour l'ingénieur et microtechniques
UNIVERSITÉ DE TECHNOLOGIE BELFORT-MONTBÉLIARD

Contribution à la théorie de la
commande par modes glissants
d'ordre supérieur et à la commande
des systèmes mécaniques
sous-actionnés.



Mohamed HARMOUCHE

SPIM

Thèse de Doctorat



école doctorale sciences pour l'ingénieur et microtechniques
UNIVERSITÉ DE TECHNOLOGIE BELFORT-MONTBÉLIARD

N° 2 1 4

THÈSE présentée par

Mohamed HARMOUCHE

pour obtenir le

Grade de Docteur de

l'Université de Technologie de Belfort-Montbéliard

Spécialité : **Automatique**

Contribution à la théorie de la commande par modes
glissants d'ordre supérieur et à la commande des
systèmes mécaniques sous-actionnés.

Soutenue le 21 Novembre 2013 devant le Jury :

Nicolas MARCHAND	Rapporteur	HDR à l'Université de Grenoble
Wilfrid PERRUQUETTI	Rapporteur	Professeur à l'Ecole Centrale de Lille
Franck PLESTAN	Examineur	Professeur à l'Ecole Centrale de Nantes
Mohammed EL-BAGDOURI	Directeur de thèse	Professeur à l'Université de Technologie de Belfort-Montbéliard
Yacine CHITOUR	Co-Directeur	Professeur à l'Université Paris XI
Salah LAGHROUCHE	Co-Directeur	Maître de Conférences à l'Université de Technologie de Belfort-Montbéliard

Acknowledgment

I would like to thank all the people in my life, who helped in completing my thesis from the start to finish.

Starting by my three dear friends, Ahmad Haddad, Mohamad Dib and Mostafa Kerdi for their recommendations that led to the start of the thesis. Also, Assad and Vahé for opening their doors for me when I lacked a roof over my head. Then Rihab, Sonya, Imad, Fayez, Mona, Adnan, Hayat, Adeel, Maya, Rana, Zakaria, Athman, Rola, Houssam, Dr. Raed and little Nissrine for their technical and moral support throughout the journey and for making it comfortable.

I would like to thank my family, specially my parents and my sister Jihane. And of course I can never forget my dear Hanane.

I would like the members of jury of my thesis, who put in the effort to go through my work and contributed actively to the defense. I would specially like to mention Yacine here for his support and our (often heated) exchanges, and specially for his support during my defense.

In the end I thank myself for this contribution towards the humanity.

List of Publications

Peer-reviewed journal papers

S. Laghrouche, Y. Chitour, M. Harmouche, F.S. Ahmed. *Path Following for a Target Point Attached to a Unicycle Type Vehicle*, Acta Applicandae Mathematicae, Vol. 121, Issue 1, 2012.

M. Harmouche, S. Laghrouche, F.S. Ahmed, M. El Bagdouri. *Second-order sliding mode controllers: an experimental comparative study on a mechatronic actuator* Proceedings of the Institution of Mechanical Engineers, Part I: Journal of Systems and Control Engineering, Vol. 226, Issue 9, 2012.

Journal papers submitted for peer-review

M. Harmouche, S. Laghrouche, Y. Chitour. *Stabilization of perturbed integrator chains using Lyapunov-Based Homogeneous Controllers*, Submitted to IEEE Transactions on Automatic Control, <http://arxiv.org/abs/1303.5330>.

M. Harmouche, S. Laghrouche, Y. Chitour. *A Lyapunov approach to Robust and Adaptive finite time stabilization of integrator chains with bounded uncertainty*, Submitted to IEEE Transactions on Automatic Control, <http://arxiv.org/abs/1303.5117>.

S. Laghrouche, M. Harmouche, Y. Chitour. *Target-point based path following controller for a car-type vehicle using bounded controls*, Submitted to International Journal of Robust and Nonlinear Control, <http://arxiv.org/abs/1303.5127>.

S. Laghrouche, M. Harmouche, Y. Chitour. *Global tracking for an underactuated ships with bounded feedback controllers*, Submitted to International Journal of Control, <http://arxiv.org/abs/1303.5120>.

Peer-reviewed international conference papers

M. Harmouche, S. Laghrouche, Y. Chitour. *Robust and adaptive Higher Order Sliding mode controllers*, 51st IEEE Conference on Decision and Control 2012, Maui, Hawaii USA, pp. 6436-6441.

S. Laghrouche, M. Harmouche, Y. Chitour. *Target-point based path following controller for car-type vehicle using bounded feedback*, 51st IEEE Conference on Decision and Control 2012, Maui, Hawaii USA, pp. 562-567.

M. Harmouche, I. Matraji, S. Laghrouche, M. El Bagdouri. *Homogeneous Higher Order Sliding Mode Control for PEM Fuel Cell*, The 12th International Workshop on Variable Structure Systems 2012, Mumbai India, pp. 161-166.

J.X. Liu, S. Laghrouche, M. Harmouche, M. Wack. *Adaptive sliding mode observer design for switching power converters*, The 8th Power Plant and Power System Control Symposium 2012, Toulouse France.

M. Harmouche, S. Laghrouche, M. El Bagdouri. *Robust Homogeneous Higher Order Sliding Mode Control*, 50th IEEE Conference on Decision and Control and European Control Conference 2011, Orlando, Florida USA, pp. 5665-5670.

Contents

Acknowledgment	i
List of Publications	iii
Contents	v
General Introduction	1
I Sliding Mode Control Design	9
1 Sliding Mode and Higher Order Sliding Mode Control	11
1.1 Introduction	11
1.2 Sliding Mode Control	12
1.2.1 Design of Sliding Manifold	13
1.2.2 Controller Design	14
1.3 Higher Order Sliding Mode Control	15
1.3.1 Problem Formulation	16
1.3.2 Examples of Second Order Sliding Mode Controllers	17
1.3.2.1 Supertwisting Algorithm [54, 11]	18
1.3.2.2 Twisting Algorithm [54]	18
1.3.2.3 Sub-optimal Algorithm [54]	19
1.3.3 Arbitrary Order Sliding Mode Controllers	19
1.3.3.1 Homogeneity	20
1.4 Adaptive Sliding Mode Controllers	21
1.4.1 Adaptive First Order Sliding Mode Controller [73]	22

1.4.2	Adaptive Supertwisting Controller [81]	23
1.4.3	Adaptive Twisting Controller [47]	23
1.5	Summary	24
2	Lyapunov based robust and adaptive HOSM controllers	27
2.1	Design of robust Higher Order Sliding Mode Controller	28
2.1.1	Preliminaries	28
2.1.2	Lyapunov-based Arbitrary HOSM Controller	29
2.2	Adaptive Controller	32
2.3	Experimental results : PEM Fuel Cell System	34
2.3.1	PEMFC air-feed system model	35
2.3.2	Control Objective	36
2.3.3	Test Bench Description	37
2.3.4	Controller design and Experimental Results	38
2.4	Summary	45
3	Lyapunov-Based Homogeneous HOSM Controller	47
3.1	Introduction and motivation	47
3.1.1	Contribution	49
3.2	Controller design	49
3.2.1	Useful definitions, lemmas and theorems	49
3.2.2	Stabilization of a pure chain of integrator	51
3.2.3	Stabilization of an r -perturbed integrator chain	54
3.3	Discussion of Special Cases	55
3.3.1	Robust Homogeneous Arbitrary HOSM Controller	55
3.3.2	Homogeneous controller with minimum discontinuous control	56
3.3.3	Fixed-time Homogeneous controller	57
3.4	Simulation Results	58
3.5	Summary	58
II	Underactuated Systems Control	65
4	Preliminary Concepts and introduction to problems	67
4.1	Stabilization of Integrator Chain Using Bounded Control	67
4.1.1	Nested bounded controls approach for integrator chains	68

4.1.2	Nested bounded controls approach for null controllable systems . . .	68
4.2	Input-to-State Stability Concept	69
4.3	Stabilization of Double Integrator Subject to Input Saturation [15]	71
4.4	Two important underactuated systems	72
4.4.1	Car-type robotic vehicle	72
4.4.1.1	Control Objective	73
4.4.2	Surface marine vessel	74
4.4.2.1	Control Objective	76
4.5	Summary	76
5	Path Following of Robotic Vehicles	79
5.1	State-of-the-Art and contributions	79
5.1.1	Contribution	80
5.2	Problem Formulation	81
5.3	Control design and Lyapunov Function	84
5.3.1	L_2 -gain Υ_L	88
5.3.2	Estimation of P_k for large k_2	88
5.3.3	ISS bounds for ξ and η	89
5.3.4	Estimation of \dot{V} for $y \notin Y_{k_2}$	90
5.3.5	Final step	91
5.4	Stabilization of the original system	92
5.5	Simulations	94
5.6	Summary	97
6	Tracking of a Underactuated Marine Vessel	99
6.1	State-of-the-art and contribution	99
6.1.1	Contribution	100
6.2	Problem Formulation	101
6.3	Controller design	102
6.4	Tracking without velocity measurement	106
6.5	Simulations	109
6.6	Summary	110
	Conclusion and Perspectives	115

Bibliography	119
Appendices	131
A Proof of technical lemmas	131
A.A Proof of Lemma 5.3.4	131
A.B Proof of Lemma 5.3.5	132
A.C Proof of Proposition 5.3.6	135
A.D Proof of Lemma 5.3.7	135
A.E Proof of Lemma 5.3.10	136

General Introduction

In 1868, J. C. Maxwell's paper "On Governors" explained the instability of flyball governor using differential equations. This marked the beginning of mathematical control and systems theory, which has undergone numerous developments – from classical to modern – in the last century. New mathematical techniques made it possible to control, more accurately, significantly more complex dynamical systems. In the first half of the 20th century, the focus remained on linear time-invariant (LTI) systems and the extensive work resulted in a rich set of mathematical tools for their analysis and control (e.g., root-locus, Bode plot, Nyquist criterion, PID, pole placement). A detailed history of these developments has been compiled in [4]. However, it also became evident that these methods cannot necessarily be applied directly to plants where the system, the controller, or both are nonlinear. Nonlinear control theory required more rigorous mathematical analysis to justify its conclusions. Since late 50s, nonlinear control has been the topic of hundreds of publications, numerous monographs and several comprehensive textbooks, such as [46], [42] and [91]. The major methods include developments in optimal control in the 1950's and 1960's and stochastic, robust and adaptive control in the 1970's and 1980's. Among other innumerable applications, these nonlinear control methods made possible aviation and space travel, satellite communication, efficient automotive systems and safe and clean chemical processes.

In spite of these developments during recent years, our increasing technological demands continue to impose challenging and widely varying control problems. These problems range from aircraft and underwater vehicles to automobiles and space telescopes, from chemical processes and the environment to manufacturing, robotics and communication networks. In addition, systems are becoming more complex, while less information is available about their dynamics. In order to meet these challenges, we need novel ideas

and interdisciplinary approaches along with further development and refining of existing methods.

The research conducted in the context of this thesis addresses two distinct, yet equally important branches of nonlinear control theory: uncertain nonlinear systems and under-actuated systems. Let us first describe the nature of these two fields.

Nonlinear uncertain systems

Lyapunov's theory of stability of the motion of systems with a finite number of degrees of freedom can safely be considered as the foundation of modern nonlinear control theory. However, in its original form, it is based upon an implicit assumption that the parameters of the system are fixed and do not change during the motion (within the accuracy of measurements) [62]. On the other hand, nonlinear dynamic physical systems, such as complex engineering systems, are difficult to characterize and model. In addition, their parameters are hard to estimate and often uncertain. Parametric uncertainty arises from varying operating conditions and external perturbations that affect the physical characteristics of systems [87, 89].

In recent years, stabilization of systems with parametric uncertainty has been studied intensely. In order to achieve true automation, the control should be capable of maintaining the system's dynamic performance in spite of this uncertainty. In other words, while developing a system design, provisions need to be made for long life of its practical operation under the conditions of uncertainty [62]. This needs to be considered during control design so that the controller counteracts the effect of variations. Specially, finite-time stabilization of uncertain systems is one of the principle problems studied under nonlinear control theory.

Underactuated systems

Underactuated systems have fewer control inputs than degrees of freedom and arise in applications, such as space and undersea robots, mobile robots, flexible robots, walking, brachiating, and gymnastic robots. The dynamics of these systems may contain feedforward nonlinearities, non-minimum phase zero dynamics, nonholonomic constraints, and other properties that place this class of systems at the forefront of research in nonlinear control [82]. Furthermore, dynamic constraints due to underactuation are often coupled

with other system constraints, such as mechanical and power limits etc. Many examples of such systems exist, including among others, underactuated robot manipulators, inverted pendulums, the Planar Vertical Takeoff and Landing (PVTOL) aircrafts, marine vehicles and car-type robots.

The class of underactuated systems is rich in both applications and control problems, and thus too broad to survey. The control of underactuated systems is an open and interesting problem in controls. Although there are a number of special cases where underactuated systems have been controlled, there are relatively few general principles [82]. Classical control techniques typically override the dynamics, whereas in underactuated systems, we need controllers that can take advantage of the dynamics and not cancel them out. These issues have created a formal class of systems, the underactuated systems, in which the dynamics of systems are studied carefully in the context of control. Seminal works, which led to the formalization of these problems, are [10, 66, 92, 9, 52].

Objectives of the Thesis

The two domains of nonlinear control, which form the basis of this thesis, have been described briefly. From their nature, it is clear that these problems require specific attention and consideration. In the first part of this thesis, the focus is on the control and finite time stabilization of nonlinear uncertain systems. Higher Order Sliding Mode Control, a popular technique for dealing with uncertain and disturbed system, has been studied and refined. In the second part of the thesis, the control of underactuated systems is addressed. A brief overview of the specific problems and our contributions is presented in this section.

Higher order sliding mode control

Sliding mode control (SMC) [89, 83] is a technique that is known for its insensitivity to parametric uncertainty and external disturbance. This technique is based on applying discontinuous control on a system which ensures convergence of the output function (sliding variable) in finite time to a manifold of the state-space, called the sliding manifold [93]. It has been shown in [89, 27, 83], that if the control forces the system states to remain on the sliding manifold, then their dynamics are defined by the manifold only, no longer influenced by parametric variations or disturbances in the system itself. An improved technique, Higher Order Sliding Mode Control (HOSMC), overcomes certain disadvantages of classical sliding mode control by acting on a higher time derivative of the sliding variable

[27]. This reduces unwanted oscillations due to unmodeled dynamics and finite switching frequency, known as chattering.

Today, many robust and adaptive forms of HOSMC exist in literature, each having its advantages and disadvantages. However, HOSMC theory lacks in generalized methods for the proof of its stability. This is specially true for arbitrary order SMC, for orders greater than two. Our contribution in this field is the development of arbitrary order robust and adaptive SMC algorithms, using a Lyapunov based approach for proof of stability. Lyapunov design is a powerful tool for control system design that allows to estimate an upper bound on convergence time [7]. To the best of our knowledge, this is the first work on a Lyapunov based approach for arbitrary HOSMC. The proposed adaptive controller also has significant design improvements as compared to other controllers of this type in the literature.

The class of robust and adaptive HOSM controllers developed in this thesis are based on a class of controllers for finite time stabilization of pure integrator chains. Using this development, a universal homogeneous controller is proposed, based on modifications introduced in Hong's controller for finite time stabilization of pure integrator chains [39]. Furthermore, the homogeneity property has also been exploited in order to produce some important properties in the controllers. Homogeneity control is used to obtain a bounded controller with minimum amplitude of discontinuity after convergence and a controller with fixed-time convergence property. It is also demonstrated that for a particular choice of degree of homogeneity, Levant's homogeneous controller [55] becomes a particular case of our universal controller.

The details of these contributions are presented in Part I of the thesis, along with extensive bibliographical references for highlighting their significance in the context of contemporary research.

Control of underactuated systems

As mentioned earlier, a wide variety of systems can be categorized as underactuated. The second part of this thesis is on the control problems related with two underactuated robotic vehicles: path following of car-type vehicles using target-point and precise tracking control of surface marine vessels.

The first problem arises in camera based autonomous vehicle guidance, navigation and control applications. The vehicle is guided on a path by a target point ahead of the vehicle, within the visual range of the camera [13, 72]. In contemporary literature, larger

effort has been made on tracking problems. The problem of path following differs from pure stabilization or tracking problems because a path is defined in space only, not in time [80, 18, 44]. Therefore it has unique challenges associated to it. Specifically, for car-type vehicles, the development produces a first order nonlinear non-globally Lipschitz differential equation that can explode in finite time. In this thesis, it is demonstrated that this problem is overcome through the application of saturated controls with arbitrary small amplitude [15]. Saturated controls are also feasible from the point of view of practical implementation as real controllers are physically limited.

The second problem, precise tracking control of surface marine vessels such as ships and boats, is often required in critical operations such as support around off-shore oil rigs [69]. Literature shows that stabilization of this system is impossible with continuous or discontinuous time-invariant state feedback. Furthermore, the underactuated ship cannot be transformed into a driftless chained system [76]; which means that the control techniques used for the similar problem of nonholonomic mobile robot control cannot be applied directly to the underactuated ship control. This has led researchers to pay particular attention to this problem, as seen in [70, 32, 5, 79, 14].

In this thesis, we have addressed a particular case of the general tracking problem, as discussed in [23], in which the yaw angle of the tracked trajectory does not admit a limit as time goes to infinity. Our algorithm is again based on saturated controls which ensure global asymptotic stability while the amplitudes of the control inputs remain bounded.

As the two problems discussed here differ widely in their structure, their solutions required separate study and analysis. Therefore, they can be considered as separate contributions, each having its own research context established by its contemporary bibliography. These contexts and the details of the contributions are presented in Part II of the thesis.

Structure of the Thesis

As mentioned before, this report has been divided into two parts, one dealing with Higher order sliding mode control, and the other with control of underactuated systems. The complete structure of these parts is presented here.

Part I : Lyapunov-based Higher Order Sliding Mode Control

Chapter 1 introduces the basic concepts of Sliding Mode and Higher Order Sliding Mode control.

Chapter 2 presents Lyapunov-based robust and adaptive Sliding Mode Controllers of arbitrary order, for nonlinear SISO systems with bounded uncertainty. The design of the robust controller requires that the bounds of uncertainty be known. The main contribution in this chapter is the Lyapunov-based approach, which is a first for arbitrary order SMC, to the best of our knowledge. In addition, the gain dynamics of the presented adaptive controller design are fast in both directions, in comparison with contemporary adaptive controllers [81, 73, 86]. The practical applicability of these controllers is demonstrated on a fuel cell system. The controllers have been designed for the net power output optimization of the fuel cell, which is achieved by minimizing the internal power consumption of the fuel cell air-feed compressor. Hardware-in-Loop tests have shown that the robust and adaptive controllers fulfil this control objective well, in spite of parametric uncertainty in the fuel cell system.

Chapter 3 deals with the control of homogeneity and the additional properties that can be produced in a controller through switching homogeneity degree. A homogeneous HOSMC controller is developed through generalization of an existing finite-time controller for pure integrator chains [39]. Using this controller it is shown that homogeneity control can result in a controller whose amplitude of discontinuity can be kept to its minimum possible. Furthermore, the recently developed “Fixed-Time” stability notion can be achieved by changing the homogeneity degree. These properties are demonstrated through simulation examples.

Part II : Control of underactuated systems

Chapter 4 introduces the mathematical tools employed in the thesis, for the control of underactuated systems. These include the stabilization of perturbed integrator chains, Input-to-State Stability (ISS) of perturbed double integrators and saturated control.

Chapter 5 is related to the problem of path following of car-type vehicles using target-point. A global asymptotically stable controller is developed by parameterizing the path

as a “virtual vehicle”, which is tracked by the actual vehicle. In this way, the path following problem is converted into a tracking problem. It has been shown that this problem requires saturated control in order to avoid the divergence of states in finite time. The convergence analysis of the controller is based on Lyapunov analysis and bootstrap technique. The performance of this controller is shown through simulation examples.

Chapter 6 is related to global tracking control of underactuated surface marine vessels using saturated state feedback control. This chapter treats a specific case, i.e. the yaw angle of the tracked trajectory does not admit a limit as time goes to infinity. The controller converges the system to the tracked trajectory asymptotically, from any initial point. The advantage of using saturated controls in this case is that the global asymptotic stability is ensured while the control inputs remain bounded. Based on the (ISS) concept, it has been proven that the controller will work with state measurements, as well as with state observers. The performance has been demonstrated through simulations.

In the end, some concluding remarks and perspectives on expansion of the work are presented in the chapter **Conclusion and perspectives**.

Part I

Sliding Mode Control Design

Chapter 1

Sliding Mode and Higher Order Sliding Mode Control

1.1 Introduction

Nonlinear dynamic physical systems suffer from parametric uncertainty and are difficult to characterize. Parametric uncertainty arises from varying operating conditions and external perturbations that affect the physical characteristics of systems. The variation limits or the bounds of this uncertainty might be known or unknown. This needs to be considered during control design so that the controller counteracts the effect of variations and guarantees performance under different operating conditions. Sliding Mode Control (SMC) [89, 83] is a well-known method for control of nonlinear systems, renowned for its insensitivity to parametric uncertainty and external disturbance. This technique is based on applying discontinuous control on a system which ensures convergence of the output function (sliding variable) in finite time to a manifold of the state-space, called the sliding manifold [93]. In practice, SMC suffers from *chattering*; the phenomenon of finite-frequency, finite-amplitude oscillations in the output which appear because the high-frequency switching excites unmodeled dynamics of the closed loop system [90]. Higher Order Sliding Mode Control (HOSMC) is an effective method for chattering attenuation [27]. In this method the discontinuous control is applied on a higher time derivative of the sliding variable, such that not only the sliding variable converges to the origin, but also its higher time derivatives. As the discontinuous control does not act upon the system input directly, chattering is automatically reduced.

This chapter is an introductory synthesis of the existing notions of SMC and HOSMC. A general survey of the basic concepts and performance of Sliding Mode is presented. Then, HOSMC is introduced along with some examples of existing HOSM controllers, there advantages and disadvantages. In the last part, adaptive first and second order Sliding Mode Control is introduced and the benefits of adaptive controllers are discussed.

1.2 Sliding Mode Control

The principle of SMC design is to force the state variables of the system to reach a given manifold (or a *surface*) of the state-space in finite-time and to stay there. This manifold is defined by a set of relationships between the state variables of the system, which determine the desired dynamics of the system. Once the states are on this manifold, provided that they stay there, the dynamics of the system are completely determined by the surface and do not depend on the system itself. Thus any perturbation, to which the system may be subjected, are rejected.

Typically, an SMC controller is designed in two steps

1. a manifold is determined in accordance with the control objective and the desired static and dynamic properties of the closed loop system,
2. a discontinuous control law is designed for the state trajectories of the system to reach this surface in finite-time and to stay on it, in spite of external disturbance and modeling uncertainty.

Consider the nonlinear system, affine in the control, defined in the Brunovsky canonical form as

$$\left\{ \begin{array}{lcl} \dot{x}_1 & = & x_2, \\ & \vdots & \\ \dot{x}_n & = & \psi(x, t) + \varphi(x, t) + \gamma(x, t)u, \\ y & = & x_1, \end{array} \right. \quad (1.1)$$

where $x \in X \subset \mathbb{R}^n$ is the state vector with X an open set of \mathbb{R}^n , and $u \in U \subset \mathbb{R}$ is the control input with U an open set of \mathbb{R} . The term y is a measured smooth output-feedback function. The nominal system dynamics are represented by $\psi(x, t)$, a known function defined on X . The functions $\varphi(x, t)$ and $\gamma(x, t)$ defined for $x \in X$, are sufficiently smooth but uncertain.

System (1.1) can be written in input-output terms as

$$y^{(n)} = \psi(\tilde{y}, t) + \varphi(\tilde{y}, t) + \gamma(\tilde{y}, t)u \quad (1.2)$$

where $\tilde{y} = [y \ \dot{y} \ \cdots \ y^{(n-1)}]$. We assume that, the functions $\gamma(x, t)$ and $\varphi(x, t)$ are bounded by some positive constants γ_m , γ_M and $\bar{\varphi}$, such that

$$0 < \gamma_m \leq \gamma(x, t) \leq \gamma_M, \quad |\varphi(x, t)| \leq \bar{\varphi}. \quad (1.3)$$

Then we are dealing with the following differential inclusion [89]

$$y^{(n)} \in \psi(\tilde{y}, t) + [-\bar{\varphi}, \bar{\varphi}] + [\gamma_m, \gamma_M] u, \quad (1.4)$$

where $\bar{\varphi}$ is the limit or bound of parameter uncertainty in the model, due to some possible simplification, unmodeled dynamics and/or external perturbation. The terms γ_m and γ_M represent the bounds of the uncertainty in the gain with respect to the controller u .

1.2.1 Design of Sliding Manifold

Let $s(x, t) : X \times \mathbb{R}^+ \rightarrow \mathbb{R}$ be a measured smooth output-feedback function, and we assume that the control objective is to force s to zero. Here the function $s(x, t)$ is called *sliding variable*, and the set

$$S = \{x \in X \mid s(x, t) = 0\} \quad (1.5)$$

represents a sub-manifold of X of dimension $n-1$, called the *sliding surface*.

Definition 1.2.1. [89] *There exists an ideal sliding regime on S , if there exists a finite-time T_s such that all solutions of System (1.1) satisfy the condition $s(x, t) = 0$ for any time $t \geq T_s$.*

In this case, the dynamics of System (1.1) belong to a system of a dimension lower than the dimension of System (1.1). This autonomous system is called reduced system, and its dynamics are determined only by the choice of the sliding surface.

For our example (1.1), the control objective is to force the output y to track a reference signal y_{ref} , which is a sufficiently smooth function. In other words, the objective is to ensure the convergence of the tracking error $e = y - y_{ref}$ to zero. One of the simplest sliding manifolds for this case is the hypersurface constructed from linear combination of the tracking error e and its higher time derivatives. We consider the following sliding variable

$$s(x, t) = e^{(n-1)} + l_{n-2}e^{(n-2)} + \cdots + l_1\dot{e} + l_0e, \quad (1.6)$$

with l_i , $i = 0, \dots, n-2$ are positive constants such that the polynomial

$$P(\theta) = \theta^{n-1} + l_{n-2}\theta^{n-2} + \dots + l_1\theta + l_0, \quad (1.7)$$

is Hurwitz. Therefore, after establishment of ideal sliding regime on S , the dynamics of the reduced system is determined by the stable associated differential equation

$$e^{(n-1)} + l_{n-2}e^{(n-2)} + \dots + l_1\dot{e} + l_0e = 0. \quad (1.8)$$

As a result, the tracking error e will converge to zero exponentially.

In this section, we determined the dynamics of reduced system presented by the sliding surface. The next step is to tune a control law u , which forces the state trajectory of System (1.1) to reach the sliding surface in a finite-time, i.e. to force sliding variable $s(x, t)$ to converge to zero in finite time.

1.2.2 Controller Design

The control law u should be designed in such way that the trajectories of System (1.1) reach and stay on the sliding surface S in spite of perturbation and uncertainty. It should be remembered that the sliding variable $s(x, t)$ of Equation (1.6) is null on S . Consider the dynamics of $s(x, t)$ given as follow

$$\dot{s}(x, t) \in \psi(x, t) + [-\bar{\varphi}, \bar{\varphi}] + [\gamma_m, \gamma_M]u + \sum_{i=0}^{n-2} l_i e^{(i+1)} - y_{ref}^{(n)}. \quad (1.9)$$

The controller u should ensure a *local attractivity* to S in its neighborhood, i.e. the trajectory of System (1.1) should be directed to S . A condition of stability of $s(x, t) = 0$, called *condition of attractivity*, should be satisfied by the controller. The well-known Lyapunov's direct method requires a positive $C^{(1)}$ radially-unbounded function $V(s)$, called *Lyapunov Function*, satisfying $V(0) = 0$ and $V(\infty) = \infty$. The function $V(s)$ represents a fictitious energy and give a global information of the System, and its time derivative \dot{V} gives an information of the stability of the system. If $\dot{V}(s)$ is negative for $s \neq 0$, then the system is asymptotically stable.

One of the proposed Lyapunov function is the classical quadratic function

$$V(s) = \frac{1}{2}s^2 \quad (1.10)$$

The function $V(s)$ is clearly positive definite. Its time derivative should be negative to ensure the convergence of $s(x, t)$ to zero

$$\dot{V} = s\dot{s} \leq 0. \quad (1.11)$$

The previous condition (attractivity condition) ensures only the asymptotic convergence of s . Otherwise, for purpose of finite-time stability, a stronger condition needs to be imposed. In Classical Sliding Mode, a non-linear condition, called condition of η -attractivity [89], is used

$$\dot{V} = s\dot{s} < \eta|s|, \quad \eta > 0. \quad (1.12)$$

Condition (1.12) is satisfied, if the controller u takes the form

$$u = -U \operatorname{sign}(s), \quad (1.13)$$

where U is chosen sufficiently large to compensate the perturbation, uncertainty and the deviation between the system's dynamics and Sliding variable dynamics. Usually, U is a sufficiently large constant. In order to satisfy Condition (1.12), U can be tuned as

$$U \geq \max_{x \in X} \left(\frac{1}{\gamma_m} \left(\left| \psi(x, t) + \sum_{i=0}^{n-2} l_i e^{(i+1)} - y_{ref}^{(n)} \right| + \bar{\varphi} + \eta \right) \right). \quad (1.14)$$

To summarize, we can describe the behavior of system in two steps:

1. **Reaching phase:** It corresponds to the time $t \in [0, T_s]$. During this phase, the state trajectory converges to the sliding surface S .
2. **Sliding phase:** It corresponds to the time interval $t \in [T_s, \infty]$, in which the state trajectories are confined to the sliding surface S . During this phase, the behavior of the system is entirely determined by the choice of the sliding surface.

In ideal Sliding Mode regime, the requested controller u should be able to switch at an infinite frequency. This is not possible in real life, due to the delay between the measurement and the generation of the command. This may cause the system to leave the sliding surface. Then, once the sign of the control is reversed order, the trajectories return on this surface and on the other side, and so on. This undesirable phenomena of oscillation around the sliding surface is called *Chattering*. One of the most effective methods to reduce chattering is the use of Higher Order Sliding Mode Control, which will be addressed in next Section.

1.3 Higher Order Sliding Mode Control

Higher Order Sliding Mode Control (HOSMC) is an effective method for chattering attenuation [27]. In this method the discontinuous control is applied on a higher time derivative

of the sliding variable, such that not only the sliding variable converges to the origin, but also its higher time derivatives. As the discontinuous control does not act upon the system input directly, chattering is automatically reduced. In this section, we will look at the problem formulation of HOSM and recall some well-known Second Order Sliding Mode Control algorithms.

1.3.1 Problem Formulation

Let us consider an uncertain nonlinear system:

$$\begin{cases} \dot{x}(t) = f(x, t) + g(x, t)u, \\ y(t) = s(x, t), \end{cases} \quad (1.15)$$

where $x \in \mathbb{R}^n$ is the state vector and $u \in \mathbb{R}$ is the control input. The sliding variable s is a measured smooth output-feedback function and $f(x, t)$ and $g(x, t)$ are uncertain smooth functions. Let us recall the definition of relative degree of a system:

Definition 1.3.1. [42, 58] *The relative degree r of System (1.15), with respect to the output $y(t)$, is the minimum order of time derivatives of the output $y(t)$ in which the control input u appears explicitly.*

It is assumed that the relative degree, r of System (1.15) is globally well defined, uniform and time invariant [22] and the associated zero dynamics are asymptotically stable. This means that, for suitable functions $\tilde{\varphi}(x, t)$ and $\tilde{\gamma}(x, t)$, we obtain

$$y^{(r)}(t) = \tilde{\varphi}(x(t), t) + \tilde{\gamma}(x(t), t)u(t). \quad (1.16)$$

The functions $\tilde{\gamma}(x(t), t)$ and $\tilde{\varphi}(x(t), t)$ are assumed to be bounded by positive constants γ_m , γ_M and $\tilde{\varphi}$, such that

$$0 < \gamma_m \leq \tilde{\gamma}(x(t), t) \leq \gamma_M, \quad |\tilde{\varphi}(x(t), t)| \leq \tilde{\varphi}. \quad (1.17)$$

Defining $s^{(i)} := \frac{d^i}{dt^i}y$; the higher order sliding manifold of degree r is defined as

$$S^{(r)} = \left\{ x \in \mathbb{R}^n \mid s^{(0)} = s^{(1)} = \dots = s^{(r-1)} = 0 \right\}. \quad (1.18)$$

Then Higher Order Sliding Mode is defined as

Definition 1.3.2. *There exists an ideal Higher Order Sliding Mode regime of r^{th} order if there exists a finite time T_s such that all solutions of System (1.16) are in $S^{(r)}$ for all $t > T_s$.*

More precisely, let us introduce $z = [z_1 \ z_2 \ \dots z_r]^T := [s \ \dot{s} \ \dots \ s^{(r-1)}]^T$. Then (1.18) is equivalent to $z = 0$. Since the only available information on $\tilde{\varphi}(x, t)$ and $\tilde{\gamma}(x, t)$ are the bounds (1.17), it is natural to consider a more general control system instead of System (1.15), such as

$$\begin{aligned} \dot{z}_i &= z_{i+1}, \quad i = 1, \dots, r-1, \\ \dot{z}_r &= \varphi(t) + \gamma(t)u, \end{aligned} \quad (1.19)$$

where the new functions φ and γ are arbitrary measurable functions that verify the condition

$$(H1) \quad \varphi(t) \in I_\varphi := [-\bar{\varphi}, \bar{\varphi}], \quad \gamma(t) \in I_\gamma := [\gamma_m, \gamma_M], \quad (1.20)$$

where $\bar{\varphi}, \gamma_m, \gamma_M$ are positive constants. In consequence, we are in fact dealing with the differential inclusion

$$z_1^{(r)} \in I_\varphi + uI_\gamma. \quad (1.21)$$

The objective of designing HOSM controllers for System (1.15), with respect to s , is equivalent to the stabilization of System (1.21) to the origin, ideally in finite time. Since these controllers are to be discontinuous feedback laws $u = U(z)$, solutions of (1.21) need to be understood here in Filippov sense, defined as follows:

Definition 1.3.3. *The right hand vector set is enlarged at the discontinuity points of (1.21) to the convex hull of the set of velocity vectors obtained by approaching z from all the directions in \mathbb{R}^r , while avoiding zero-measure sets [29].*

Another important notion concerning our work is that of Real Sliding Modes, defined by Levant in [54] as

Definition 1.3.4. [54] *A control algorithm is said to establish real sliding mode of order r with respect to s when for any local set of initial conditions and for any finite time interval $[t_1, t_2]$, there exist constants $\Delta_1 \dots \Delta_r$ such that for all $t > t_1$, the following inequalities are satisfied*

$$|s| \leq \Delta_1, \quad |\dot{s}| \leq \Delta_2, \quad \dots \quad |s^{(r-1)}| \leq \Delta_r. \quad (1.22)$$

1.3.2 Examples of Second Order Sliding Mode Controllers

After the introduction to Higher Order Sliding Mode, let us examine some popular Second Order Sliding Mode algorithms, the *supertwisting*, the *twisting* and the *sub-optimal*. Second Order Sliding Mode (SOCM) means that the sliding variable s and its first time derivative \dot{s} should converge to zero in a finite time.

1.3.2.1 Supertwisting Algorithm [54, 11]

Supertwisting is a continuous SOSM controller for systems of relative degree 1. It requires the boundedness of the time derivative of perturbation, i.e. for the system $\dot{z}_1 = \varphi(t) + \gamma(t)u$, the condition $|\dot{\varphi}| \leq \bar{\varphi}$ needs to be satisfied. Let us introduce $\varphi = z_2$, then the control objective becomes the stabilization of the following differential inclusion.

$$\begin{aligned} \dot{z}_1 &\in z_2 + [\gamma_m, \gamma_M] u, \\ \dot{z}_2 &\in [-\bar{\varphi}, \bar{\varphi}]. \end{aligned} \quad (1.23)$$

Supertwisting algorithm is expressed as follows:

$$u = -K_p |z_1|^{1/2} \text{sign}(z_1) - \int_0^t K_i \text{sign}(z_1) dt, \quad (1.24)$$

where K_p and K_i are positive constants, chosen as in [11],

$$\begin{aligned} K_p &= k_p \sqrt{L}, \quad K_i = k_i L, \\ L &= \frac{\bar{\varphi}}{\gamma_m}, \quad k_i > 1, \quad k_p > \sqrt{-2k_i + 2\sqrt{k_i^2 + 2k_i + 2}}. \end{aligned} \quad (1.25)$$

It should be noted that the structure of Supertwisting algorithm can be considered as a nonlinear finite time version of the PI Controller.

1.3.2.2 Twisting Algorithm [54]

The Twisting algorithm is a discontinuous SOSM controller that is generally used for systems of relative degree 2. The amplitude of this algorithm switch between two values depending on the quadrant wherein lies the system state.

Considering the following differential inclusion, arising from Equation (1.21),

$$\begin{cases} \dot{z}_1 = z_2, \\ \dot{z}_2 \in [-\bar{\varphi}, \bar{\varphi}] + [\gamma_m, \gamma_M] u. \end{cases} \quad (1.26)$$

The twisting controller is given as

$$u = \begin{cases} -K_m \text{sign}(z_1) & \text{if } z_1 z_2 < 0, \\ -K_M \text{sign}(z_1) & \text{if } z_1 z_2 \geq 0, \end{cases} \quad (1.27)$$

where K_m and K_M are some positive constants. Twisting algorithm can be written in another compact form

$$u = -l_1 \text{sign}(z_1) - l_2 \text{sign}(z_2), \quad (1.28)$$

where l_1 and l_2 satisfy

$$\begin{aligned}\gamma_m(l_1 + l_2) - \bar{\varphi} &> \gamma_M(l_1 - l_2) + \bar{\varphi}, \\ \gamma_m(l_1 - l_2) &> \bar{\varphi}.\end{aligned}\tag{1.29}$$

This algorithm can be considered as a nonlinear robust version of the classical PD controller.

1.3.2.3 Sub-optimal Algorithm [54]

The Sub-optimal algorithm is a discontinuous SOSM controller that is generally used for systems of relative degree 2, therefore its formulation is similar to that of the twisting algorithm. The sub-optimal controller is given as

$$\begin{aligned}u &= \lambda(t)u_M \operatorname{sign}\left(z_1(t) - \frac{z_1(t_M)}{2}\right) \\ \lambda(t) &= \begin{cases} 1 & \text{if } z_1(t) \geq z_1(t_M), \\ \lambda^* & \text{if } z_1(t) < z_1(t_M), \end{cases}\end{aligned}\tag{1.30}$$

where t_M is the last moment at which $z_2 = 0$. In order to ensure finite time convergence, the gains λ^* and u_M should fulfill the following condition:

$$\begin{aligned}\lambda^* &\in (0, 1] \cap \left(0, \frac{3\gamma_m}{\gamma_M}\right) \\ u_M &> \max\left(\frac{\bar{\varphi}}{\lambda^*\gamma_m}, \frac{4\bar{\varphi}}{3\gamma_m\lambda^*\gamma_M}\right)\end{aligned}\tag{1.31}$$

Like twisting, this algorithm can also be considered as a nonlinear robust version of the classical PD controller.

1.3.3 Arbitrary Order Sliding Mode Controllers

Besides Second Order Sliding Mode controllers, there exist many HOSM controllers that can be extended to establish sliding mode of any arbitrary order. For example, Laghrouche et al. [51] have proposed a two part integral sliding mode based control to deal with the finite time stabilization problem and uncertainty rejection problem separately. Dinuzzo et al. have proposed another method in [22], where the problem of HOSM has been treated as Robust Fuller's problem. Defoort et al. [21] have developed a robust Multi Input Multi Output (MIMO) HOSM controller, using a constructive algorithm with geometric homogeneity based finite time stabilization of an integrators chain. Among these, Levant has presented a method of designing arbitrary order sliding mode controllers for Single Input Single Output (SISO) systems in [55], which is presented below :

Theorem 1.3.5. *Provided $l_1, \dots, l_{r-1}, M > 0$ are chosen sufficiently large in the listed order, the bounded controller $u = -M \text{sign}(\phi_{r-1})$ provides finite-time stability for System (1.21), where ϕ_{r-1} is defined inductively as*

$$\begin{aligned} N_1 &= |z_1|^{r-1/r}, \\ N_i &= \left(|z_1|^{d/r} + |z_2|^{d/(r-1)} + \dots + |z_i|^{d/(r-i+1)} \right)^{(r-i)/d}, \quad i = 2, \dots, r-1. \\ \phi_0 &= z_1, \\ \phi_i &= z_{i+1} + l_i N_i \text{sign}(\phi_{i-1}), \quad i = 2, \dots, r-1. \end{aligned} \quad (1.32)$$

with $d > r$ is an arbitrary positive constant.

While this algorithm ensures the finite time convergence, there is a problem in the choice of parameters l_1, l_2, l_{r-1} and M , since there is no necessary or sufficient condition based on Lyapunov analysis proposed yet.

1.3.3.1 Homogeneity

At this point, it is important to introduce the notion of homogeneity, which provides an equivalence between local asymptotic convergence and global finite time convergence. This property facilitates the design of finite time controllers. Let us first recall some important definitions concerning homogeneity.

Consider the following time invariant system (1.33):

$$\dot{z} = f(z), \quad f(0) = 0, \quad z \in \mathbb{R}^r. \quad (1.33)$$

Definition 1.3.6. [39] *The family of dilations ζ_ϵ^p , $\epsilon > 0$, are the linear maps defined on \mathbb{R}^r given by*

$$\zeta_\epsilon^p(z_1, \dots, z_r) = (\epsilon^{p_1} z_1, \dots, \epsilon^{p_r} z_r),$$

where $p = (p_1, \dots, p_r)$ with the dilation coefficients $p_i > 0$, for $i = 1, \dots, r$.

Definition 1.3.7. [39] *The vector field $f(z) = (f_1(z), \dots, f_r(z))^T$ is homogeneous of degree $\kappa \in \mathbb{R}$ with respect to the family of dilation ζ_ϵ^p if, for every $z \in \mathbb{R}^r$ and $\epsilon > 0$,*

$$f_i(\epsilon^{p_1} z_1, \dots, \epsilon^{p_r} z_r) = \epsilon^{p_i + \kappa} f_i(z_1, \dots, z_r), \quad i = 1, \dots, r, \quad \epsilon > 0.$$

System (1.33) is called homogeneous, if the vector field $f(z)$ is homogeneous.

The following lemma establishes the equivalence between local and global stability of homogeneous systems.

Lemma 1.3.8. *Lemma 3.3 [8]. Suppose f is homogeneous with respect to the family of dilations δ_ϵ^p and 0 is an attractive equilibrium under f . Then, 0 is a globally asymptotically stable equilibrium under f .*

Lemma 1.3.9. *Lemma 3.1 [39]. Suppose that System (1.33) is homogeneous of degree $k < 0$ with respect to the family of dilations δ_ϵ^p , $f(z)$ is continuous and $z = 0$ is its asymptotically stable equilibrium. Then the equilibrium of system (1.33) is globally finite-time stable.*

Remark 1.3.10. *The homogeneity concept can be extended for the case of differential inclusion [57]*

$$\dot{z} \in F(z). \quad (1.34)$$

The property of finite-time convergence will hold true in this case.

From these lemmas, it is clear that if a closed loop system (with a controller u) is homogeneous of negative degree, then it is sufficient to prove its local asymptotic stability to deduce that it is globally finite-time stable. In this regard, let us recall that many Higher Order Sliding Mode Controllers are homogenous. For example, The closed loop system with the supertwisting algorithm is homogeneous of degree $\kappa = -\frac{1}{2}$ with respect to the family of dilation $(1, \frac{1}{2})$. The twisting algorithm and sub-optimal are also homogeneous of negative degree. In his recent works [56, 57], homogeneity approach has been used to demonstrate finite time stabilization of his initial work in [55]. The concept of homogeneity has been used extensively in Chapter 3 of the thesis.

1.4 Adaptive Sliding Mode Controllers

In the previous section, it was seen that SMC and HOSMC require the uncertainty in the system to be bounded. In many cases, these bounds need to be known in order to calculate the gains of the control algorithms. However, the exact identification of uncertainty bounds is challenging from the physical point of view, as it requires extensive experimentation in worst case conditions of the system. The case where the bounds on uncertainty exist, but are unknown, is an interesting problem in the field of arbitrary HOSMC. A simple solution would be to use overestimated gains, resulting in high amplitude discontinuous control. In practice, such controllers are not applicable as they lead to a high amplitude chattering in physical systems. Therefore, a good control strategy is expected to have two

essential properties (a) non-requirement of the uncertainty bounds and (b) avoidance of gain overestimation [73].

A more effective method of dealing with uncertain systems with unknown uncertainty bounds is to employ dynamically adapting the controller gains, such that the controller's output amplitude remains just sufficient for compensating the parametric drifts and external disturbance. Such adaptive controllers efficiently avoid oscillations due to unnecessarily large control inputs, while maintaining the robustness property. Huang et al. [41] were the first to use dynamic gain adaptation in SMC for the problem of unknown uncertainty bound. They presented an adaptation law for first order SMC, which depends directly upon the sliding variable; the control gains increase until sliding mode is achieved, and afterward the gains become constant. This method worked without a-priori knowledge of uncertainty bounds, however it does not solve the gain overestimation problem. Since then, many improved adaptive SMC algorithms have been published. Let us review some of the adaptive sliding mode control algorithms that have been published in contemporary literature.

1.4.1 Adaptive First Order Sliding Mode Controller [73]

This controller is applicable on systems of relative degree 1. The idea of the algorithm is to increase the amplitude of the control when the system is far from the sliding manifold, and to reduce the amplitude when $s \approx 0$.

The proposed control law defined as:

$$u = K(t) \text{sign}(s), \quad (1.35)$$

and the gain K is defined by the following dynamics

$$\dot{K} = \begin{cases} \bar{K}|s| \text{sign}(|s| - \epsilon) & , \quad K > 0 \text{ or } \text{sign}(|s| - \epsilon) > 0 \\ 0 & , \quad K = 0 \text{ and } \text{sign}(|s| - \epsilon) < 0 \end{cases} \quad (1.36)$$

where \bar{K} is an arbitrary positive constant.

The controller u ensures the convergence of s in finite time to the domain $|s| < \epsilon$, therefore it establishes real sliding mode. However it does not guarantee that the states would remain inside the neighborhood after convergence; the states actually overshoot in a known region around the neighborhood $|s| \leq \mu$, where

$$\mu = \sqrt{\epsilon^2 + \frac{\bar{\varphi}^2}{\bar{K}\gamma_m}}. \quad (1.37)$$

Due to the presence of the term $|s|$ in the dynamics of adaptation, the gain K has a fast rate of increase, but a very slow rate of decrease.

1.4.2 Adaptive Supertwisting Controller [81]

This adaptive controller is based on the Supertwisting algorithm. Therefore, its control output is continuous, and defined as follows

$$u = -K_p(t)|z_1|^{1/2}\text{sign}(z_1) - \int_0^t K_i(t)\text{sign}(z_1)dt, \quad (1.38)$$

where the dynamics of K_p and K_i are defined as

$$\begin{aligned} \dot{K}_p &= \begin{cases} \omega_1 \sqrt{\frac{\gamma_1}{2}} \text{sign}(|s| - \epsilon) & , \quad K_p > K_{pm} \\ \eta & , \quad K_p \leq K_{pm} \end{cases} \\ \dot{K}_i &= 2aK_p \end{aligned} \quad (1.39)$$

where ω_1 , γ_1 , K_{pm} , η and a are arbitrary positive constants. The controller u ensures the convergence of s in finite time to the domain $|s| < \epsilon$, thereby establishing real sliding mode. However, as in [73], this algorithm also does not guarantee that the states would remain inside the neighborhood after convergence; furthermore the region of is not determined. However, the dynamics of adaptation are fast in both increasing and decreasing directions.

1.4.3 Adaptive Twisting Controller [47]

This adaptive controller, based on the twisting algorithm, was proposed for systems with relative degree 2. The proposed controller takes the following form

$$u = -K(t)(\text{sign}(z_1) + 0.5\text{sign}(z_2)) \quad (1.40)$$

where the gain $K(t)$ is given by

$$\dot{K} = \begin{cases} \frac{\frac{\omega_1}{\sqrt{2\gamma_1}} \text{sign}(N(z_1, z_2) - \epsilon)}{\frac{1}{\gamma_1} - \frac{2Kz_1^2 + |z_1|z_2^2}{|K - K^*|^3}} & , \quad K \geq K_m, \\ \xi & , \quad K < K_m, \end{cases} \quad (1.41)$$

with $N(z_1, z_2)$ defined by

$$N(z_1, z_2) = \frac{z_1^2}{a} + \frac{z_2^2}{b}, \quad (1.42)$$

where a and b are positive constants. The controller aims to ensure the convergence to the domain which represents an ellipse $N(z_1, z_2) \leq \epsilon$.

where ω_1 , γ_1 , K_m , ϵ , ξ are arbitrary positive constants, and K^* is a sufficiently large positive constant.

This algorithm ensures the finite-time convergence of (z_1, z_2) to domain $N(z_1, z_2) \leq \epsilon$, but the states remain in a larger domain $N(z_1, z_2) \leq \mu$, with $\mu > \epsilon$. However, there is no estimation of a bound of μ .

Remark 1.4.1. *One particular point to be noted in the description of the adaptive SMC algorithms, is that all of these controllers establish real sliding mode. Effectively, as the gains are decreased, the perturbation in the system may switch instantly, provoking the sliding variable to leave zero. Therefore, in the case of adaptive controllers convergence of sliding variable is can only be ensured to neighborhood of the origin.*

1.5 Summary

In this chapter, we recalled the basic concepts of SMC, HOSMC, Homogeneity and Adaptive SMC, for the control of uncertain nonlinear systems. Different contemporary algorithms for robust SMC and HOSMC were reviewed and it was shown that HOSMC controllers can be designed using the concept of homogeneity. While there exists vast literature on these methods, there are certain problems that still remain to be resolved. One of the major problems of HOSMC for an order greater than 2 is the tuning of controller gains, which have so far been done through simulations. While generalized methods, such as Lyapunov functions, exist for tuning the gains of First and Second Order SMC, to the best of our knowledge, there are no such methods for the analysis and tuning of arbitrary sliding mode controllers.

Then, we discussed the case where the bounds of uncertainty may be unknown. It was shown that adaptive controllers solve this problem effectively, by dynamically adjusting the controller gains to compensate the uncertainty. However, research in adaptive SMC controllers has remained limited. In contemporary literature, no adaptive controllers were found for SMC of orders greater than 2.

These two problems, related to robust and adaptive controllers are the focus of this part of the thesis. In the following chapter, a Lyapunov-based method is presented for the design of arbitrary order robust and adaptive sliding mode controllers for uncertain

nonlinear systems. The problem is formulated as the finite-time stabilization of perturbed integrator chains, and the solution is based on a class of controllers for the finite-time stabilization of pure integrator chains.

The results of Chapter 2 are then further elaborated in Chapter 3, in which, the degree of homogeneity of the controllers is used to obtain different useful characteristics. A generalized arbitrary order SMC algorithm is presented and it has been shown that for a particular choice of homogeneity degree, Levant's arbitrary order HOSM controller [55] becomes a particular case of our controller. Then, it has been demonstrated that by controlling the homogeneity degree, the properties of bounded control output with amplitude of discontinuity in zero and fixed time convergence can also be acquired.

Chapter 2

Lyapunov based robust and adaptive HOSM controllers

As discussed in the previous chapter, Higher Order Sliding Mode Control (HOSMC) is an effective method for control of uncertain nonlinear systems. This method retains the disturbance and parameter insensitivity property of classical sliding mode, and also reduces chattering. The last 15 years have seen outstanding developments in the field of HOSMC. The important works in robust and adaptive HOSMC were presented in the previous chapter. It was concluded that there is a lack of general methods for design and tuning of arbitrary order sliding mode controllers. Furthermore, adaptive controllers for sliding mode of orders greater than 2 are so far unavailable.

This chapter is based on our contributions in arbitrary order robust and adaptive HOSMC. We present Lyapunov-based robust and adaptive Higher Order Sliding Mode Controllers for nonlinear SISO systems with bounded uncertainty. This problem has been formulated as the stabilization of a chain of integrators with bounded uncertainty. There are two main contributions in this chapter. First, a Lyapunov-based approach for arbitrary HOSMC is developed. The controller establishes higher order sliding mode of any arbitrary order under the condition that the bounds of the uncertainty are known. The advantage of our method is that robust HOSM controllers are developed from a class of finite time controllers for pure chain of integrators. To the best of our knowledge, this is the first work on a Lyapunov based approach for arbitrary HOSMC. As mentioned in the previous chapter, Lyapunov design is a powerful tool for control system design that allows to estimate an upper bound on convergence time [7].

The second contribution in this chapter is the extension of the robust controller to an adaptive controller for the case where the bounds on the uncertainty are unknown. This controller aims to converge the states to an arbitrarily small neighborhood of the origin. The adaptation dynamics are based on a saturation function [15, 49, 50], which results in rapid increase of gains when the sliding variable and its derivatives are outside the neighborhood, and rapid decrease when they are inside the neighborhood. The advantage of this adaptive controller design, compared to other algorithms mentioned before, is that this controller can be extended to any arbitrary order and the adaptation rates are fast in both directions. Therefore, the amplitude of the discontinuous control decreases faster as compared to [73]. However, as in all the cases of adaptive controllers discussed in the previous section, the proposed adaptive controller also establishes real HOSM.

The practical applicability and performance of the robust and adaptive controllers demonstrated through an illustrative example a fuel cell system control, which is described in detail later on.

2.1 Design of robust Higher Order Sliding Mode Controller

Let us recall the problem formulation of HOSMC, presented in Chapter 1. It was established that the problem of HOSM control of System (1.15) with respect to s is equivalent to the finite time stabilization of the auxiliary system (1.21) to the origin, and that the solutions need to be understood here in Filippov sense due to the discontinuous nature of the control. In this section, a robust controller is developed for this problem, under the assumption that the uncertainty bounds $\bar{\varphi}$, γ_m , γ_M are known. This controller has been derived from a class of Lyapunov-based controllers that guarantee finite time stabilization of pure chain of integrators, and satisfy certain additional geometric conditions.

2.1.1 Preliminaries

The HOSM controller developed in this section is based on a class of controllers for the finite time stabilization of pure integrator chains. The pure (unperturbed) integrator chain is represented as follows:

$$\begin{aligned}\dot{z}_i &= z_{i+1}, \quad i = 1, \dots, r-1, \\ \dot{z}_r &= u.\end{aligned}\tag{2.1}$$

Let us recall the theorem:

Theorem 2.1.1. [7] Consider System (2.1). Suppose there exist a continuous state-feedback control law $u = u_0(z)$, a positive definite C^1 function V_1 defined on a neighborhood $\hat{U} \subset \mathbb{R}^r$ of the origin and real numbers $c > 0$ and $0 < \alpha < 1$, such that the following condition is true for every trajectory z of System (2.1), $\dot{V}_1 + cV_1^\alpha(z(t)) \leq 0$, if $z(t) \in \hat{U}$, where \dot{V}_1 is the time derivative of $V_1(z)$. Then all trajectories of System (2.1) with the feedback $u_0(z)$ which stay in \hat{U} converge to zero in finite time. If $\hat{U} = \mathbb{R}^r$ and V_1 is radially unbounded, then System (2.1) with the feedback $u_0(z)$ is globally finite time stable with respect to the origin.

2.1.2 Lyapunov-based Arbitrary HOSM Controller

Based on Theorem 2.1.1, we now present the main result of this section:

Theorem 2.1.2. Consider System (1.15) subject to Hypothesis **H1**. Then the following control law establishes Higher Order Sliding Mode with respect to s :

$$u = \frac{1}{\gamma_m} (u_0 + \bar{\varphi} \text{sign}(u_0)), \quad (2.2)$$

where $u_0(z)$ is any state-feedback control law that satisfies the hypotheses of Theorem 2.1.1 and obeys the following additional conditions:

$$\frac{\partial V_1}{\partial z_r} u_0 \leq 0, \text{ and } u_0 = 0 \Rightarrow \frac{\partial V_1}{\partial z_r} = 0. \quad (2.3)$$

Proof of Theorem 2.1.2. As mentioned before, establishment of HOSM with respect to s for System (1.15) is equivalent to the finite-time stabilization of System (1.21). Let us consider System (1.21) under the control law u defined in (2.2):

$$\begin{cases} \dot{z}_i &= z_{i+1}, \quad i = 1, \dots, r-1, \\ \dot{z}_r &= \varphi + \gamma u \\ &= \frac{\gamma}{\gamma_m} u_0(z) + \frac{\gamma \bar{\varphi}}{\gamma_m} \text{sign}(u_0(z)) + \varphi. \end{cases} \quad (2.4)$$

System (2.4) defines a differential inclusion where $\text{sign}(x)$ stands for the closed interval $[-1, 1]$ when $x = 0$ and $x/|x|$ otherwise. Since the right-hand side is bounded, closed, convex and upper semi-continuous w.r.t. z , solutions of the differential inclusion are well-defined for positive times. The conditions in (3.16) mean that the quantity $\frac{\partial V_1}{\partial z_r} \text{sign}(u_0)$ defines a continuous and non positive function of the time along trajectories of System (2.4). For $u_0(z(t)) \neq 0$, this is ensured by the first part of (3.16) and the term also converges to zero

if u_0 tends to zero. On the other hand, if $u_0(z(t)) = 0$, then the second part of Condition (3.16) results in $\frac{\partial V_1}{\partial z_r} \text{sign}(u_0) = 0$.

We next compute the time derivative of the Lyapunov function V_1 provided by Theorem 2.1.1 along a non trivial trajectory of System (2.4). We obtain:

$$\begin{aligned}
 \dot{V}_1 &= \sum_{i=1}^{r-1} \frac{\partial V_1}{\partial z_i} z_{i+1} + \frac{\partial V_1}{\partial z_r} (\varphi + \gamma u) \\
 &= \sum_{i=1}^{r-1} \frac{\partial V_1}{\partial z_i} z_{i+1} + \frac{\partial V_1}{\partial z_r} \left(\frac{\gamma}{\gamma_m} u_0 + \frac{\gamma}{\gamma_m} \bar{\varphi} \text{sign}(u_0) + \varphi \right) \\
 &\leq \sum_{i=1}^{r-1} \frac{\partial V_1}{\partial z_i} z_{i+1} + \frac{\partial V_1}{\partial z_r} u_0 + \frac{\partial V_1}{\partial z_r} \text{sign}(u_0) (\bar{\varphi} - |\varphi|) \\
 &\leq \sum_{i=1}^{r-1} \frac{\partial V_1}{\partial z_i} z_{i+1} + \frac{\partial V_1}{\partial z_r} u_0 \leq -c V_1^\alpha.
 \end{aligned} \tag{2.5}$$

This implies that if a non-trivial trajectory z reaches zero, it must stay there and the zero function is the unique solution of the differential inclusion (2.4) starting from the origin. In addition, the Lyapunov function V_1 strictly decreases along any non trivial trajectory of (6) and reaches zero in finite time according to (2.5). \square

The previous result becomes non empty if controllers satisfying Theorem 2.1.1 and Condition (3.16) can be identified. It can be verified that the controllers proposed by Hong [39] and Huang et al. [40] fulfill these conditions. We present Hong's controller as an example. Let us denote $|a|^\theta := |a|^\theta \text{sign}(a)$, $\forall a \in \mathbb{R}, \theta > 0$. Then Hong's controller [39] is defined as follows:

Let $k < 0$ and l_1, \dots, l_r positive real numbers. For $z = (z_1, \dots, z_r)$, we define for $i = 0, \dots, r-1$:

$$\begin{aligned}
 p_i &= 1 + (i-1)k, \\
 v_0 &= 0, \quad v_{i+1} = -l_{i+1} [|z_{i+1}|^{\beta_i} - |v_i|^{\beta_i}]^{\alpha_{i+1}/(\beta_i)},
 \end{aligned} \tag{2.6}$$

where $\alpha_i = p_{i+1}/p_i$, for $i = 1, \dots, r$, and, for $k < 0$ sufficiently small,

$$\beta_0 = p_2, \quad (\beta_i + 1)p_{i+1} = \beta_0 + 1 > 0, \quad i = 1, \dots, r-1.$$

Consider the positive definite radially unbounded function $V_1 : \mathbb{R}^r \rightarrow \mathbb{R}^+$ given by

$$V_1 = \sum_{j=1}^r \int_{v_{j-1}}^{z_j} [s]^{\beta_{j-1}} - [v_{j-1}]^{\beta_{j-1}} ds.$$

It has been proved in [39] that for a sufficiently small k , there exist $l_i > 0$, $i = 1, \dots, r$, such that the control law $u_0 = v_r$ defined above stabilizes System (2.1) in finite time and there

exists $c > 0$ and $0 < \alpha < 1$ such that u_0 and V_1 fulfill the conditions of Theorem 2.1.1. Moreover,

$$\frac{\partial V_1}{\partial z_r} = [z_r]^{\beta_{r-1}} - [v_{r-1}]^{\beta_{r-1}}, \quad u_0 = v_r = -l_r \left[[z_r]^{\beta_{r-1}} - [v_{r-1}]^{\beta_{r-1}} \right]^{\alpha_r / \beta_{r-1}}. \quad (2.7)$$

It can be verified that $\frac{\partial V_1}{\partial z_r} u_0 \leq 0$ and $u_0 = 0 \Rightarrow \frac{\partial V_1}{\partial z_r} = 0$. The feedback law of [39] can be simplified by choosing all $\beta_i = 1$ in (2.6) as explained below:

Proposition 2.1.3. *For System (2.1), there exist a sufficiently small $k < 0$ and real numbers $l_i > 0$, such that the control law $u_0 = v_r$ defined below stabilizes System (2.1) in finite time.*

For $i = 0, \dots, r-1$,

$$v_0 = 0, \quad v_{i+1} = -l_{i+1} [z_{i+1} - v_i]^{(1+(i+2)k)/(1+(i+1)k)}. \quad (2.8)$$

Proof of Proposition 2.1.3. The proof can be developed simply by adapting the proof presented in [39] to the parameter choice of (2.8). Let $\lambda = (1 + (r+2)k)/(1 + (r+1)k)$ and f_λ be the closed-loop vector field obtained by using the feedback (2.8) in (2.1). For each $\lambda > 0$, the vector field f_λ is continuous and homogeneous of degree $k < 0$ with respect to the family of dilations (p_1, \dots, p_r) , where $p_i = 1 + (i-1)k$, $i = 1, \dots, r$. Let l_i , $i = 1, \dots, r$ be positive constants such that the polynomial $y^r + l_r(y^{r-1} + l_{r-1}(y^{r-2} + \dots + l_2(y + l_1)))$ is Hurwitz. If $k = 0$ the vector field is linear and therefore $\lambda = 1$. Therefore, there exists a positive-definite, radially unbounded, Lyapunov function $V : \mathbb{R}^r \rightarrow \mathbb{R}$ such that $L_{f_\lambda} V$ is continuous and negative definite.

Let $\mathcal{A} = V^{-1}([0, 1])$ and $\mathcal{S} = \text{bd} \mathcal{A} = V^{-1}(\{1\})$, where $\text{bd} \mathcal{A}$ is the boundary of the set \mathcal{A} , i.e. $\mathcal{A} = \{z \in \mathbb{R}^r | V(z) \in [0, 1]\}$ and $\mathcal{S} = \{z \in \mathbb{R}^r | V(z) = 1\}$. Then \mathcal{A} and \mathcal{S} are compact since V is proper. Also, $0 \notin \mathcal{S}$ as V is positive definite. Defining $\phi : (0, 1] \times \mathcal{S} \rightarrow \mathbb{R}$ by $\phi(\lambda, z) = L_{f_\lambda} V(z)$. Then V is continuous and satisfies $\phi(\lambda, z) < 0$ for all $z \in \mathcal{S}$, i.e. $\phi(\{1\} \times \mathcal{S}) \subset (-\infty, 0)$. Since \mathcal{S} is compact, by continuity there exists $\epsilon > 0$ such that $\phi((1-\epsilon, 1] \times \mathcal{S}) \subset (-\infty, 0)$. It follows that for $\lambda \in (1-\epsilon, 1]$, $L_{f_\lambda} V$ takes negative values on \mathcal{S} . Thus, \mathcal{A} is strictly positively invariant under f_λ for every $\lambda \in (1-\epsilon, 1]$. Therefore the origin is global asymptotic stable under f_λ , for $\lambda \in (1-\epsilon, 1]$. Finally, for $\lambda \in (1-\epsilon, 1)$ i.e. $|k|$ small enough, by homogeneity, the origin is globally finite time stable. \square

2.2 Adaptive Controller

Let us now consider that uncertainty bounds γ_m , γ_M and $\bar{\varphi}$ of System (1.21) are unknown. As mentioned in Chapter 1, adaptive control is an effective method for this problem. In the literature, many adaptive algorithms exist for SMC and HOSMC, the most prominent of which were presented in the previous chapter. It was remarked that no contemporary work on adaptive HOSMC has been published for orders greater than two (to the best of our knowledge). In this section, we will extend the robust controller, presented afore, in order to develop an adaptive arbitrary HOSM controller.

For any $a \in \mathbb{R}$, let $\sigma(a)$ be the standard saturation function defined by $\sigma(a) = \frac{a}{\max(1, |a|)}$.

For $\varepsilon > 0$, $a \in \mathbb{R}$, we define $v_\varepsilon(a) = \frac{1}{2} + \frac{1}{2}\sigma\left(\frac{|a| - \frac{3}{4}\varepsilon}{\frac{1}{4}\varepsilon}\right)$.

The following controller is proposed:

$$u = \hat{\gamma}u_0(z) + \hat{\varphi}\text{sign}(u_0(z)), \quad (2.9)$$

where u_0 is a homogeneous controller that satisfies the hypotheses of Theorem 2.1.1 and fulfills Condition (3.16). The adaptive function $\hat{\gamma} = \kappa + \delta|u_0(z)|$ and $\hat{\varphi}(t)$ is defined by the ODE

$$\dot{\hat{\varphi}}(t) = kv_\varepsilon(V_1(z)) - (1 - v_\varepsilon(V_1(z))) [\hat{\varphi}]^\eta,$$

with the initial condition $\hat{\varphi}(0) = 0$. The new terms are defined as $\kappa, \delta > 0, \eta \in (0, 1), k > 0$ and V_1 is a homogeneous Lyapunov function which also satisfies Theorem 2.1.1 and Condition (3.16). Then the following theorem provides the main result for the adaptive case.

Theorem 2.2.1. *Consider System (1.21) under the feedback control law (2.9). Then, $\forall \varepsilon, \exists c' > 0$ and $0 < \alpha' < 1$ such that the following conditions are satisfied for any initial condition $z_0 \in \hat{U}$*

$$(i) \liminf_{t \rightarrow \infty} V_1(z(t)) \leq \varepsilon, \limsup_{t \rightarrow \infty} V_1(z(t)) \leq \Delta;$$

$$(ii) \limsup_{t \rightarrow \infty} |\hat{\varphi}| \leq 2\bar{\Phi} + k(\Delta^{1-\alpha}/(c(1-\alpha))),$$

$$\text{where } \bar{\Phi} := \frac{1}{\gamma_m} \left(\bar{\varphi} + \frac{(\kappa\gamma_m - 1)^2}{4\gamma_m\delta} \right), \quad \Delta := \left(\varepsilon^{1-\alpha'} + \frac{c'(1-\alpha')\gamma_m}{2k} \bar{\Phi}^2 \right)^{\frac{1}{1-\alpha'}}.$$

Remark 2.2.2. *The second Inequality of (i) of Theorem 2.2.1 is equivalent to Levant's concept of real Higher Order Sliding Mode, as defined in the previous chapter. This is equivalent to practical stability of z_1, \dots, z_r . Details on real sliding mode and real HOSM can be found in Section 2 of [54].*

Proof of Theorem 2.2.1. We first demonstrate that when the system states are in the domain $V_1 > \varepsilon$, the controller brings them to the domain $V_1 \leq \varepsilon$ in finite time. Then, it is proved that once z reaches the domain $V_1 \leq \varepsilon$, it stays in the domain $V_1 \leq \Delta$ for all consecutive time instances and $\hat{\varphi}$ is upper-bounded after a sufficiently large time.

We first need the following intermediate result.

Lemma 2.2.3. *The function $\hat{\varphi}$ is non-negative and is defined as long as the trajectory of z is defined.*

Proof. It is clear that $\hat{\varphi}$ is positive in time interval $(0, \tau)$, since $\dot{\hat{\varphi}}(0) \geq 0$. Since $\hat{\varphi}$ is continuous, if there exists $\tau_1 > 0$ such that $\hat{\varphi}(\tau_1) < 0$, then there exists a time $\tau_0 \geq 0$, $\tau_0 < \tau_1$, such that $\hat{\varphi}(\tau_0) = 0$, and $\hat{\varphi}(t) < 0$, $\forall t \in]\tau_0, \tau_1]$.

In this case, $V_1(z(\tau_0)) = 0$ otherwise $\dot{\hat{\varphi}}(\tau_0) > 0$ and $\hat{\varphi}$ cannot be negative on a right interval at τ_0 . In that case, there exists a right interval at τ_0 (still denoted $] \tau_0, \tau_1]$) where $V_1 < \frac{\varepsilon}{2}$ and then $\dot{\hat{\varphi}} = -[\hat{\varphi}]^\eta > 0$. We therefore obtain $\hat{\varphi}(\tau_1) = \int_{\tau_0}^{\tau_1} \dot{\hat{\varphi}} dt > 0$, which is a contradiction. \square

We argue by contradiction in order to prove that $\liminf_{t \rightarrow \infty} V_1(z(t)) \leq \varepsilon$. Supposing there exists \bar{t} such that $V_1(t) > \varepsilon$ for every $t \geq \bar{t}$, then according to the dynamics of $\hat{\varphi}$, we get $\dot{\hat{\varphi}} = k$ for $t \geq \bar{t}$. This implies that for $t \geq \bar{t}$, $\hat{\varphi}$ is increasing and $\hat{\varphi} > \bar{\Phi}$. Since we have

$$\begin{aligned}
 \dot{V}_1 &= \frac{\partial V_1}{\partial z_1} z_2 + \dots + \frac{\partial V_1}{\partial z_r} (\gamma [\hat{\gamma} u_0 + \hat{\varphi} \text{sign}(u_0)] + \varphi), \\
 &= \frac{\partial V_1}{\partial z_1} z_2 + \dots + \frac{\partial V_1}{\partial z_r} u_0 + \frac{\partial V_1}{\partial z_r} (-u_0 + \kappa \gamma u_0 + \gamma \delta |u_0|^2 + \gamma \hat{\varphi} \text{sign}(u_0) + \varphi), \\
 &\leq -cV_1^\alpha - \left| \frac{\partial V_1}{\partial z_r} \right| ((\kappa \gamma_m - 1) |u_0| + \gamma_m \delta |u_0|^2 + \gamma_m \hat{\varphi} - \bar{\varphi}), \\
 &= -cV_1^\alpha - \left| \frac{\partial V_1}{\partial z_r} \right| \left[\gamma_m \delta \left(|u_0| + \frac{\kappa \gamma_m - 1}{2 \gamma_m \delta} \right)^2 \right] - \left| \frac{\partial V_1}{\partial z_r} \right| \left[-\left(\bar{\varphi} + \frac{(\kappa \gamma_m - 1)^2}{4 \gamma_m \delta} \right) + \gamma_m \hat{\varphi} \right], \\
 &\leq -cV_1^\alpha - \gamma_m \left| \frac{\partial V_1}{\partial z_r} \right| (\hat{\varphi} - \bar{\Phi}) \leq -cV_1^\alpha.
 \end{aligned} \tag{2.10}$$

Then $V_1(z)$ converges to zero in finite time, which contradicts the hypothesis. The functions u_0 and V_1 are homogeneous, which according to [8], means that

$$\exists c', \alpha' > 0 : |\partial V_1 / \partial z_r| \leq c' V_1^{\alpha'}, \tag{2.11}$$

where $c' = \max_{\{z: V_1(z)=1\}} \left| \frac{\partial V_1}{\partial z_r} \right|$, $\alpha' = \frac{\kappa_2}{\kappa_1}$. The terms κ_2 and κ_1 are the respective degrees of homogeneity of $\partial V_1 / \partial z_r$ and V_1 .

We suppose now that $V_1 < \varepsilon$. Considering (2.11), let us estimate the overshoot in the worst case condition with respect to uncertainty. For $V_1(z(0)) = \varepsilon$ and $\hat{\phi}(0) = 0$, we get

$$\dot{V}_1 \leq -cV_1^\alpha - \gamma_m c' V_1^{\alpha'} (\hat{\phi} - \bar{\Phi}), \quad \dot{\hat{\phi}} = k. \quad (2.12)$$

The overshoot Δ of V_1 holds for $\dot{V}_1 = 0$ at $t = T_M$. We get $\hat{\phi}(T_M) = \bar{\Phi} - \frac{c\Delta^{\alpha-\alpha'}}{c'\gamma_m} \leq \bar{\Phi}$, and then $T_M \leq \bar{\Phi}/k$. An upper bound of Δ can be estimated as $\Delta = \left(\varepsilon^{1-\alpha'} + \frac{c'(1-\alpha')\gamma_m \bar{\Phi}^2}{2k} \right)^{\frac{1}{1-\alpha'}}$.

We now estimate an upper bound of $\limsup_{t \rightarrow \infty} \hat{\phi}$. Consider the case $V_1(z(0)) = \varepsilon$ with $\dot{V}_1(z(0)) \geq 0$, in this case we have $\hat{\phi}(0) < \bar{\Phi}$. For $t = T_M$, i.e., $\dot{V}_1 = 0$, we get $\hat{\phi}(T_M) \leq \bar{\Phi} + \hat{\phi}(0) \leq 2\bar{\Phi}$. $\hat{\phi}$ will increase until time T_f where $\dot{\hat{\phi}}(T_f) = 0$ and $V_1(z(T_f)) \geq 0$. The worst case is calculated with respect to the boundary of $\hat{\phi}$, using $\dot{V}_1 \leq -cV_1^\alpha$ and $\dot{\hat{\phi}} = k$. Here T_f corresponds to $V_1(z(T_f)) = 0$, i.e. $T_f - T_M = (\Delta^{(1-\alpha)}) / (c(1-\alpha))$, which implies that

$$\hat{\phi}(T_f) \leq \hat{\phi}(T_M) + k(T_f - T_M) = 2\bar{\Phi} + \frac{k\Delta^{(1-\alpha)}}{c(1-\alpha)}.$$

□

Discussion: The adaptive functions $\hat{\gamma}$ and $\hat{\phi}$ are chosen non-negative and $\hat{\gamma}$ is strictly positive with a term proportional to $|u_0|$. It satisfies the condition $\frac{\partial \hat{\gamma}}{\partial |u_0|} > 0$, which is sufficient to ensure that the states will not diverge, irrespectively of $\hat{\phi}$. The second adaptive function $\hat{\phi}$ ensures the convergence of the state to a neighborhood of zero. Its dynamics can be defined explicitly by: $\dot{\hat{\phi}} = k$ for $V_1 \leq \frac{\varepsilon}{2}$, $\dot{\hat{\phi}} = \frac{2k}{\varepsilon}(V_1 - \varepsilon/2) - \frac{2}{\varepsilon}(\varepsilon - V_1)[\hat{\phi}]^\eta$ for $\frac{\varepsilon}{2} \leq V_1 \leq \varepsilon$ and $\dot{\hat{\phi}} = -[\hat{\phi}]^\eta$ for $V_1 \leq \frac{\varepsilon}{2}$. These dynamics mean that $\hat{\phi}$ is increasing for $V_1 \geq \varepsilon$, decreasing for $V_1 \leq \frac{\varepsilon}{2}$, and with indefinite sign for $\frac{\varepsilon}{2} \leq V_1 \leq \varepsilon$.

2.3 Experimental results : PEM Fuel Cell System

The practical applicability of the proposed controllers is demonstrated on the air-feed system of Polymer Electrolyte Membrane Fuel Cell (PEMFC) System, in which, a moto-compressor is used to feed air (as a source of oxygen) to the PEMFC's cathode. The control problem in this application is to optimize the net power output of the PEMFC by operating the compressor at its optimal point, thereby reducing the internal power consumption of the fuel cell. This is achieved by maintaining the oxygen excess ratio in the cathode at a certain optimal value. Some sliding mode based solutions of this problem have been published in [48] and [63]. In the first, the oxygen excess ratio is assumed to

have a static relationship with the compressor flow rate; and the compressor is controlled using a SOSMC. In the latter, the authors have proposed a dual loop cascade SOSMC controller. In this method, the outer loop generates the compressor speed reference and the inner loop forces the motor to follow this reference. This approach is more practical as both control loops are robust, however its implementation requires different loop rates for controllers. We have approached this problem by designing third order sliding mode based oxygen excess ratio controllers, using the proposed techniques. The advantage of our method in this context, is that the third order extension generates smooth control input, which results in continuous current control of the moto-compressor. Both the robust and adaptive controllers are designed for this problem, and validated on a Hardware in Loop test bench, which consists of a commercial twin screw compressor with inverter drive and a real-time fuel cell emulation system. The robustness property of the controllers has also been verified by varying the parameters of the fuel cell emulator to their extreme values.

2.3.1 PEMFC air-feed system model

The dynamic model of a PEMFC air-feed system is as follows [63]:

$$\begin{aligned}
 \dot{x}_1 &= c_1(x_4 - x_1 - x_2 - c_2) - \frac{c_3 x_1}{c_4 x_1 + c_5 x_2 + c_6} c_{17} \sqrt{x_1 + x_2 + c_2 - c_{11}} - c_7 \zeta, \\
 \dot{x}_2 &= c_8(x_4 - x_1 - x_2 - c_2) - \frac{c_3 x_2}{c_4 x_1 + c_5 x_2 + c_6} c_{17} \sqrt{x_1 + x_2 + c_2 - c_{11}}, \\
 \dot{x}_3 &= -c_9 x_3 - c_{10} \left[\left(\frac{x_4}{c_{11}} \right)^{c_{12}} - 1 \right] + c_{13} u, \\
 \dot{x}_4 &= c_{14} \left[1 + c_{15} \left[\left(\frac{x_4}{c_{11}} \right)^{c_{12}} - 1 \right] \right] [W_{cp} - c_{16}(x_4 - x_1 - x_2 - c_2)],
 \end{aligned} \tag{2.13}$$

$$u = I_q \quad , \quad \zeta = I_{st}, \quad W_{cp} = c_{21} \omega_{cp}. \tag{2.14}$$

The physical quantities that form the state vector x are

$$x = [x_1 \ x_2 \ x_3 \ x_4]^T = [p_{O_2} \ p_{N_2} \ \omega_{cp} \ p_{sm}]^T,$$

where p_{O_2} and p_{N_2} represent the oxygen partial pressure and the nitrogen partial pressure, respectively. The compressor speed is denoted by ω_{cp} and the supply manifold pressure by p_{sm} . The control input u is the motor current, whereas the fuel cell stack current ζ is considered as measurable input disturbance. The compressor air flow is denoted by W_{cp} and it is proportional to the compressor speed. The parameters c_i are considered as uncertain constants. These parameters represent the variation/uncertainty of the system's

physical parameters, as given in Table 2.1:

$$\begin{aligned}
c_1 &= c_{01} + \delta c_1, & c_2 &= c_{02} + \delta c_2, \\
c_3 &= c_{03} + \delta c_3, & c_6 &= c_{06} + \delta c_6, \\
c_7 &= c_{07} + \delta c_7, & c_8 &= c_{08} + \delta c_8, \\
c_9 &= c_{09} + \delta c_9, & c_{10} &= c_{010} + \delta c_{10}, \\
c_{13} &= c_{013} + \delta c_{13}, & c_{14} &= c_{014} + \delta c_{14}, \\
c_{19} &= c_{019} + \delta c_{19}, & c_{17} &= c_{017} + \delta c_{17},
\end{aligned} \tag{2.15}$$

where c_{0i} and δc_i are the nominal value and the uncertainty of c_i , respectively. Complete details and physical significance of these parameters can be found in [63].

TABLE 2.1: *Variations of system parameters*

Parameter	Variation
Fuel cell temperature (T_{fc})	+10% in $^{\circ}\text{C}$
Cathode volume (V_{ca})	+5%
Supply manifold volume (V_{sm})	−10%
Atmospheric temperature (T_{atm})	+10% in $^{\circ}\text{C}$
Cathode inlet orifice constant ($k_{ca,in}$)	+5%
Cathode outlet orifice constant ($k_{ca,out}$)	+5%

2.3.2 Control Objective

The oxygen excess ratio can be written as [63].

$$\lambda_{O_2} = \frac{c_{19}}{c_{20}\zeta} (x_4 - x_1 - x_2 - c_2). \tag{2.16}$$

The net electrical power is optimized by reducing the consumption of the compressor, i.e. maintaining the oxygen excess ratio λ_{O_2} at its optimal value $\lambda_{O_2,ref}$. Depending upon the stack current, this optimal value exists between 2 and 2.5 [75]. Conventionally, $\lambda_{O_2,ref}$ has been taken as a fixed value [48, 75]. A more precise method has been presented in [63], where $\lambda_{O_2,ref}$ has been modeled as a function of the stack current:

$$\lambda_{O_2,ref} = 5 \times 10^{-8} \zeta^3 - 2.87 \times 10^{-5} \zeta^2 + 2.23 \times 10^{-3} \zeta + 2.5. \tag{2.17}$$

Our objective is to force λ_{O_2} to follow $\lambda_{O_2,ref}$ in finite time.

2.3.3 Test Bench Description

The experiments have been conducted on a Hardware-In-Loop (HIL) test bench (See Fig. 2.1), the HIL simulator structure can be seen in Fig.2.2. It consists of a twin screw compressor and a real time fuel cell emulation system. The twin screw compressor is driven by a permanent magnet synchronous motor (PMSM). The 3-phase currents of PMSM are calculated from dq coordinates and supplied by an inverter. The control input Iq , for the inverter, is generated by the proposed controllers installed in a real time controller. The measured compressor air flow W_{cp} is fed to the real time fuel cell emulation system. The PEMFC emulator receives the flow rate W_{cp} , in order to generate the states x_1 , x_2 , x_4 and λ_{O_2} .

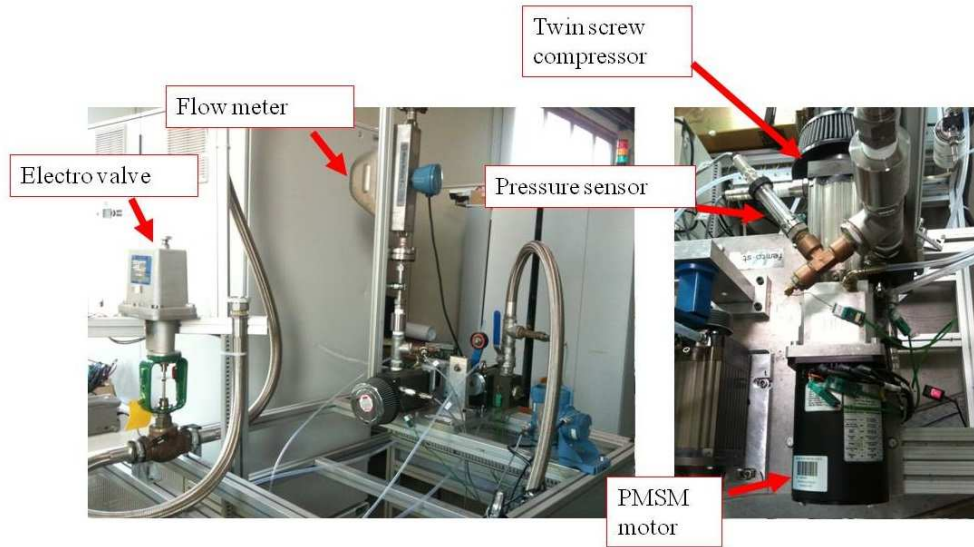
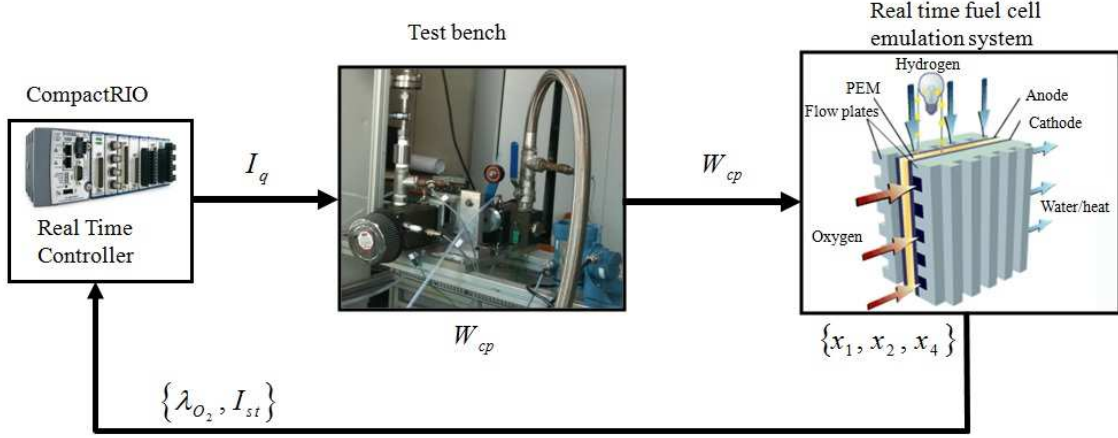


Figure 2.1. Test bench

Figure 2.2. *HIL Simulator*

2.3.4 Controller design and Experimental Results

The sliding variable is defined as $z_1 = s = \lambda_{O_2} - \lambda_{O_2,ref}$. In our case, the sliding variable s depends on x_1 , x_2 and x_4 . The first and second time derivative of s are

$$\begin{aligned} \dot{s} = z_2 &= \frac{\partial}{\partial x_1} s(x_1, x_2, x_4) \cdot \dot{x}_1(x_1, x_2, x_4) + \frac{\partial}{\partial x_2} s(x_1, x_2, x_4) \cdot \dot{x}_2(x_1, x_2, x_4) \\ &\quad + \frac{\partial}{\partial x_4} s(x_1, x_2, x_4) \cdot \dot{x}_4(x_1, x_2, x_3, x_4), \\ \ddot{s} = z_3 &= \frac{\partial}{\partial x_1} \dot{s}(x_1, x_2, x_3, x_4) \cdot \dot{x}_1(x_1, x_2, x_4) + \frac{\partial}{\partial x_2} \dot{s}(x_1, x_2, x_4) \cdot \dot{x}_2(x_1, x_2, x_4) \\ &\quad + \frac{\partial}{\partial x_3} \dot{s}(x_1, x_2, x_3, x_4) \cdot \dot{x}_3(x_3, x_4, u) + \frac{\partial}{\partial x_4} \dot{s}(x_1, x_2, x_3, x_4) \cdot \dot{x}_4(x_1, x_2, x_3, x_4), \\ &= \varphi + \gamma u. \end{aligned}$$

where φ and γ are given in [63] (See Equation (54) of [63], where φ and γ are denoted by ϕ_1 and γ_1 , respectively).

The control input u appears for the first time, in the second time derivative of s . In order to obtain a continuous control u , the discontinuous control is applied on the higher derivative \dot{u} . We get

$$s^{(3)} = \dot{z}_3 = \underbrace{\dot{\varphi} + \dot{\gamma}u}_{\Phi} + \gamma \dot{u},$$

where $v = \dot{u}$, Φ and γ are uncertain bounded functions that satisfy

$$\Phi \in [-\bar{\varphi}, \bar{\varphi}], \quad \gamma \in [\gamma_m, \gamma_M] \quad (2.18)$$

For the PEMFC under consideration, the bounding values of the parameters were determined through precise physical analyses, as presented as percentage deviations in Table I. The following numerical values of the uncertainty limits were obtained:

$$\bar{\varphi} = 0.03, \quad \gamma_m = 5, \quad \gamma_M = 15.$$

From here, the control objective becomes equivalent to forcing s and its first and second time derivatives to zero in finite time, through

$$s^{(3)} \in [-\bar{\varphi}, \bar{\varphi}] + [\gamma_m, \gamma_M]v. \quad (2.19)$$

We first develop a 3^{rd} -order SMC robust controller using Equations (2.2) and (2.6). According to Theorem 2, the controller takes the following structure:

$$\begin{aligned} v_1 &= -l_1 |s|^{\alpha_1}, \\ v_2 &= -l_2 [|s|^{\beta_1} - |v_1|^{\beta_1}]^{\alpha_2/\beta_1}, \\ v_3 &= -l_3 [|s|^{\beta_2} - |v_2|^{\beta_2}]^{\alpha_3/\beta_2}, \\ v &= \dot{u} = \frac{1}{\gamma_m} (v_3 + \bar{\varphi} \text{sign}(v_3)). \end{aligned} \quad (2.20)$$

In this test, the parameters have been tuned to the following values: $l_1 = 5$, $l_2 = 10$, $l_3 = 40$, $\beta_0 = 0.8$, $\beta_1 = 1.25$, $\beta_2 = 2$, $\alpha_1 = 4/5$, $\alpha_2 = 3/4$, $\alpha_3 = 2/3$, $\gamma_m = 5$, $\bar{\varphi} = 0.03$.

During the tests, the stack current was varied between 150A and 400A, in steps. The current profile is shown in Fig. 2.3. The performance of the controller in response to the variation in the λ_{O_2} due to these stack current variations, is shown in Fig.2.4. It is clear that λ_{O_2} tracks the desired value $\lambda_{O_{2,ref}}$ successfully, with a response time between 3 and 7 seconds practically. The control input (I_q) is shown in Fig.2.5, which varies between 0 and 3 A. As the controller establishes third order HOSM, it can be seen that the oscillations in I_q are negligible.

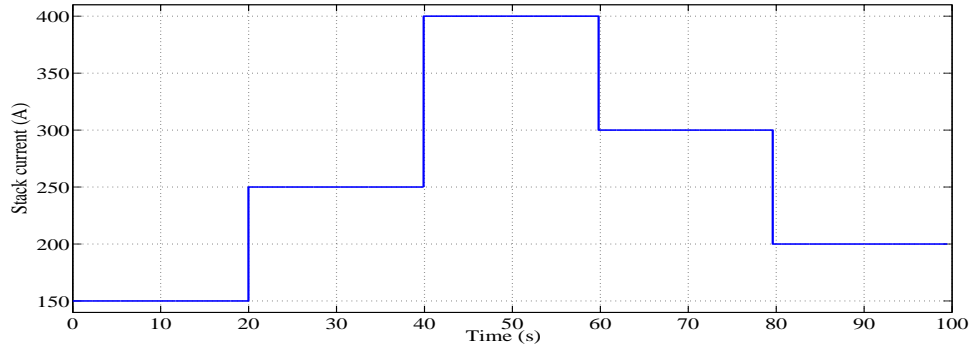


Figure 2.3. Stack current (A)

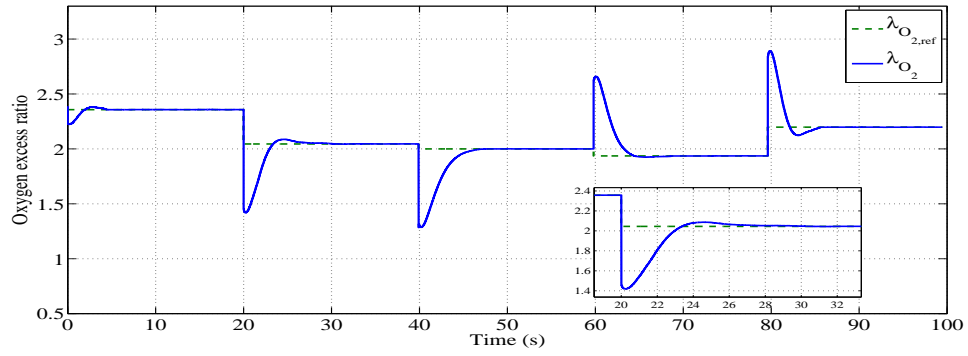


Figure 2.4. λ_{O_2} and $\lambda_{O_{2,ref}}$ versus time (s)

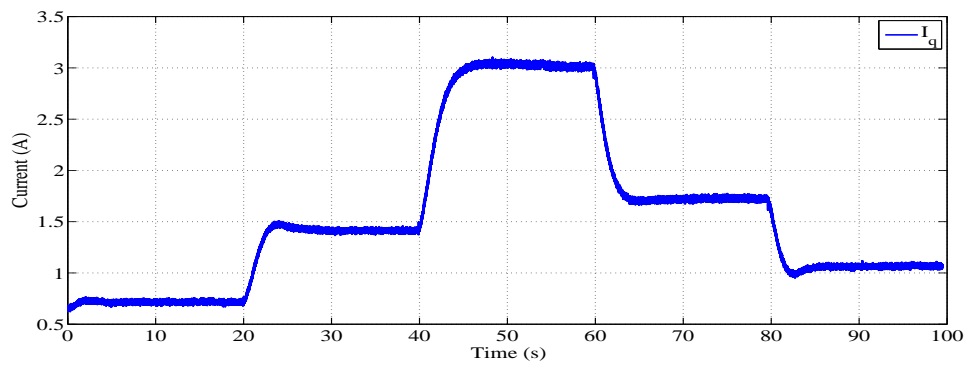


Figure 2.5. Quadratic current I_q versus time (s)

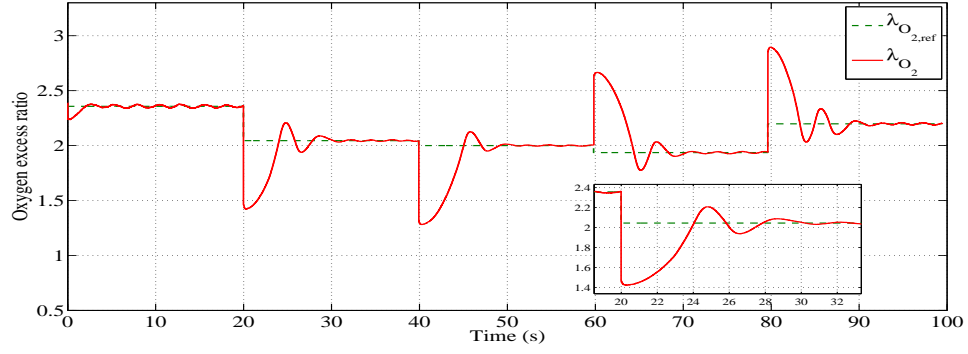


Figure 2.6. λ_{O_2} and $\lambda_{O_{2,ref}}$ versus time (s)

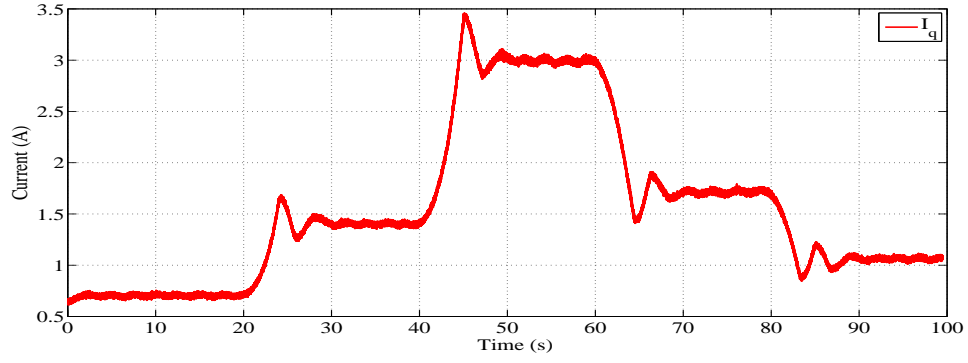


Figure 2.7. Quadratic current I_q versus time (s)

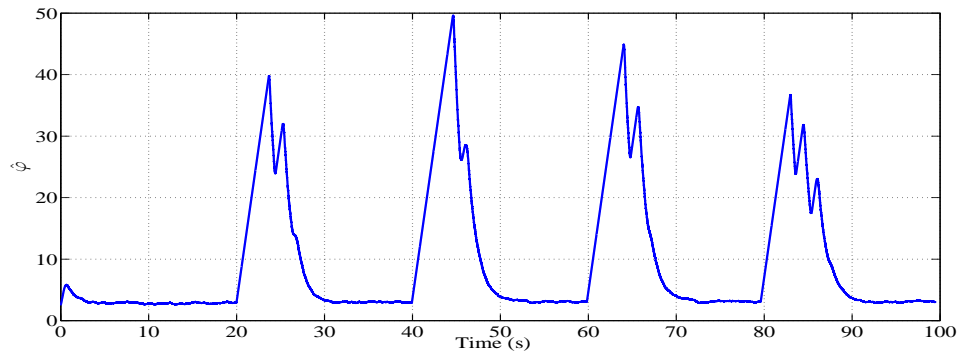


Figure 2.8. $\hat{\phi}$ versus time (s)

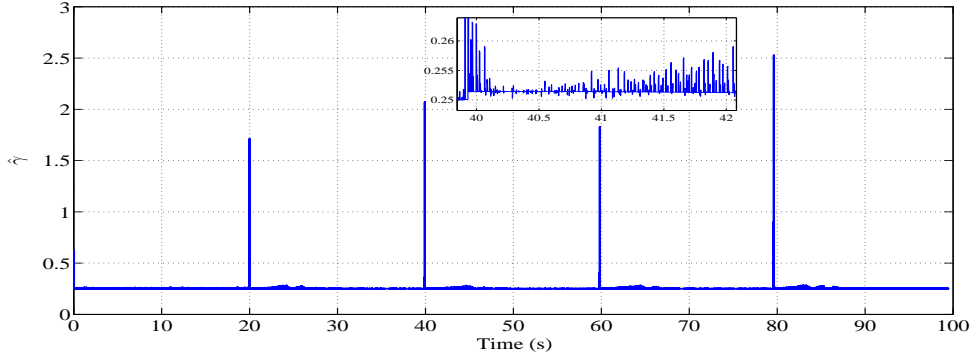


Figure 2.9. $\hat{\gamma}$ versus time (s)

While the uncertainty bounds $(\gamma_m, \bar{\varphi})$ of the system under consideration are known, they are very hard to estimate in many cases of fuel cell systems. We will now demonstrate that the proposed adaptive controller can be applied to overcome this problem. The 3rd-order SMC adaptive controller is designed using Equations (2.9) and (2.6), under the assumption that the system parameters are unknown. According to Theorem 3, the controller has the following structure:

$$v = \dot{u} = \hat{\gamma} v_3 + \hat{\varphi} \text{sign}(v_3), \quad (2.21)$$

where v_3 is the same as in Equation (2.20). The controller parameters used in adaptive case are as follows: $l_1 = 5$, $l_2 = 10$, $l_3 = 40$, $\beta_0 = 0.8$, $\beta_1 = 1.25$, $\beta_2 = 2$, $\alpha_1 = 4/5$, $\alpha_2 = 3/4$, $\alpha_3 = 2/3$, $k = 5$, $\eta = 0.95$, $\varepsilon = 0.001$, $\kappa = 0.25$, $\delta = 0.001$.

The results of the adaptive controller are shown in Figures 2.6, 2.7, 2.8 and 2.9. Fig.2.6 shows that λ_{O_2} converges and remains inside a small and acceptable neighborhood around the desired value $\lambda_{O_2,ref}$. The control input, I_q is shown in Fig.2.7 and the behaviors of the adaptive parameters $\hat{\varphi}$ and $\hat{\gamma}$ are shown in Figures 2.8 and 2.9 respectively. It can be seen that $\hat{\varphi}$ increases at each stack current step, and then decreases rapidly after the convergence of the tracking error. As real sliding mode is achieved, small oscillations can be seen in $\hat{\gamma}$. In general, these results show the effectiveness of both the robust and adaptive controllers for a wide range of stack current variation, i.e. external perturbation.

In order to validate the robustness of our controllers in dealing with parametric uncertainty, another series of experiments was conducted using the designed controllers (with

the same controller parameters). The parameters of the PEMFC emulator were varied to their extreme values, as specified in Table I. The results of the robust controller in these tests are shown in Figures 2.10 and 2.11. It can be seen that this controller performs as well as in the previous tests with defined system parameter values. The results of the adaptive controller are shown in Figures 2.12, 2.13, 2.14 and 2.15. We see again, in Fig. 2.12 a similar behavior of tracking error as compared to the previous tests. However, the static value of the quadratic current Fig. (2.13) changes in order to accommodate the emulated parametric drift. The adaptive gains $\hat{\phi}$ and $\hat{\gamma}$ adapt to counteract the uncertainty, ensuring convergence. These tests demonstrate that both the robust and adaptive controllers are capable of handling parametric uncertainty, albeit with different mechanisms.

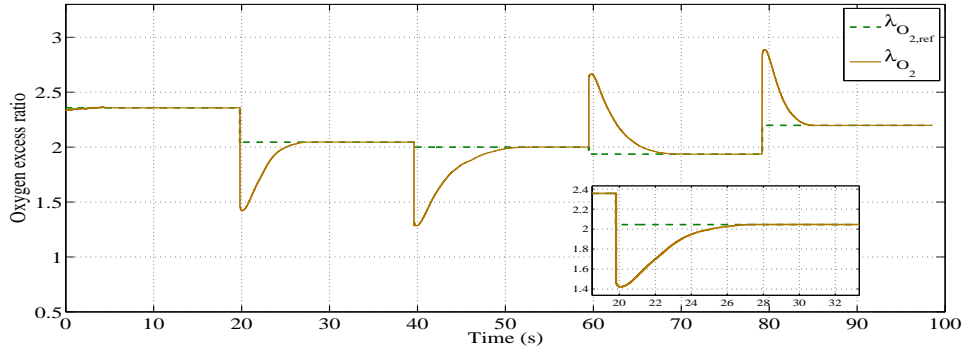


Figure 2.10. λ_{O_2} and $\lambda_{O_{2,ref}}$ versus time (s)

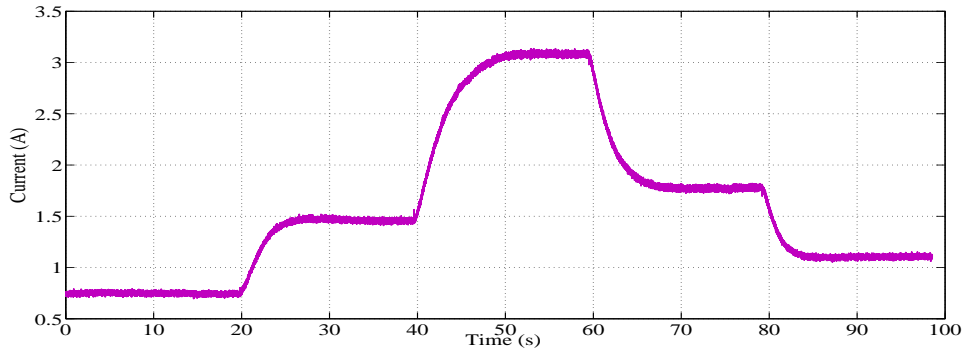


Figure 2.11. Quadratic current I_q versus time (s)

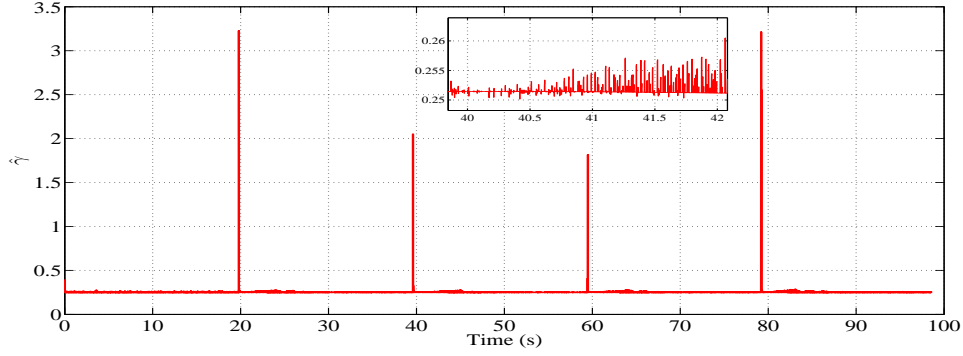


Figure 2.15. $\hat{\gamma}$ versus time (s)

2.4 Summary

In this chapter, we have presented two arbitrary HOSM controllers for uncertain nonlinear systems with bounded uncertainty, as represented by System (1.15). The control design is based on a class of controllers for stabilization of pure integrator chains. The first controller is robust and its design requires the knowledge of the bounds or limits of system uncertainty. The second controller is adaptive, therefore its design does not require any quantitative knowledge of the uncertainty bounds. The latter establishes real HOSM i.e. forces the states to remain within a region around the origin that depends upon the uncertainty bounds. It can be noted that convergence of states to a defined neighborhood, such that they remain inside it, is still an open problem in adaptive control theory.

The effectiveness and practical applicability of the proposed controllers were evaluated through simulations and experiments. These controllers showed good performance in simulations, as well as in experiments concerning a practical control problem of a PEMFC air-feed system. However, the fact that these controllers are unbounded may raise concerns in certain practical applications. In the next chapter, we will see that certain interesting properties, including bounded control input, can be achieved by manipulating the degree of homogeneity of the controllers.

Chapter 3

Lyapunov-Based Homogeneous HOSM Controller

3.1 Introduction and motivation

In the previous chapter, two Lyapunov-based arbitrary HOSM controllers were developed for the control of uncertain nonlinear systems, and their performance was evaluated through simulations and experiments. The class of controllers is studied in detail in this chapter, and a universal homogenous controller is developed through modification of Hong's algorithm [39]. It is shown that for a particular choice of the degree of homogeneity, Levant's universal controller [55] becomes a particular case of our controller. Furthermore, the influence of controlling the degree of homogeneity of the controllers is also studied, in order to identify additional properties that may result in better performance of our controllers. Namely, the homogeneity degree can be manipulated or controlled to bound the control input, to minimize the amplitude of discontinuous control after convergence and to obtain a fixed-time control. In order to elucidate this point, let us consider the following one-dimensional differential equation:

$$\dot{z} = \omega(z) = -c [z]^\alpha, \quad (3.1)$$

where $\alpha \geq 0$, $c > 0$ and $[z]^\alpha := |z|^\alpha \text{sign}(z)$. The term $\text{sign}(z)$ is a multi-valued function, equal to $z/|z|$ if $z \neq 0$ and $[-1, 1]$ if $z = 0$. The degree of homogeneity of Equation (3.1) is $\kappa = \alpha - 1$ and this system is stable for all $c > 0$ and $\alpha \geq 0$. Depending upon the value of α , different characteristics can be obtained in the system:

$\alpha = 0$: the convergence to zero occurs in finite-time. The controller $\omega(z)$ is uniformly bounded for $z \in \mathbb{R}$ but discontinuous at $z = 0$;

$0 < \alpha < 1$: the convergence to zero occurs in finite-time. The controller $\omega(z)$ is unbounded and tends to zero as $|z| \rightarrow 0$;

$\alpha > 1$: the convergence to zero is asymptotic, however the convergence time to the sphere $\mathbf{B}(0, 1) = \{z \in \mathbb{R} : \|z\| < 1\}$ is uniformly bounded by a constant. The controller $\omega(z)$ is unbounded.

Based on these observations, we can construct controllers forcing z to converge to zero in finite-time by changing α :

an unbounded controller obtained by changing κ from $\kappa_1 > 0$ to $\kappa_2 < 0$ when z reaches the sphere $\mathbf{B}(0, 1)$. This ensures the convergence to zero in finite-time, bounded by a constant.

a uniformly bounded controller whose amplitude tends to zero as z converges to zero. This controller is obtained by changing the homogeneity degree from $\kappa_1 = -1$ to $-1 < \kappa_2 < 0$.

The second point is of particular importance as bounded controllers are more practical in real life cases than unbounded ones. In the case of a perturbed integrator, (3.1) is replaced by the following differential inclusion:

$$\dot{z} \in u(z) [\gamma_m, \gamma_M] + [-\bar{\varphi}, +\bar{\varphi}], \quad (3.2)$$

where $\gamma_m \leq \gamma_M$ and $\bar{\varphi}$ are arbitrary positive constants. This is similar to System (1.21) for a single integrator. In the previous chapter, it was demonstrated that the controller

$$u(z) = \frac{1}{\gamma_m} (\omega(z) + \bar{\varphi} \text{sign}(\omega(z))),$$

defined for $0 < \alpha < 1$, forces z to converge to zero in finite-time, and thereby establishes HOSM with respect to s for System (1.15). According to the standard comparison principle [46] the rate of convergence of (3.2) is faster than (3.1). It can be noted that the controller is valid for $0 \leq \alpha \leq 2$.

3.1.1 Contribution

In this chapter, these observations (related to homogeneous controllers for a single integrator) are extended to the arbitrary sliding mode controllers developed in the previous chapter. The main focus is to obtain various properties in the controller by changing the degree of homogeneity. In this regard, a modified form of Hong's homogeneous controller [39] is developed, which satisfies the conditions of Theorem 2.1.2 in Chapter 2. A universal homogeneous HOSMC controller is developed using this modified form, and the effect of switching its homogeneity degree is studied. This yields three important results:

1. With a particular choice of homogeneity degree, Levant's well known homogeneous robust arbitrary HOSM controller [55] is a particular case of our modified controller
2. The amplitude of discontinuous control can be kept to its minimum possible value after the states have converged, by controlling the homogeneity degree in the neighborhood of zero
3. The recently developed "Fixed-Time" stability notion can be achieved by changing the homogeneity degree.

3.2 Controller design

Based on the problem formulation introduced in Chapter 1, the homogeneous controller is developed in two steps. In the first step, the modified form of Hong's controller [39] for stabilization of a pure integrator chain is considered. Then, using this modified controller and the results of Chapter 2, a universal HOSM controller is developed for System (1.15).

3.2.1 Useful definitions, lemmas and theorems

Let us first establish some definitions, which would aid in the statement of our results. Consider the differential system

$$\dot{z} = f(t, z), \quad z \in \mathbb{R}^r. \quad (3.3)$$

Definition 3.2.1. [74, 7] *The equilibrium point $z = 0$ of System (3.3) is said to be locally **finite-time** stable in a neighborhood $\hat{U} \subset \mathbb{R}^r$ if (i) it is asymptotically stable in \hat{U} ; (ii) it is finite-time convergent in \hat{U} , i.e. for any initial condition z_0 , $z(t, z_0) = 0, \forall t \geq T(z_0)$, where $T(z_0)$ is called the settling-time function. The equilibrium point $z = 0$ is globally finite-time*

stable if $\hat{U} = \mathbb{R}^r$. The equilibrium point is **fixed-time** stable if (i) it is globally finite-time stable; (ii) the settling-time function is bounded by a constant T_{max} , i.e. $\exists T_{max} > 0 : \forall z_0 \in \mathbb{R}^r, T(z_0) \leq T_{max}$.

Definition 3.2.2. [74] The set S is said to be globally **finite-time** attractive for (3.3), if for any initial condition z_0 , the trajectory $z(t, z_0)$ of (3.3), achieves S in finite-time $T(z_0)$. Moreover, the set S is said to be **fixed-time** attractive for (3.3), if (i) it is globally finite-time stable; (ii) the settling-time function is bounded by a constant T_{max} .

Let us recall the following theorem:

Theorem 3.2.3. [8, 7] Suppose there exists a positive definite C^1 function V defined on a neighborhood $\hat{U} \subset \mathbb{R}^r$ of the equilibrium point $z = 0$ and real numbers $C > 0$ and $\alpha \geq 0$, such that the following condition is true for every trajectory z of System (3.3),

$$\dot{V} + CV^\alpha(z(t)) \leq 0, \text{ if } z(t) \in \hat{U}, \quad (3.4)$$

where \dot{V} is the time derivative of $V(z(t))$.

Then all trajectories of System (3.3) which stay in \hat{U} converge to zero. If $\hat{U} = \mathbb{R}^r$ and V is radially unbounded, then System (3.3) is globally stable with respect to the equilibrium point $z = 0$.

Depending on the value α , we have different types of convergence: if $0 \leq \alpha < 1$, the equilibrium point $z = 0$ is finite-time stable ([7]), if $\alpha = 1$, it is exponentially stable and if $\alpha > 1$ the equilibrium point $z = 0$ is asymptotically stable equilibrium and, for every $\epsilon > 0$, the set $\mathbf{B}(0, \epsilon) = \{z \in \hat{U} : V(z) < \epsilon\}$ is fixed-time attractive.

Let us now present some further notions related to the concept of homogeneity, which was introduced in Chapter 1. Consider the time-invariant differential system

$$\dot{z} = f(z), \quad z \in \mathbb{R}^r. \quad (3.5)$$

Definition 3.2.4. [39] A function $\Omega(z)$ is homogeneous of degree $a \in \mathbb{R}^{+*}$ with respect to the family of dilation ζ_ϵ^p if, for every $z \in \mathbb{R}^r$ and $\epsilon > 0$,

$$\Omega(\epsilon^{p_1} z_1, \dots, \epsilon^{p_r} z_r) = \epsilon^a \Omega(z_1, \dots, z_r).$$

Definition 3.2.5. The homogeneous norm $\Gamma_i(z)$ for $z \in \mathbb{R}^i$ is defined by

$$\Gamma_i(z) \equiv \Gamma_i(z_1, \dots, z_i) = \left(\sum_{j=1}^i |z_j|^{c/p_j} \right)^{1/c},$$

$$c \geq \max(p_1, \dots, p_r) > 0,$$

where $\Gamma_i(\epsilon^{p_1} z_1, \dots, \epsilon^{p_i} z_i) = \epsilon \Gamma_i(z_1, \dots, z_i)$, $\epsilon > 0$.

In this case, the unit sphere S_i is given by

$$S_i = \{z \in \mathbb{R}^i : \Gamma_i(z) = 1\}.$$

Lemma 3.2.6 (Lemma 4.2 of [8]). *Suppose Ω_1 and Ω_2 are continuous real-valued functions on \mathbb{R}^r , homogeneous with respect to ζ_ϵ^p of degrees $d_1 > 0$ and $d_2 > 0$, respectively, and Ω_1 is positive definite. Then, for every $z \in \mathbb{R}^r$,*

$$\left[\min_{\{z: \Omega_1(z)=1\}} \right] [\Omega_1(z)]^{\frac{d_2}{d_1}} \leq \Omega_2(z) \leq \left[\max_{\{z: \Omega_1(z)=1\}} \right] [\Omega_1(z)]^{\frac{d_2}{d_1}}. \quad (3.6)$$

Proposition 3.2.7 (Proposition 1 of [77]). *Let Ω be a positive definite C^1 function, homogeneous of degree a with respect to ζ_ϵ^p . Then, for all $i = 1, \dots, r$; $\frac{\partial \Omega}{\partial z_i}$ is homogeneous of degree $(a - p_i)$.*

3.2.2 Stabilization of a pure chain of integrator

Consider the following pure integrator chain:

$$\begin{cases} \dot{z}_i &= z_{i+1}, \quad i = 1, \dots, r-1, \\ \dot{z}_r &= u. \end{cases} \quad (3.7)$$

The following result guarantees the stabilization of (3.7).

Theorem 3.2.8. *Let r be the order of the pure integrator chain given in (3.7). For $\kappa \in [-1/r, 1/r]$, set*

$$p_i = 1 + (i-1)\kappa, \quad i = 1, \dots, r,$$

and finally let c be a positive constant such that $c \geq \max(p_1, \dots, p_r)$. Then there exist constants $l_i > 0$, $i = 1, \dots, r$, independent on κ , such that the feedback control law $u = \omega_\kappa(z) := v_r$ defined inductively by

$$\begin{cases} v_0 &= 0, \\ v_i &= -l_i N_i \text{sign}(z_i - v_{i-1}), \\ &i = 1, \dots, r, \end{cases} \quad (3.8)$$

stabilizes System (3.7), where $N_i, i = 1, \dots, r$ are defined by

$$N_i = \left(\sum_{j=1}^i |z_j|^{c/p_j} \right)^{\frac{p_i + \kappa}{c}}. \quad (3.9)$$

There also exists a homogeneous Lyapunov function $V_\kappa(z)$ for the closed-loop system (3.7) under u , that satisfies $\dot{V}_\kappa \leq -C V_\kappa^{\frac{c+1+\kappa}{c+1}}$, for some positive constant C .

Proof. For $1 \leq i \leq r$, we define

$$\begin{aligned} w_i &:= \left(\sum_{j=1}^i |z_j|^{c/p_j} \right) \text{sign}(z_i - v_{i-1}), \\ W_i &:= \int_{v_{i-1}(z_1, \dots, z_{i-1})}^{z_i} w_i(z_1, \dots, z_{i-1}, s) ds, \\ &= \left(|z_1|^{\frac{c}{p_1}} + \dots + |z_{i-1}|^{\frac{c}{p_{i-1}}} \right) |z_i - v_{i-1}| + \frac{\left| \lfloor z_i \rfloor^{\frac{c}{p_i}+1} - \lfloor v_{i-1} \rfloor^{\frac{c}{p_i}+1} \right|}{\frac{c}{p_i} + 1}. \end{aligned} \quad (3.10)$$

It can be seen that W_i is positive definite function with respect to $v_{i-1} - z_i$, homogeneous with respect to ξ_ϵ^p of degree $(c + p_i)$. We introduce $\bar{W}_i := W_i^{\delta_i}$, where $\delta_i = \frac{c+1}{c+p_i}$, so that all functions \bar{W}_i are homogeneous of the same homogeneity degree $(c+1)$.

Lemma 3.2.9. *With the notations above and $1 \leq i \leq r$, there exist positive constants k_i , such that:*

$$\bar{W}_i \leq k_i |w_i|^{\frac{c+1}{c}}. \quad (3.11)$$

Proof. We can get that $\left(\sum_{j=1}^i |z_j|^{c/p_j} \right)$ is a homogeneous function with respect to ξ_ϵ^p of degree c . Then according to Lemma 3.2.6, and for a given κ , there exists a constant K_i depending on κ , such that

$$\bar{W}_i \leq K_i(\kappa) \left(\sum_{j=1}^i |z_j|^{c/p_j} \right),$$

where $K_i(\kappa) = \max_{z \in S_i} \bar{W}_i$. Then, the choice of k_i , as $k_i = \max_{\kappa \in [-1/r, 1/r]} K_i(\kappa)$, implies (3.11). \square

We proceed to prove the theorem by induction on r .

Step 1: Consider $\dot{z}_1 = u$. For any $l_1 > 0$, taking $u = \omega_\kappa(z_1) = -l_1 \lfloor z_1 \rfloor^{(p_1+\kappa)/p_1}$ stabilizes the closed-loop system. The Lyapunov function $V_1 = W_1 = |z_1|^{1+c}/(1+c)$ is homogeneous of degree $c+1$ and

$$\dot{V}_1 = -l_1 |z_1|^{c+p_2} \leq -\eta_1 V_1^{\frac{c+1+\kappa}{c+1}}, \quad (3.12)$$

for some constant $\eta_1 > 0$.

Step i: Assume that the conclusion holds true till $i-1$. Define the Lyapunov function V_i by $V_i = V_{i-1} + \bar{W}_i = \sum_{j=1}^i \bar{W}_j$. We get

$$\begin{aligned}
\dot{V}_i &= \sum_{j=1}^{i-1} \frac{\partial \bar{W}_i}{\partial z_j} z_{i+1} + w_i v_i W_i^{\frac{-(i-1)\kappa}{c+p_i}} + \dot{V}_{i-1} + \frac{\partial V_{i-1}}{\partial z_{i-1}} (z_i - v_{i-1}), \\
&= \sum_{j=1}^{i-1} \frac{\partial \bar{W}_i}{\partial z_j} z_{i+1} - l_i |w_i|^{\frac{c+p_i+\kappa}{c}} \bar{W}_i^{\frac{-\kappa(i-1)}{c+p_i}} + \dot{V}_{i-1} + \frac{\partial V_{i-1}}{\partial z_{i-1}} (z_i - v_{i-1}), \\
&\leq \sum_{j=1}^{i-1} \frac{\partial \bar{W}_i}{\partial z_j} z_{i+1} - l_i \frac{\bar{W}_i^{\frac{c+p_i+\kappa}{c+p_i}}}{k_i^{\frac{c}{c+p_i}}} \bar{W}_i^{\frac{-\kappa(i-1)}{c+p_i}} + \dot{V}_{i-1} + \frac{\partial V_{i-1}}{\partial z_{i-1}} (z_i - v_{i-1}), \\
&\leq \sum_{j=1}^{i-1} \frac{\partial \bar{W}_i}{\partial z_j} z_{i+1} - \frac{l_i}{k_i^{\frac{c}{c+p_i}}} \bar{W}_i^{\frac{c+p_2}{c+p_i}} + \dot{V}_{i-1} + \frac{\partial V_{i-1}}{\partial z_{i-1}} (z_i - v_{i-1}).
\end{aligned} \tag{3.13}$$

The fact that \bar{W}_i are homogeneous with respect to ζ_ϵ^p of degree $(c+1)$ for each $i = 1, \dots, r$, implies that V_i are homogeneous of degree $(c+1)$ with respect to ζ_ϵ^p as well. In addition, according to Proposition 3.2.7, \dot{V}_i are homogeneous of degree $(c+1-\kappa)$ with respect to ζ_ϵ^p . Then without loss of generality, the study can be restricted to the unit sphere S_i .

By taking l_i such that

$$l_i > 2k_i^{\frac{c}{c+1}} \max_{z \in S_i} \left\{ \sum_{j=1}^{i-1} \frac{\partial \bar{W}_i}{\partial z_j} z_{i+1} + \frac{\partial V_{i-1}}{\partial z_{i-1}} (z_i - v_{i-1}) \right\}, \forall \kappa \in [-1/r, 1/r], \tag{3.14}$$

and setting $\eta_i := l_i / 2k_i^{\frac{c}{c+1}}$, we get

$$\dot{V}_i \leq - \sum_{j=1}^i \eta_j \bar{W}_j^{\frac{c+1+\kappa}{c+1}}. \tag{3.15}$$

At the final step, all parameters l_i are determined, with $V_\kappa(z) = V_r = \sum_{j=1}^r \bar{W}_j$ and

$$\dot{V}_\kappa(z) \leq - \sum_{j=1}^i \eta_j \bar{W}_j^{\frac{c+1+\kappa}{c+1}} \leq -\eta \sum_{j=1}^i \bar{W}_j^{\frac{c+1+\kappa}{c+1}},$$

where $\eta := \min \eta_i$ for $i = 1, \dots, r$.

According to Lemma 3.2.6, for all $\kappa \in [-1/r, 1/r]$, we get

$$\sum_{j=1}^i \bar{W}_j^{\frac{c+1+\kappa}{c+1}} \geq 2^{\frac{r-1}{r(c+1)}} \left(\sum_{j=1}^i \bar{W}_j \right)^{\frac{c+1+\kappa}{c+1}},$$

which can be seen as a generalization of Jensen's inequality.

Finally we get $\dot{V}_\kappa \leq -C V_\kappa^{(c+1+\kappa)/(c+1)}$, with $C \geq \eta 2^{\frac{r-1}{r(c+1)}}$.

□

3.2.3 Stabilization of an r -perturbed integrator chain

From the result obtained in Theorem 3.2.8, we now proceed to the stabilization of the perturbed integrator chain presented in System (1.21). The extension of Theorem 3.2.8 to the case of System (1.21) is based on the following result of [38].

Theorem 3.2.10. [38] *Let $\omega(z)$ and $V(z)$ be respectively, a state-feedback control law stabilizing System (3.7) and a Lyapunov function for the closed-loop system, which satisfy the hypotheses of Theorem 3.2.3 and obey the following additional conditions: for every $z \in \hat{U}$,*

$$\frac{\partial V}{\partial z_r}(z)\omega(z) \leq 0, \quad \omega(z) = 0 \Rightarrow \frac{\partial V}{\partial z_r}(z) = 0.$$

Then, for arbitrary constants $m, n \geq 1$, the following control law stabilizes System (1.21):

$$u(z) = \frac{m}{\gamma_m}(\omega(z) + n\bar{\varphi} \text{sign}(\omega(z))). \quad (3.16)$$

The function $V(z)$ remains a Lyapunov function for the closed-loop system (1.21) with the feedback $u(z)$, and satisfies Condition (3.4). If $\hat{U} = \mathbb{R}^r$ and $V(z)$ is radially unbounded, then the closed-loop system (1.21) with the feedback $u(z)$ is globally stable with respect to the origin.

Proof. This theorem is a generalization of Theorem 2.1.2, presented in previous Chapter, and can be proven in the same way. \square

It can be shown that the controller presented in Theorem 3.2.8 satisfies the conditions presented in Theorem 3.2.10. We calculate $\frac{\partial V_\kappa}{\partial z_r}\omega_\kappa = \frac{\partial \bar{W}_r}{\partial z_r}v_r \leq -\frac{l_r}{k_r^{\frac{c}{c+1}}}\bar{W}_r^{\frac{c+1+\kappa}{c+1}} \leq 0$, and

$$\omega_\kappa = 0 \Rightarrow -l_r |w_r|^{\frac{pr+\kappa}{c}} \text{sign}(z_r - v_{r-1}) = 0 \Rightarrow \frac{\partial V_\kappa}{\partial z_r} \equiv \frac{\partial \bar{W}_r}{\partial z_r} = 0.$$

Remark 3.2.11. *It should be noted that this controller is not unique, and all homogeneous controllers satisfying the conditions of Theorem 3.2.10 are valid (e.g. [39]).*

As indicated in Section 2 of [57], in order to stabilize the uncertain System (1.21) by a state-feedback controller $u = u(z)$, it is necessary that the controller be discontinuous at $z = 0$, and satisfy

$$\lim_{\|z\| \rightarrow 0} |u(z)| \geq \frac{\bar{\varphi}}{\gamma_m} =: M_{\min}.$$

3.3 Discussion of Special Cases

In this section, we consider some specific choices of the homogeneity degree, in order to obtain further results. First, it is shown that for a particular choice of homogeneity degree, the homogeneous HOSM controller presented in [55] becomes a special case of our controller. Then, a bounded controller with minimum amplitude M_{min} of discontinuous control at $z = 0$ is designed. Finally, a controller with fixed-time convergence is synthesized.

3.3.1 Robust Homogeneous Arbitrary HOSM Controller

Let us consider the controller presented in [55].

Proposition 3.3.1. *Provided $l_1, \dots, l_{r-1}, M > 0$ are chosen sufficiently large in the listed order, the bounded controller $u = -M \text{sign}(\phi_{r-1})$ stabilizes System (1.21) in finite time, ensuring HOSM w.r.t. s for System (1.15), ϕ_{r-1} is defined inductively as*

$$\begin{aligned} N_1 &= |z_1|^{\frac{r-1}{r}}, \\ N_i &= \left(|z_1|^{\frac{d}{r}} + |z_2|^{\frac{d}{r-1}} + \dots + |z_i|^{\frac{d}{r-i+1}} \right)^{\frac{r-i}{d}}, \\ &\quad i = 2, \dots, r-1. \\ \phi_0 &= z_1, \\ \phi_i &= z_{i+1} + l_i N_i \text{sign}(\phi_{i-1}), \\ &\quad i = 2, \dots, r-1. \end{aligned} \tag{3.17}$$

with $d > r$ is an arbitrary positive constant.

Proof. Consider the functions N_i in Equation (3.9). Let us fix the parameters κ and c as follows $\kappa = -1/r$ and $c = d/r$. Then, defining $\phi_i = z_{i+1} - v_i$, we find:

$$\begin{aligned} N_1 &= |z_1|^{\frac{r-1}{r}}, \\ N_i &= \left(|z_1|^{\frac{d}{r}} + |z_2|^{\frac{d}{r-1}} + \dots + |z_i|^{\frac{d}{r-i+1}} \right)^{\frac{r-i}{d}}, \\ &\quad i = 2, \dots, r. \\ \phi_0 &= z_1, \\ \phi_i &= z_{i+1} + l_i N_i \text{sign}(\phi_{i-1}), \\ &\quad i = 2, \dots, r-1. \end{aligned} \tag{3.18}$$

According to Theorem 3.2.10 and by taking $m = n = 1$, the state-feedback control law for the stabilization of System (1.21) can be expressed as: $u = -(l_r N_r / K_m + \bar{\varphi} / K_m) \text{sign}(\phi_{r-1})$. It can be seen that this particular choice of parameter κ gives $N_r \equiv 1$, then for the positive

constant M defined by

$$M := \left(\frac{l_r}{\gamma_m} + \frac{\bar{\varphi}}{\gamma_m} \right),$$

the controller $u = -M \text{sign}(\phi_{r-1})$ stabilizes System (1.21) in finite time, ensuring HOSM w.r.t. s for System (1.15). \square

3.3.2 Homogeneous controller with minimum discontinuous control

The amplitude of discontinuous control, in the case of [55], is equal to $M = \left(\frac{l_r}{\gamma_m} + \frac{\bar{\varphi}}{\gamma_m} \right)$. We shall now see that this amplitude can be reduced to its minimum level M_{min} when the state z tends to zero, by changing the degree of homogeneity.

Proposition 3.3.2. *For $k \in (-1/r, 0)$ and $A > 0$ satisfying*

$$\max_{V_k(z) \leq A} |\omega_k(z)| \leq l_r, \quad (3.19)$$

we define the function

$$U_{k,A}(z) := \begin{cases} \omega_{-1/r}(z) & \text{if } V_k(z) > A, \\ \omega_k(z) & \text{if } V_k(z) \leq A. \end{cases}$$

Then the controller $u(z) := \frac{1}{\gamma_m} (U_{k,A}(z) + \bar{\varphi} \text{sign}(U_{k,A}(z)))$ stabilizes System (1.21) in finite time, ensuring HOSM w.r.t. s for System (1.15), and $u(z)$ is bounded with minimum amplitude of discontinuity M_{min} at $z = 0$.

Proof. Consider the following sets

$$\begin{aligned} \mathbf{S}_1 &= \{z \in \mathbb{R}^r : |\omega_k(z)| \leq l_r\}, \\ \mathbf{S}_2 &= \{z \in \mathbb{R}^r : V_k(z) \leq A\}. \end{aligned} \quad (3.20)$$

According to Condition (3.19), we have $\mathbf{S}_2 \subset \mathbf{S}_1$. As $\dot{V}_{-1/r}(z) < 0, \forall z \notin \mathbf{S}_2$, z will reach \mathbf{S}_1 and \mathbf{S}_2 successively in finite-time. Once $z \in \mathbf{S}_2$, $U_{k,A}(z)$ is equal to $\omega_k(z)$, with $|\omega_k(z)| \leq l_r$. Therefore, z will stay in \mathbf{S}_2 and converges to zero in finite-time, as $\dot{V}_k(z) < 0, \forall z \notin \mathbf{S}_1, \forall z \neq 0$. Eventhough the feedback is discontinuous, there is no chattering regime since the derivative of V_k is strictly negative in an open neighborhood of the level line $V_k(z) = A$, regardless of the value of the feedback. In consequence, the system trajectory crosses transversally the

level line $V_k(z) = A$.

Clearly $U_{k,A}(z)$ tends to zero as z tends to zero. As a result

$$\begin{aligned} \lim_{\|z\| \rightarrow 0} |u(z)| &= \frac{\bar{\varphi}}{\gamma_m} = M_{min}, \\ \forall z \in \mathbb{R}^r, |u(z)| &\leq M_{min} + \frac{l_r}{\gamma_m}. \end{aligned}$$

□

3.3.3 Fixed-time Homogeneous controller

In certain cases, it is required that the controller converges within a fixed interval of time, irrespective of its initial condition. This can also be achieved by changing the homogeneity degree.

Proposition 3.3.3. *For $k \in (-1/r, 0)$ and $B > 0$, define*

$$E := \min_{V_k(z)=B} V_{-k}(z) > 0, \quad (3.21)$$

and the function

$$U_{k,B}(z) = \begin{cases} \omega_{-k}(z) & \text{if } V_k(z) > B, \\ \omega_k(z) & \text{if } V_k(z) \leq B. \end{cases}$$

Then the controller $u(z) := \frac{1}{\gamma_m}(U_{k,B}(z) + \bar{\varphi} \text{sign}(U_{k,B}(z)))$ stabilizes System (1.21) in fixed-time $T \leq T_u + T_f$, ensuring HOSM w.r.t. s for System (1.15). The values of T_u and T_f are given by

$$T_u = \frac{E^{\frac{k}{c+1}}}{\frac{-k}{c+1}C}, \quad T_f = \frac{B^{\frac{-k}{c+1}}}{\frac{-k}{c+1}C}. \quad (3.22)$$

Proof. Note that there is no chattering regime for the same reason as in the previous proposition. The conclusion follows by integrating the differential equation $\dot{V} = -CV^\alpha$ on appropriate time intervals. Consider first the following sets

$$\begin{aligned} \mathbf{S}_1 &= \{z \in \mathbb{R}^r : V_{-k}(z) \leq E\}, \\ \mathbf{S}_2 &= \{z \in \mathbb{R}^r : V_k(z) \leq B\}. \end{aligned} \quad (3.23)$$

According to Condition (3.21), we get that $\mathbf{S}_1 \subset \mathbf{S}_2$. Clearly, z will reach \mathbf{S}_2 in a fixed-time, bounded by a constant T_u , calculated as follows:

$$\text{for } \alpha = 1 - \frac{k}{c+1}, \quad \int_E^{+\infty} \frac{dV}{V^\alpha} = -C \int_0^{T_u} dt, \text{ then } T_u = \frac{E^{\frac{k}{c+1}}}{\frac{-k}{c+1}C}.$$

When z reaches \mathbf{S}_2 , i.e. $V_k(z) = B$, z will converge to zero in a finite-time, bounded by T_f , calculated as follows:

$$\text{for } \alpha = 1 + \frac{k}{c+1}, \quad \int_B^0 \frac{dV}{V^\alpha} = -C \int_{T_u}^{T=T_u+T_f} dt, \text{ then } T_f = \frac{B^{\frac{-k}{c+1}}}{\frac{-k}{c+1}C}.$$

□

3.4 Simulation Results

In this section, we illustrate the performance of our proposed controllers using the following perturbed triple integrator defined by:

$$\dot{z}_1 = z_2, \quad \dot{z}_2 = z_3, \quad \dot{z}_3 = \varphi + \gamma u,$$

with $\varphi = \sin(t)$ and $\gamma = 3 + \cos(t)$. Then, we have

$$\gamma_m = 2, \quad \gamma_M = 4, \quad \bar{\varphi} = 1.$$

The parameters of the controller are chosen as follows:

$$l_1 = 1, \quad l_2 = 4, \quad l_3 = 7.$$

We start first by fixing the parameter κ for different values $\{\frac{1}{8}, -\frac{1}{8}, -\frac{1}{3}\}$.

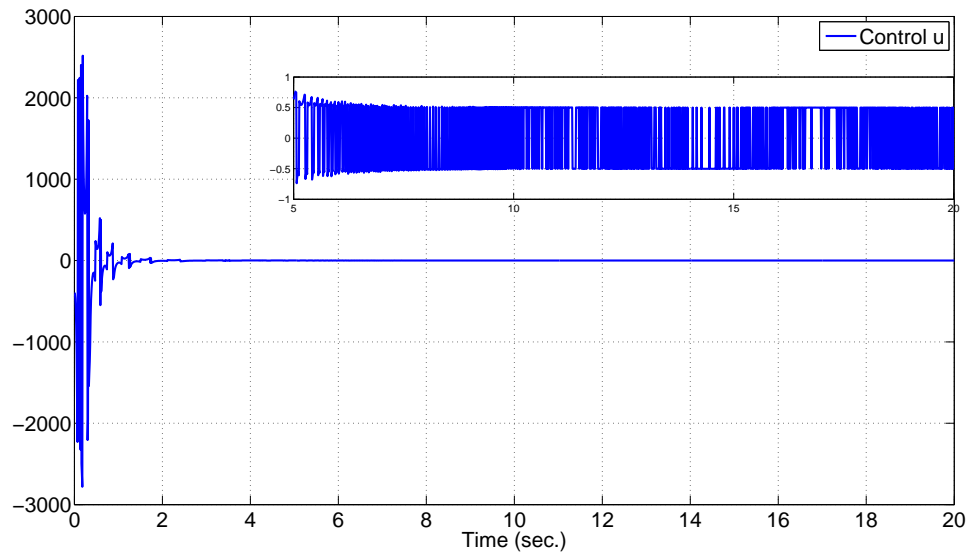
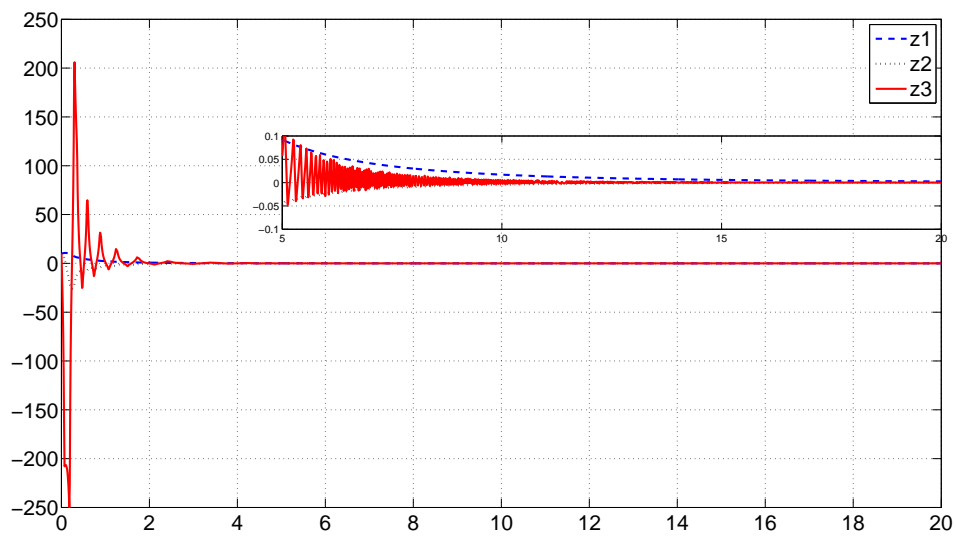
For $\kappa > 0$, Figure 3.1 shows a fast convergence of the states to a neighborhood of zero by an unbounded controller, otherwise the convergence to zero is asymptotic. For $-1/3 < \kappa < 0$, the convergence of the states to zero in finite-time is obtained by an unbounded controller with a minimum amplitude of the discontinuous control at $z = 0$, as shown in Figure 3.2. The finite-time convergence of the states is also shown in Figure 3.3 for $\kappa = -1/3$, using a bounded controller with a large discontinuous control at $z = 0$.

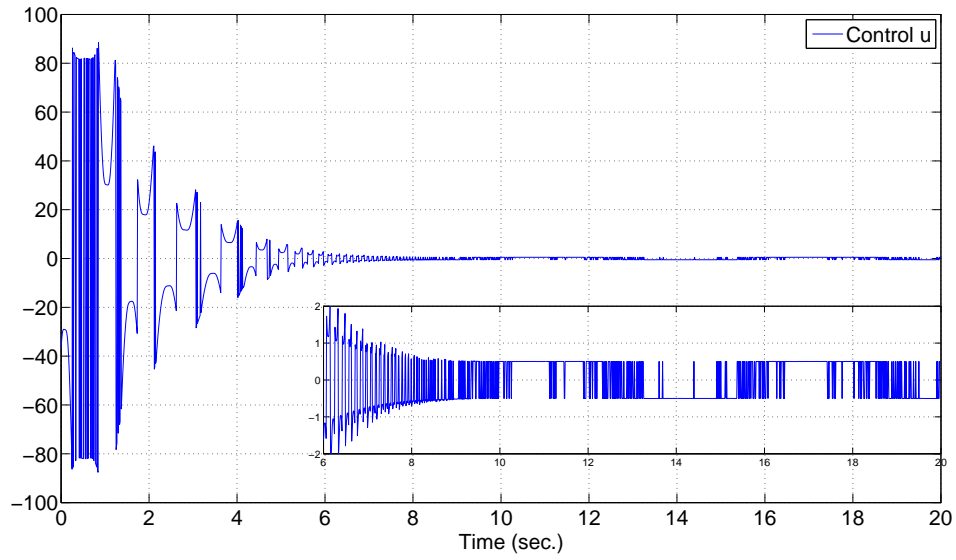
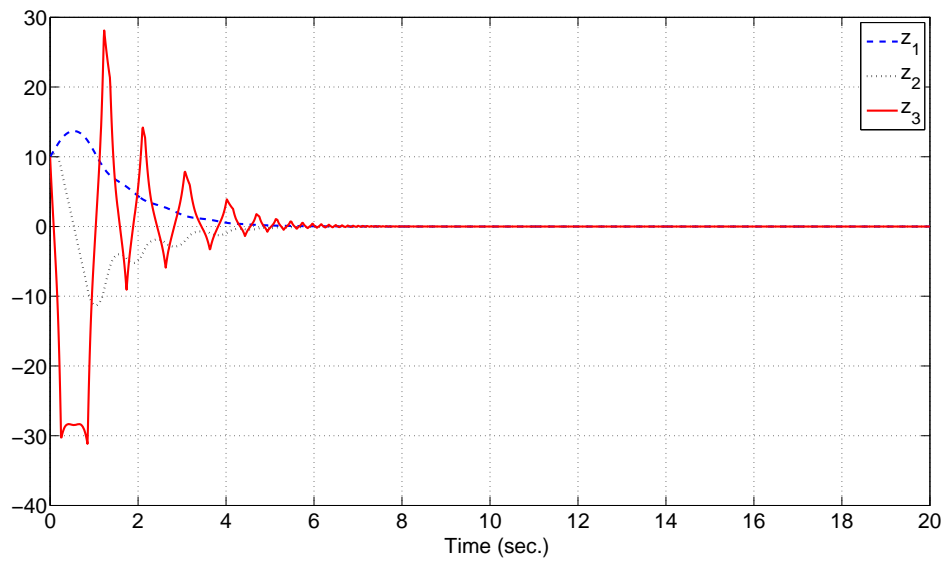
A bounded controller which ensures a minimum discontinuous control amplitude at zero is shown in Figure 3.4 by switching κ in neighborhood of zero, from $-1/3$ to $-1/8$.

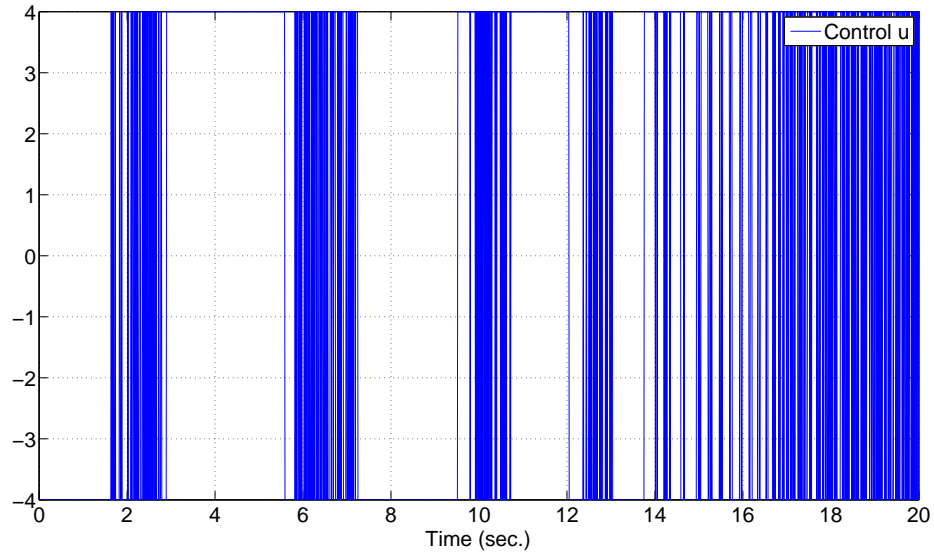
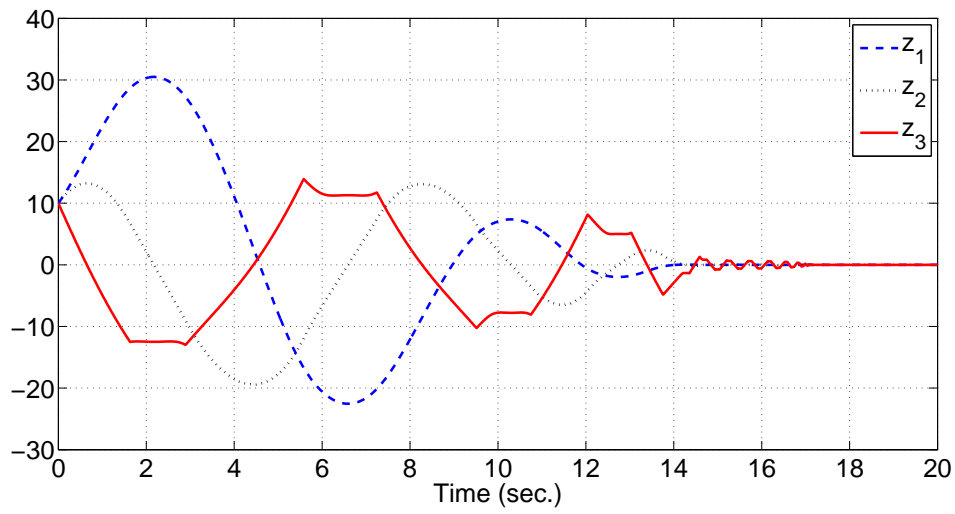
A fixed-time controller is shown in Figure 3.5. Figure 3.6 shows that the convergence time will not exceed 8.5 sec for any initial condition. Fixed-time stability is assumed to be established by the time after which, $|z_1|$, $|z_2|$, $|z_3|$ are less than 1×10^{-4} .

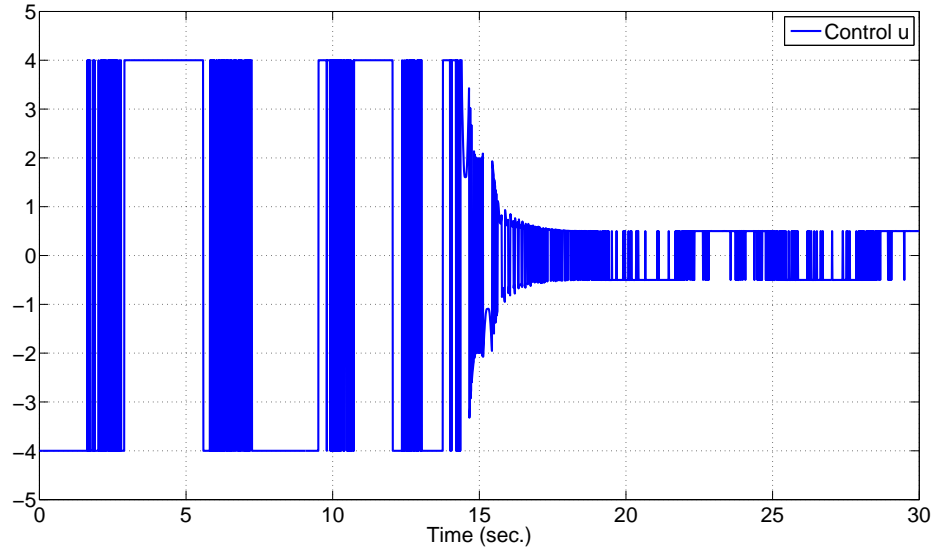
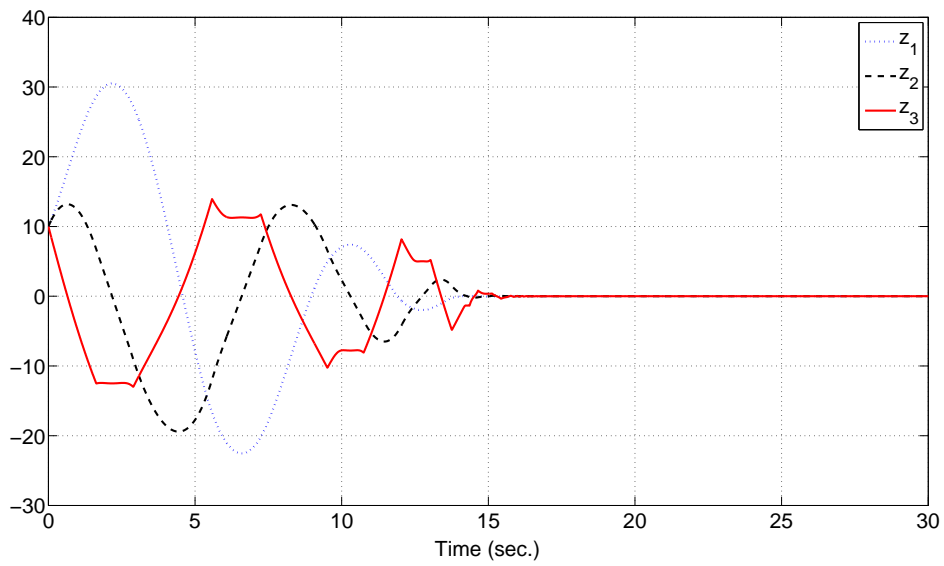
3.5 Summary

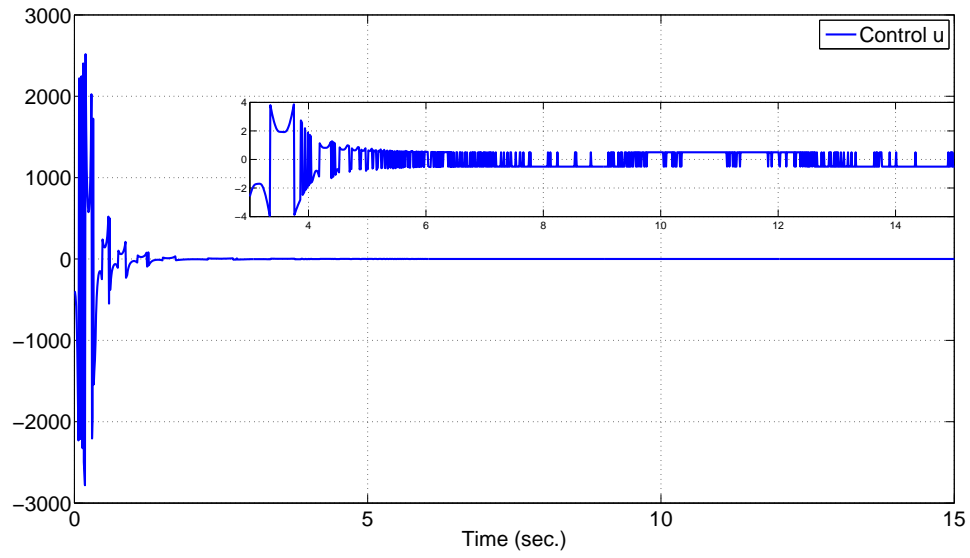
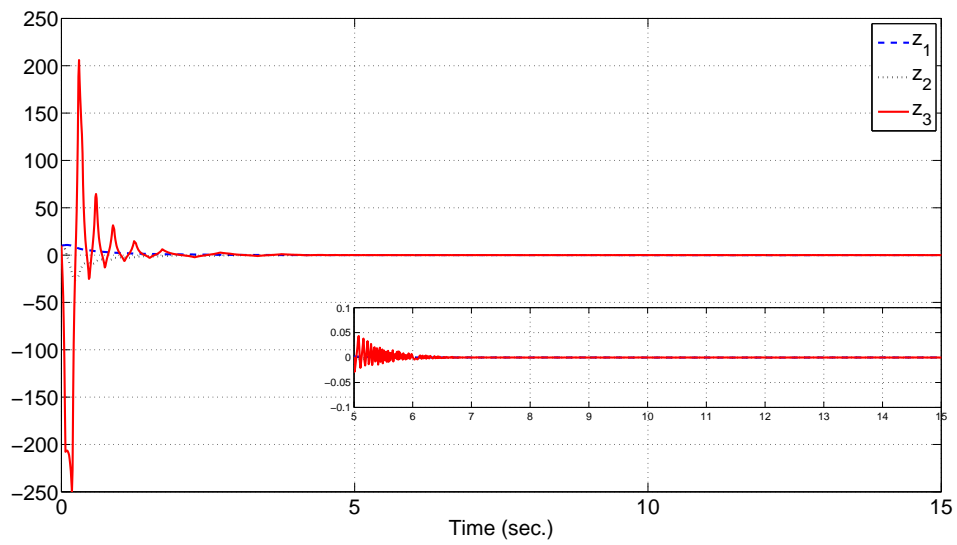
In this chapter, further properties of the Lyapunov-based finite-time convergent controllers, presented in the previous chapter, were discussed in detail. A generalized bounded controller was developed and the influence of homogeneity degree on the nature of control

(a) control law u versus time (s).(b) z_1 and z_2 versus time (s).**Figure 3.1.** test for $\kappa > 0$

(a) control law u versus time (s).(b) z_1 and z_2 versus time (s).**Figure 3.2.** test for $-1/r < \kappa < 0$

(a) control law u versus time (s).(b) z_1 and z_2 versus time (s).**Figure 3.3.** test for $\kappa = -1/r$ (case of [55])

(a) control law u versus time (s).(b) z_1 and z_2 versus time (s).**Figure 3.4.** test for κ switching from $-1/r$ to $k \in (-1/r, 0)$

(a) control law u versus time (s).(b) z_1 and z_2 versus time (s).**Figure 3.5.** test for κ switching from $-k$ to k , $k \in (-1/r, 0)$

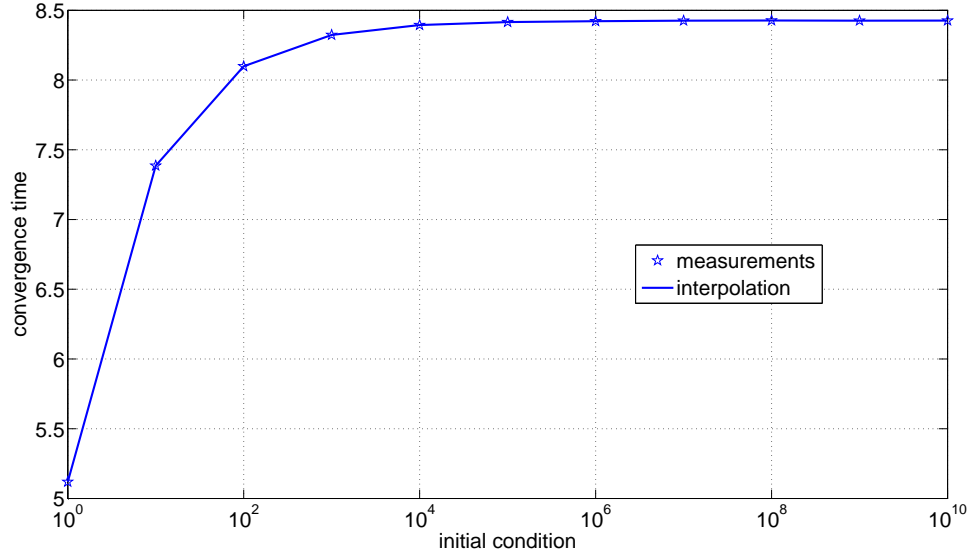


Figure 3.6. *Convergence time versus initial condition.*

was elaborated. It was observed that Levant's arbitrary HOSM controller [55] is a particular case of our controller, under a particular choice of the homogeneity degree. It was also shown that the properties of minimum discontinuity amplitude of the controller and fixed-time convergence can be obtained by changing the homogeneity degree of the controller.

This chapter ends the part of this thesis related to HOSM controllers.

Part II

Underactuated Systems Control

Chapter 4

Preliminary Concepts and introduction to problems

In this part of the thesis, control problems related to underactuated systems are discussed. As mentioned in the introduction, the control of under-actuated physical systems, with more degrees of freedom than control inputs, is a challenging task in nonlinear control systems [28, 67]. An additional consideration is that in practice, the available control inputs are also physically constrained or bounded. In this regard, stabilization using saturated controls [84] appears to be an interesting approach for control of such systems.

In this chapter, we will first review some existing bounded control methods for systems that can be modeled as integrator chains. The notion of Input-to-State Stability will also be introduced. Then, we will introduce the two underactuated systems, the control of which is studied in this thesis. Let us first recall some popular bounded controllers for the stabilization of pure integrator chain, as present in the contemporary literature.

4.1 Stabilization of Integrator Chain Using Bounded Control

Bounded or saturated controls have been the subject of many studies, such as [88, 85, 84] and [36]. In [85], it was demonstrated that stabilization of integrator chains of order greater than two is not possible with with saturated linear state feedback. Teel [88] introduced the method of nested saturated controls for integrator chains of higher orders. Sussmann

et al. [85] extended method to null controllable systems of higher orders. Let us review these two approaches.

4.1.1 Nested bounded controls approach for integrator chains

A pure integrator chain is represented as

$$\begin{cases} \dot{x}_1 &= x_2, \\ &\vdots \\ \dot{x}_n &= u, \end{cases} \quad (4.1)$$

Teel [88] introduced a non-linear control law with nested saturation functions in the following form:

$$u(x) = -sat_{M_n}(h_n(x) + sat_{M_{n-1}}(h_{n-1}(x) + \dots sat_{M_1}(h_x))), \quad (4.2)$$

where h_i is a linear coordinate change and sat_{M_i} is a linear saturation function. For a given positive constant M and L with $L \leq M$, sat_M is an increasing function defined by:

$$psat_M(p) > 0 \text{ for a real } p \neq 0$$

$$sat_M(p) = p \text{ when } |p| \leq L$$

$$sat_M(p) \leq M$$

The global stability of the integrators chain (4.1) is guaranteed by the application of the controller u presented in (4.2), with the of linear coordinate change given by:

$$h_{n-i} = \sum_{j=0}^i \frac{i!}{j!(i-j)!} x_{n-j}, \quad (4.3)$$

where M_i and L_i are positive constants which satisfy

$$L_i \leq M_i \leq \frac{1}{2} L_{i+1}. \quad (4.4)$$

4.1.2 Nested bounded controls approach for null controllable systems

Sussmann et al. generalized the control laws with nested saturation functions for global stabilization linear *null controllable* system with control constraints [85]. A *null controllable* system is a stabilizable systems with poles of null or negative real part. The controller u is the sum of saturated functions :

$$u = \sum_{i=1}^n \epsilon^{n-i+1} \sigma(y_i) \quad (4.5)$$

with $0 < \epsilon < \frac{1}{4}$, and σ is the standard saturation function with $\sigma(y) = \text{sat}_1(y)$. The linear change of coordinate $(x_1, \dots, x_n) \longrightarrow (y_1, \dots, y_n)$ is given by:

$$\begin{cases} y_n &= h_1(x_n), \\ y_{n-1} &= h_2(x_{n-1}, x_n), \\ &\vdots \\ y_1 &= h_n(x_1, x_2, \dots, x_n), \end{cases} \quad (4.6)$$

where

$$\begin{cases} h_1(s_1) &= s_1, \\ h_2(s_1, s_2) &= \epsilon h_1(s_1) + h_1(s_2), \\ &\vdots \\ h_n(s_1, s_2, \dots, s_n) &= \epsilon^{n-1} h_{n-1}(s_1, s_2, \dots, s_{n-1}) + h_1(s_2, s_3, \dots, s_n). \end{cases} \quad (4.7)$$

Remark 4.1.1. *This approach ensures the global asymptotic convergence to zero, however the rate of convergence becomes slower when the order of the system is increased [64]. This problem related to the small rate of convergence comes essentially from the presence of small ϵ [37]. Hably [37] overcomes this problem by proposing a choice of the parameter $\bar{\epsilon}$, an upper bound of ϵ as :*

$$\bar{\epsilon} > 0 \text{ if } n = 1$$

$$\bar{\epsilon} = 1 \text{ if } n = 2$$

$$\bar{\epsilon} \text{ is the unique solution in } (0, 1) \text{ of the equation } \epsilon^{n+1} - 2\epsilon^2 + \epsilon \text{ if } n > 2$$

The robustness to the measurement and modeling error is shown in [37] without mathematical proof.

4.2 Input-to-State Stability Concept

Input-to-State Stability is a notion often employed for the robustness of closed-loop under-actuated systems. Before presenting another approach of saturated control, let us revise this concept.

Consider the system

$$\dot{x} = f(t, x, u), \quad (4.8)$$

where $f : [0, \infty) \times \mathbb{R}^n \times \mathbb{R}^m \rightarrow \mathbb{R}^n$ is piecewise continuous in t and locally Lipschitz in x and u . The control input $u(t)$ is piecewise continuous, bounded function of t for all $t \geq 0$. Suppose that the unforced system

$$\dot{x} = f(t, x, u), \quad (4.9)$$

has a globally uniformly asymptotically stable equilibrium point at the origin $x = 0$. We introduce below the *input-to-state stability*.

Definition 4.2.1. [46] System (4.8) is said to be input-to-state stable if there exist a class \mathcal{KL} function β and a class \mathcal{K} function γ such that for any initial state $x(t_0)$ and any bounded input $u(t)$, the solution $x(t)$ exists for all $t \geq t_0$ and satisfies

$$\|x(t)\| \leq \beta(\|x(t_0)\|, t - t_0) + \gamma\left(\sup_{t_0 \leq \tau \leq t} \|u(\tau)\|\right). \quad (4.10)$$

Where the Class \mathcal{K} and Class \mathcal{KL} function are defined next.

Definition 4.2.2. [46] A continuous function $\alpha : [0, a) \rightarrow [0, \infty)$ is said to belong to class \mathcal{K} if it is strictly increasing and $\alpha(0) = 0$.

Definition 4.2.3. [46] A continuous function $\beta : [0, a) \times [0, \infty) \rightarrow [0, \infty)$ is said to belong to class \mathcal{KL} , if for each fixed s , the mapping $\beta(r, s)$ belongs to class \mathcal{K} , with respect to r and, for each fixed r , the mapping $\beta(r, s)$ is decreasing with respect to s and $\beta(r, s) \rightarrow 0$ as $s \rightarrow \infty$.

Let us elucidate this ISS with the following example, as stated in [46] for a linear time-invariant system

$$\dot{x} = Ax + Bu, \quad (4.11)$$

where A is a Hurwitz matrix, B is a non null arbitrary matrix, and u is a bounded input. The solution of (4.11) can be written as

$$x(t) = e^{(t-t_0)A}x(t_0) + \int_{t_0}^t e^{t-\tau}Bu(\tau)d\tau, \quad (4.12)$$

and use the bound $\|e^{(t-t_0)A}\| \leq ke^{-\lambda(t-t_0)}$, for some positive constant k and λ . We estimate the solution by

$$\begin{aligned} \|x(t)\| &\leq ke^{-\lambda(t-t_0)}\|x(t_0)\| + \int_{t_0}^t ke^{-\lambda(t-\tau)}\|B\|\|u(\tau)\|d\tau, \\ &\leq ke^{-\lambda(t-t_0)}\|x(t_0)\| + \frac{k\|B\|}{\lambda} \sup_{t_0 \leq \tau \leq t} \|u(\tau)\|. \end{aligned} \quad (4.13)$$

The function $ke^{-\lambda(t-t_0)}x(t_0)$ is a class \mathcal{K} function as λ is positive, and $\frac{k\|B\|}{\lambda} \sup_{t_0 \leq \tau \leq t} \|u(\tau)\|$ is a class \mathcal{KL} function. Inequality (4.13) guarantees that x will be bounded for u bounded, and x will converge exponentially to a neighborhood of zero defined by $\|x\| \leq \frac{k\|B\|}{\lambda} \limsup_{\tau \rightarrow \infty} \|u(\tau)\|$.

4.3 Stabilization of Double Integrator Subject to Input Saturation [15]

We now recall the work of [15] for the stabilization of perturbed double integrator system using a bounded control. The robustness of this controller is mathematically proved using ISS. Let us consider the following system

$$\begin{aligned}\dot{x}_1 &= x_2 + v_1, \\ \dot{x}_2 &= \sigma(-x_1 - x_2 + u) + v_2,\end{aligned}\tag{4.14}$$

where $\sigma(a)$ is the standard saturation function defined for any $a \in \mathbb{R}$, as follows

$$\sigma(a) = \frac{a}{\max(1, |a|)},\tag{4.15}$$

$v = (v_1, v_2)$ and u are bounded functions.

Based on the following Lyapunov function for System (4.14) proposed in [15] :

$$V(x_1, x_2) = x_2^2 + \int_0^{x_1} \sigma(s) ds + \int_0^{x_1+x_2} \sigma(s) ds,\tag{4.16}$$

it has been proven that: for every $\epsilon > 0$, there exists a bounded input $v^{(\epsilon)}$ with $\|v^{(\epsilon)}\|_\infty \leq \epsilon$ and a compactly supported input $u^{(\epsilon)}$ such that the trajectory of System (4.14) starting at $(0,0)$ and associated to $(u^{(\epsilon)}, v^{(\epsilon)})$ tends to infinity. However, by following the arguments of [15] (see in particular the paragraphs 5.3 till 5.5 pages 323–326), it is easy to obtain the following result: there exists $\epsilon_0 > 0$ such that for every bounded input $v = (v_1, 0)$ with $\|v_1\|_\infty \leq \epsilon_0$, the following inequality hold true: for every bounded input u ,

$$\limsup_{t \rightarrow \infty} (|x_1| + |x_2|) \leq C (\|v_1\|_\infty + \|u\|_\infty + \|u\|_\infty^2),\tag{4.17}$$

where C is a universal positive constant and (x_1, x_2) is a trajectory of System (4.14) associated to u and v_1 .

Equation (4.17) will imply that for sufficiently small v_1 , u , i.e. $\|v_1\|_\infty \ll 1$ and $\|u\|_\infty \ll 1$, we get

$$\limsup_{t \rightarrow \infty} (|x_1| + |x_2|) \ll 1,\tag{4.18}$$

which implies that after a sufficiently large time, we will obtain $(|x_1| + |x_2| + u) < 1$ and System (4.14) will become

$$\begin{aligned}\dot{x}_1 &= x_2 + v_1, \\ \dot{x}_2 &= -x_1 - x_2 + u,\end{aligned}\tag{4.19}$$

which is clearly ISS as we saw in the example presented in the previous section.

Remark 4.3.1. *In the studied underactuated systems, the functions v_1 and u can model the observation error coming of velocity observer, or some controls which serve to stabilize other states in the global system*

4.4 Two important underactuated systems

In this thesis, we have studied two particular problems related with two different underactuated systems: path-following of a car-type robotic vehicle and trajectory tracking of a surface marine vessel. The development and proofs are established on the stabilization of perturbed double integrator based on bounded control input, presented in [15] and recalled in the previous section. In this section these the dynamic models of these two underactuated systems are introduced and their control problems are formalized.

4.4.1 Car-type robotic vehicle

The first problem, addressed in Chapter 5, is the path following control of a robot car-type vehicle using target point. This control problem arises from camera-vision applications [13, 72], where the vehicle is guided by a target point ahead of the vehicle, within the visual range of the camera [6, 13]. The target point is fixed at a known distance $d > 0$ from the center of gravity on the axis of the vehicle. The control objective is to drive the vehicle, such that the target point follows the desired path (as shown in Figure 4.1).

The state equations for the vehicle dynamics are

$$\begin{cases} \dot{x} &= V_x \cos \psi, \\ \dot{y} &= V_x \sin \psi, \\ \dot{\psi} &= V_x \kappa, \\ \dot{\kappa} &= V_x \rho_0. \end{cases}\tag{4.20}$$

These equations represent the vehicle's motion with a velocity V_x , along the curve defined by the its geodesic curvature κ . The control variable ρ_0 will be defined later. The

variable ψ represents the angle between the abscissa axis and the velocity vector $(\dot{p}, \dot{q})^T$, and κ represents the geodesic curvature of the driving path.

4.4.1.1 Control Objective

The control problem of path following differs from pure stabilization or tracking problems because the path, described by its curvature $\kappa(\cdot)$, is defined in space only, not in time. However, it can be converted into trajectory tracking problem in the following manner:

Let us consider a path Γ with geodesic curvature κ_r whose absolute value is bounded by $\kappa_{max} > 0$, i.e., for all $t \geq 0$, we have

$$|\kappa_r(t)| \leq \kappa_{max}. \quad (4.21)$$

The path Γ will be parameterized as a vehicle trajectory with a forward velocity $u(t)$ such that $\Gamma(t) = (p_r(t), q_r(t))$ is described by the following state equations

$$\begin{cases} \dot{p}_r &= u \cos \psi_r, \\ \dot{q}_r &= u \sin \psi_r, \\ \dot{\psi}_r &= u \kappa_r, \\ \dot{\kappa}_r &= u \rho_r, \end{cases} \quad (4.22)$$

where the variables have the same definitions as in (4.20) and the subscript r is used to differentiate between the reference variables and the actual vehicle variables. The arc length s of Γ is given by $s(t) = s_0 + \int_0^t u(\tau) d\tau$ and the scalar curvature $\kappa_r(t)$ is hence equal to $\kappa_r^*(s(t))$.

For the target point, the equations for the coordinates p and q are defined as

$$\begin{aligned} p &= x + d \cos \psi, \\ q &= y + d \sin \psi, \end{aligned} \quad (4.23)$$

and their dynamics are

$$\begin{cases} \dot{p} &= V_x \cos \psi - d V_x \sin \psi \kappa, \\ \dot{q} &= V_x \sin \psi + d V_x \cos \psi \kappa, \end{cases} \quad (4.24)$$

The control objective is therefore to force the coordinates of the target point in the p, q reference, to track p_r, q_r .

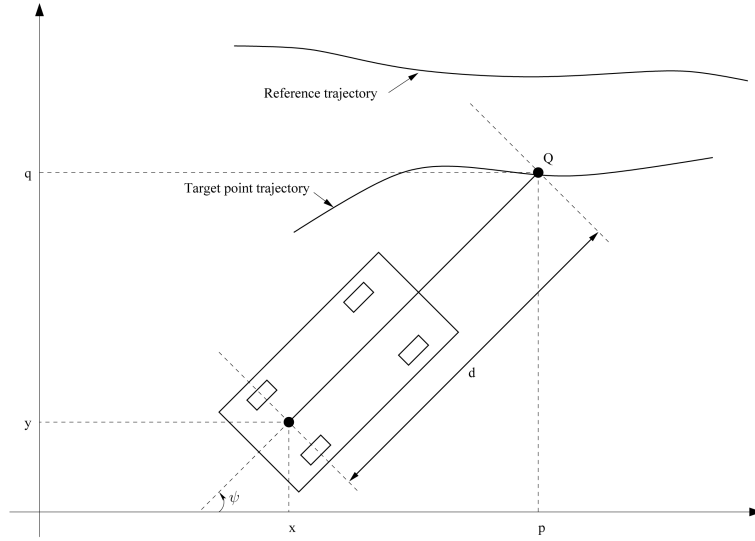


Figure 4.1. *The reference trajectory, the vehicle and its target point.*

4.4.2 Surface marine vessel

The next problem, addressed in Chapter 6, is the precise trajectory tracking of a surface marine vessel, such as a boat or a ship. The general 6-DOF rigid body model for surface marine vessels presented in [31] can be reduced by considering surge, sway and yaw motions only, under the following assumptions [17],

- (H1) Heave, roll and pitch motions induced by drift forces of wind, wave and ocean current are neglected.
- (H2) The inertia, added mass and hydrodynamic damping matrices are diagonal.

The aft propeller configuration provides only the surge force τ_u and the yaw moment τ_r . The kinematic and dynamic equations of the vessel can therefore be written as

$$\begin{cases} \dot{x} &= u \cos(\psi) - v \sin(\psi), \\ \dot{y} &= u \sin(\psi) + v \cos(\psi), \\ \dot{u} &= \frac{1}{c} v r - a u + \bar{\tau}_1, \\ \dot{v} &= -c u r - b v, \\ \dot{\psi} &= r, \\ \dot{r} &= \kappa u v - d r + \bar{\tau}_2, \end{cases} \quad (4.25)$$

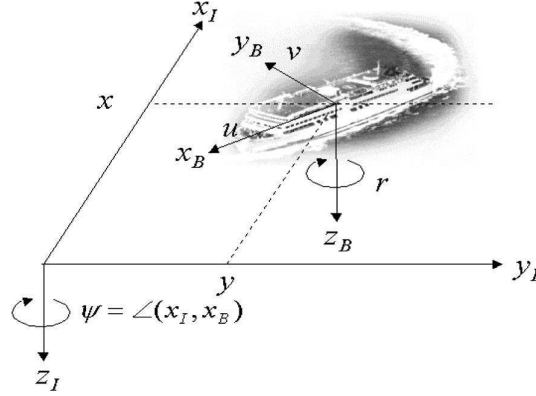


Figure 4.2. Surface marine vessel

where (x, y) and ψ are the coordinates and the yaw angle of the vessel in the earth-fixed frame, and u , v and r denote the surge, sway and yaw velocities respectively. The control inputs $\bar{\tau}_1$ and $\bar{\tau}_2$ are the normalized expressions of the surge force and yaw moment, given as $\bar{\tau}_1 = \frac{1}{m_1}\tau_u$ and $\bar{\tau}_2 = \frac{1}{m_3}\tau_r$. The parameters a , b , c , d and κ are positive constants that represent the mechanical properties of the system, namely the inertia $m_i > 0$ and hydrodynamic damping d_i , where $i = 1, 2, 3$ corresponds to surge, sway and yaw motions respectively. The constants are defined as follows $a = \frac{d_1}{m_1}$, $b = \frac{d_2}{m_2}$, $c = \frac{m_1}{m_2}$, $d = \frac{d_3}{m_3}$, $\kappa = \frac{m_1 - m_2}{m_3}$.

For control design, the system model (4.25) can be simplified by normalizing the physical parameters through straightforward variable and time-scale changes. For the sake of clarity, let us rewrite System (4.25) as follows,

$$(\tilde{S}) \begin{cases} \begin{pmatrix} \dot{x} \\ \dot{y} \end{pmatrix} = R_\psi \begin{pmatrix} u \\ v \end{pmatrix}, \\ \begin{pmatrix} \dot{u} \\ \dot{v} \end{pmatrix} = -D_0 \begin{pmatrix} u \\ v \end{pmatrix} - r A_c \begin{pmatrix} u \\ v \end{pmatrix} + \begin{pmatrix} 1 \\ 0 \end{pmatrix} \bar{\tau}_1, \\ \dot{\psi} = r, \quad \dot{r} = \kappa uv - dr + \bar{\tau}_2, \end{cases} \quad (4.26)$$

where the matrices D_0 , R_ψ and A_c are given as

$$\begin{aligned} D_0 &= \begin{pmatrix} a & 0 \\ 0 & b \end{pmatrix}, \quad R_\psi = \begin{pmatrix} \cos(\psi) & -\sin(\psi) \\ \sin(\psi) & \cos(\psi) \end{pmatrix}, \\ A_c &= \begin{pmatrix} 0 & -1/c \\ c & 0 \end{pmatrix}. \end{aligned} \quad (4.27)$$

Let us consider the following matrix $D_\rho = \text{diag}(\rho, c\rho)$, where ρ is a positive constant to be chosen later. Then we obtain $A_1 = D_\rho^{-1} A_c D_\rho$. The time scale $s := dt$ is introduced in System (4.26) as well as the linear changes of variables $(u(t)/d\rho, v(t)/dc\rho)$ and $r(t)/d$, still denoted $(u(s), v(s))$ and $r(s)$ respectively.

After easy computations and by setting $\beta := \frac{\kappa}{c\rho^2}$, $\tau_1 := \frac{\bar{\tau}_1}{\rho d^2}$, $\tau_2 := \frac{\bar{\tau}_2}{d^2}$ and $D = \text{diag}(a/d, b/d)$, the dynamics of the vessel, denoted by (S), is rewritten as follows,

$$(S) \begin{cases} \begin{pmatrix} \dot{x} \\ \dot{y} \end{pmatrix} &= R_\psi D_\rho \begin{pmatrix} u \\ v \end{pmatrix}, \\ \begin{pmatrix} \dot{u} \\ \dot{v} \end{pmatrix} &= -D \begin{pmatrix} u \\ v \end{pmatrix} - r A_1 \begin{pmatrix} u \\ v \end{pmatrix} + \tau_1 \begin{pmatrix} 1 \\ 0 \end{pmatrix}, \\ \dot{\psi} &= r, \quad \dot{r} = \beta uv - r + \tau_2. \end{cases} \quad (4.28)$$

4.4.2.1 Control Objective

Concerning this system, our objective is tracking control of the presented underactuated marine vessel by controlling its position and orientation. The vessel is forced to follow a reference trajectory which is generated by a “virtual vessel”, as follows,

$$(S_{re}) \begin{cases} \begin{pmatrix} \dot{x}_{re} \\ \dot{y}_{re} \end{pmatrix} &= R_{\psi_{re}} D_\rho \begin{pmatrix} u_{re} \\ v_{re} \end{pmatrix}, \\ \begin{pmatrix} \dot{u}_{re} \\ \dot{v}_{re} \end{pmatrix} &= -D \begin{pmatrix} u_{re} \\ v_{re} \end{pmatrix} - r_{re} A_1 \begin{pmatrix} u_{re} \\ v_{re} \end{pmatrix} \\ &\quad + \begin{pmatrix} 1 \\ 0 \end{pmatrix} \tau_{1,re}, \\ \dot{\psi}_{re} &= r_{re}, \quad \dot{r}_{re} = \beta u_{re} v_{re} - r_{re} + \tau_{2,re}, \end{cases} \quad (4.29)$$

where all variables have similar meanings as in System (6.1). Therefore, the control objective is to converge S to S_{re} .

4.5 Summary

In this chapter, the notions of ISS and stabilization of double integrator chains using saturated control were established. Then, two underactuated systems and their control problems were introduced. In the following chapters, these control problems will be addressed using the notions introduced here. The first chapter is dedicated to the path-following

problem of a car type robotic vehicle. The second chapter deals with a tracking problem associated with surface marine vehicles.

Chapter 5

Path Following of Robotic Vehicles

As introduced in the previous chapter, we will now address the problem of path-following of car-type robotic vehicles, using target-points.

5.1 State-of-the-Art and contributions

In the field of autonomous vehicle guidance, navigation and control, path-following problem of car-type vehicles is of particular interest. Many contemporary researchers have published various techniques and strategies for this problem, such as [80, 18, 44, 79, 26, 60]. Among open-loop motion planning techniques, differential flatness approach has been significant in motion planning to drive vehicles on Cartesian paths [30, 78]. In feedback control techniques, larger effort has been made on tracking problems. A backstepping approach has been presented in the context of tracking in [45]. This approach has also been used in [61], to develop a controller that is robust against vehicle skidding effects. Do et al. have further improved upon Jiang's backstepping method in [24] and [25], by adding observers to render the controller output-feedback and extending it to tracking and stabilization for parking problems of a vehicle and introducing dynamic update laws to compensate for parametric uncertainty and modeling errors. In [1] Aguiar et al. have used adaptive switched supervisory control combined with a non linear Lyapunov-based control to ensure the global convergence of the position tracking error to a small neighborhood of the origin. Bloch and Drakunov [9] have used sliding mode control for the stabilization and tracking of a nonholonomic dynamic system. This controller is global and ensures

convergence to the neighborhood of the desired trajectory. Lee et al. [53] have proposed a saturated feedback controller for tracking of a unicycle-type vehicle, using its forward velocity and angular acceleration as control inputs. They have also extended this controller for application on car-type vehicles.

The problem of path following differs from pure stabilization or tracking problems because the path, described by its curvature $\kappa(\cdot)$, is defined in space only, not in time. In this chapter, we have addressed the path following control of a robot car-type vehicle using target point. This control problem arises from camera-vision applications [13, 72], where the vehicle is guided by a target point ahead of the vehicle, within the visual range of the camera [6, 13]. The target point is fixed at a known distance $d > 0$ from the center of gravity on the axis of the vehicle. The control objective is to drive the vehicle, such that the target point follows the desired path (as shown in Figure 5.1). This problem has been addressed in [19] where a local robust path following strategy has been proposed using target point. Their solution is based on an open loop control based on inversion of the nominal model, and a closed loop control for stabilization of the resultant system. The error dynamics have been expressed in the Frénet frame associated to the followed path. This technique, also discussed in [65], is convenient only when the vehicle is close, positioned and oriented to the path.

5.1.1 Contribution

In our work, a global asymptotically stable controller is developed by parameterizing the path as a “virtual vehicle”, which is tracked by the actual vehicle. In this way, the path following problem is converted into a tracking problem, with two control inputs: the angular acceleration of the real vehicle and the velocity of the virtual vehicle. The forward velocity control of the real vehicle is not considered as part of the navigation problem, as it is controlled by other intelligent control systems in practical applications (for example, ABS, ESP [68]). It is instead assumed to be a measured state that is strictly positive, meaning that the vehicle is in continuous forward motion.

It can be noted that if there is no target point, i.e. $d = 0$, then the tracking error model obtained in this study is identical to [53], in which tracking has been achieved by using saturation on one control input while the other is unbounded. In our case, the introduction of the target point at a distance makes the dynamics of the tracking error model more complicated. Specifically, the development produces a first order nonlinear non-globally Lipschitz differential equation (see equation (5.8)) that can blow up in finite time. To

overcome this difficulty, our solution necessitates the application of saturated controls for both our control inputs with arbitrary small amplitude. Consequently, if both the control inputs are applied on the real vehicle, then the path following problem developed here becomes equivalent to the generalization of [53], as tracking problem with a target-point.

The work presented in this chapter is the continuation of [49], in which a unicycle type vehicle had been considered. However, the arguments of the Lyapunov analysis used for the convergence proof are significantly more involved than that of [49], due to the added state of the car type vehicle (essentially an integrator) and the fact that one must keep track of the small amplitudes of the saturations. Therefore, a positive definite function V is designed instead of a global Lyapunov function, whose time derivative along the closed-loop system is strictly negative outside a neighborhood of the origin. The design of V relies on an asymptotic analysis of a Ricatti equation, which is not needed in [49]. The convergence to zero is then demonstrated using a bootstrap procedure [59], i.e., once the system errors converge to a neighborhood, they continue to diminish to a smaller neighborhood, and ultimately converge asymptotically to the origin. The results so obtained can be extended to the case where only the position of the reference trajectory is directly known. One should finally notice that backstepping technics do not apply directly here (especially for the subsystem (η, ξ) defined in Eq.(5.19)) since we need to deal with (arbitrarily small) bounded inputs and we must perform precise robustness analysis in order to derive quantitative estimates for several \limsup .

5.2 Problem Formulation

Let us recall from Chapter 4, that the vehicle dynamics are represented by

$$\begin{cases} \dot{x} &= V_x \cos \psi, \\ \dot{y} &= V_x \sin \psi, \\ \dot{\psi} &= V_x \kappa, \\ \dot{\kappa} &= V_x \rho_0. \end{cases} \quad (5.1)$$

and the path Γ with geodesic curvature κ_r ($|\kappa_r(t)| \leq \kappa_{max}$) is parameterized as

$$\begin{cases} \dot{p}_r &= u \cos \psi_r, \\ \dot{q}_r &= u \sin \psi_r, \\ \dot{\psi}_r &= u \kappa_r, \\ \dot{\kappa}_r &= u \rho_r, \end{cases} \quad (5.2)$$

It can be noticed that V_x is not necessarily constant, but simply a continuous function of time, which verifies the following hypothesis: there exist two positive constants $0 < V_{min} \leq V_{max}$, such that for all $t \geq 0$

$$V_{min} \leq V_x(t) \leq V_{max}. \quad (5.3)$$

The strict positivity of the lower bound is necessary to derive our subsequent results.

For the target point, the equations for the coordinates p and q are defined as

$$\begin{aligned} p &= x + d \cos \psi, \\ q &= y + d \sin \psi. \end{aligned} \quad (5.4)$$

We will also suppose throughout that

$$(H1) \quad d\kappa_{max} < 1.$$

Remark 5.2.1. *The above assumption may be considered as a technical one or a design constraint for positioning the target point. However, it is reasonable to upper bound the curvature of the reference path in terms of the distance d . Indeed, tracking a circle of radius $d' < d$ with a point fixed at a distance d in front of a vehicle is impossible. To see that, one can see that intuitively of rely on equation (5.44) given below. At the light of the previous example, Hypothesis (H1) is almost optimal.*

The dynamics of the target point in a form similar to (5.1) can be obtained by deriving the precedent equations:

$$\begin{cases} \dot{p} &= V_x \cos \psi - d V_x \sin \psi \kappa, \\ \dot{q} &= V_x \sin \psi + d V_x \cos \psi \kappa, \end{cases} \quad (5.5)$$

The curve defined by the target point is traveled at the following speed

$$v_d = \sqrt{\dot{p}^2 + \dot{q}^2} = V_x \sqrt{1 + (\kappa d)^2}. \quad (5.6)$$

Our objective now is to define the dynamics of the target point as those of a car. For that purpose, we consider θ as the angle between the abscissa axis and the velocity vector $(\dot{p}, \dot{q})^T$. One easily gets that

$$\theta = \psi + \arctan(\kappa d), \quad (5.7)$$

then $\dot{p} = v_d \cos(\theta)$, $\dot{q} = v_d \sin(\theta)$, and the scalar curvature ω is defined by $\omega = \frac{\dot{\theta}}{v_d}$.

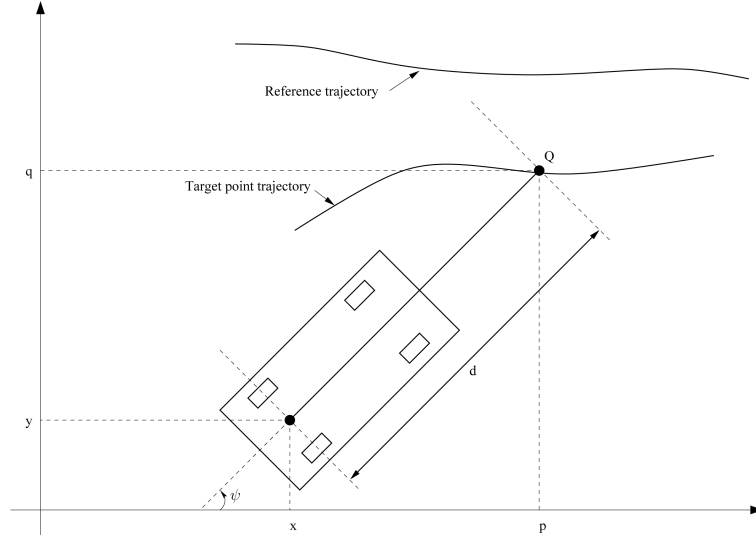


Figure 5.1. The reference trajectory, the vehicle and its target point.

We define the dynamics of ω by the new control variable $\rho := \dot{\omega}/v_d$. Deriving equation (5.7), we obtain

$$d\dot{\kappa} = V_x(1 + (\kappa d)^2)((1 + (\kappa d)^2)^{1/2}\omega - \kappa). \quad (5.8)$$

Hence the dynamics of the target point (p, q) becomes

$$\begin{cases} \dot{p} &= v_d \cos\theta, \\ \dot{q} &= v_d \sin\theta, \\ \dot{\theta} &= v_d \omega, \\ \dot{\omega} &= v_d \rho. \end{cases} \quad (5.9)$$

The error between the target point and the reference curve is defined as

$$\begin{aligned} e_p &= p - p_r, \\ e_q &= q - q_r, \\ \xi &= \theta - \psi_r, \\ \eta &= \omega - \kappa_r. \end{aligned} \quad (5.10)$$

and the error dynamics is given by

$$\begin{cases} \dot{e}_p &= v_d \cos\theta - u \cos\psi_r, \\ \dot{e}_q &= v_d \sin\theta - u \sin\psi_r, \\ \dot{\xi} &= v_d \omega - \kappa_r u, \\ \dot{\eta} &= v_d \rho - \rho_r u. \end{cases} \quad (5.11)$$

5.3 Control design and Lyapunov Function

In this section, we will present a control law $u(e_p, e_q, \xi, \eta, t)$ and $\rho(e_p, e_q, \xi, \eta, t)$, such that the system (5.11) is globally asymptotically stable (GAS for short) w.r.t. origin. Note that, from the equations (5.6) and (5.8), one recovers the control ρ_0 once v_d and ρ are determined. However, there is an issue of possible blow-up in finite time for κ (and thus for ρ_0). Indeed, assuming that one is able to stabilize (5.11) to zero, then the control ρ_0 is obtained by derivating κ , which is in turn obtained by solving (5.8), seen as an o.d.e. with unknown κ since ω tends to κ_r asymptotically. Equation (5.8) is of the type $\dot{\kappa} = f(\kappa, t)$ with the right-hand side f not globally Lipschitz w.r.t. κ , hence it is not immediate to insure global existence of κ for all $t \geq 0$. We will show later on, that an appropriate choice of u and ρ under Hypothesis (H1) solves this problem (see Lemma 5.4.1 below).

The standard saturation function $\sigma(x)$ defined for $x \in \mathbb{R}$ by

$$\sigma(x) = \frac{x}{\max(1, |x|)}. \quad (5.12)$$

Let us first of all perform a variable change on the control, as follows

$$\begin{aligned} u &= v_d(1 + u_1), \\ \rho &= \rho_r(1 + u_1) + u_2, \end{aligned} \quad (5.13)$$

where u_1, u_2 are the new control variables.

Remark 5.3.1. *In order to define ω, ρ and to perform the change of inputs variables, v_d must be greater than zero and thus V_x must also be strictly positive. It is therefore not obvious to proceed as above, if V_x only satisfies (PEC).*

With the boundedness of κ and V_x , equation (5.6) implies that v_d is bounded. If one insists on having ρ bounded, then we must assume also that ρ_r is bounded, as

$$|\rho_r| \leq \rho_{r,max}, \quad (5.14)$$

where $\rho_{r,max}$ is a known positive constant.

The system (5.11) is therefore rewritten as

$$\begin{cases} \dot{e}_p &= v_d(\cos\theta - \cos\psi_r - u_1 \cos\psi_r), \\ \dot{e}_q &= v_d(\sin\theta - \sin\psi_r - u_1 \sin\psi_r), \\ \dot{\xi} &= v_d(\eta - \kappa_r u_1), \\ \dot{\eta} &= v_d u_2. \end{cases} \quad (5.15)$$

The bounded controls u_1 and u_2 can be expressed in the following form:

$$\begin{aligned} u_1 &= C_1 \sigma(\cdot), \\ u_2 &= D \sigma(\cdot), \end{aligned} \quad (5.16)$$

with sufficiently small gains C_1 and D . Since κ is bounded, v_d also remains uniformly bounded throughout $t \geq 0$. We can hence change the time scale by considering $ds = v_d dt$. To keep the notations simple, we would continue to use t for time, and the point for the derivation with respect to s , like $\frac{df}{ds} = \dot{f}$. This has no effect on the control laws since our design is based on static feedback (w.r.t. the error). The error dynamics hence becomes

$$\begin{cases} \dot{e}_p &= \cos \theta - \cos \psi_r - u_1 \cos \psi_r, \\ \dot{e}_q &= \sin \theta - \sin \psi_r - u_1 \sin \psi_r, \\ \dot{\xi} &= \eta - \kappa_r u_1, \\ \dot{\eta} &= u_2. \end{cases} \quad (5.17)$$

Let us perform the following change of variable corresponding to a time-varying rotation in the frame of the reference trajectory

$$\begin{aligned} y_1 &= e_p \cos \psi_r + e_q \sin \psi_r, \\ y_2 &= -e_p \sin \psi_r + e_q \cos \psi_r. \end{aligned} \quad (5.18)$$

The system becomes

$$\begin{cases} \dot{y}_1 &= -u_1 + (\cos \xi - 1) + (1 + u_1) \kappa_r y_2, \\ \dot{y}_2 &= \sin \xi - (1 + u_1) \kappa_r y_1, \\ \dot{\xi} &= \eta - \kappa_r u_1, \\ \dot{\eta} &= u_2, \end{cases} \quad (5.19)$$

where u_1, u_2 will be chosen such that (5.19) becomes GAS.

The control variables u_1 and u_2 are defined as follows

$$\begin{aligned} u_1 &= C_1 \sigma(y_1), \\ u_2 &= -D \sigma\left(\frac{k_1}{D} \xi + \frac{k_2}{D} \eta + \frac{C_2}{D} \sigma(y_2)\right), \end{aligned} \quad (5.20)$$

where k_1, k_2, C_1, C_2, D are positive real numbers and $\sigma(\cdot)$ is the standard saturation function defined in (5.12). Typically, we want to stabilize the system with arbitrarily small saturation levels C_1 and D . In conclusion, the final system, noted (Σ) becomes

$$(\Sigma) \quad \begin{cases} \dot{y}_1 &= -C_1\sigma(y_1) + (\cos\xi - 1) + \mu y_2, \\ \dot{y}_2 &= \sin\xi - \mu y_1, \\ \dot{\xi} &= \eta - \kappa_r C_1\sigma(y_1), \\ \dot{\eta} &= -D\sigma\left(\frac{k_1}{D}\xi + \frac{k_2}{D}\eta + \frac{C_2}{D}\sigma(y_2)\right), \end{cases} \quad (5.21)$$

where

$$\mu := \kappa_r(1 + C_1\sigma(y_1)) \text{ and } |\mu| \leq \kappa_{max}(1 + C_1). \quad (5.22)$$

In the following section, it is shown that Global Asymptotic Stability of the system (5.21) can be achieved by proper selection of C_1 , C_2 , k_1 , k_2 .

More precisely, we prove the following theorem, which is the main result of this chapter.

Theorem 5.3.2. *Consider a path Γ with geodesic curvature κ_r^* verifying (4.21) for some $\kappa_{max} > 0$. It is then possible to track asymptotically γ with a point fixed at a distance $d > 0$ in front of a vehicle, where $d\kappa_{max} < 1$, by choosing the control laws u_1, u_2 according to (5.20) with constants k_1, k_2, C_1, C_2, D , which satisfy the following conditions. Set $a := \frac{3}{16}$.*

$$k_1 = ak_2^2, \quad C_2 = \frac{1}{2\beta k_2}, \quad C_1 = \frac{aC_2}{4k_2}, \quad (5.23)$$

where β is a positive constant larger than 8, D is an arbitrary positive constant, fixed a-priori, and k_2 is large enough that $\frac{1}{k_2 D} \ll 1$.

Proof. The proof of GAS stability of System (5.21) has been carried out as an argument based on Lyapunov analysis.

The first remark consists in focusing on the last two equations in (Σ) and we will first treat the case where there is no saturation on $\dot{\eta}$.

In that case, the last two equations in the previous section define a double integrator system, which shall now be denoted as (S_k) :

$$(S_k) \quad \begin{cases} \dot{\xi} = \eta + v_1, \\ \dot{\eta} = -k_1\xi - k_2\eta + v_2, \end{cases} \quad (5.24)$$

with,

$$\begin{aligned} v_1 &= -\kappa_r C_1\sigma(y_1), \\ v_2 &= -C_2\sigma(y_2). \end{aligned} \quad (5.25)$$

The system (S_k) can be presented in the matrix form

$$\dot{Z} = AZ + BU, \quad (5.26)$$

where,

$$Z = \begin{pmatrix} \xi \\ \eta \end{pmatrix}, \quad A = \begin{pmatrix} 0 & 1 \\ -k_1 & -k_2 \end{pmatrix}, \quad B = \begin{pmatrix} 1 & 0 \\ 0 & 1 \end{pmatrix}, \quad U = \begin{pmatrix} v_1 \\ v_2 \end{pmatrix}. \quad (5.27)$$

Since A is Hurwitz, there exists a quadratic form $V_k = Z^T P_k Z$, where P_k is a positive definite square matrix, obtained by solving the following Riccati equation

$$P_k A + A^T P_k + \frac{P_k^2}{\Upsilon_L^2} = -I, \quad (5.28)$$

where, Υ_L is the L_2 -gain related to the system (S_k) . The derivative \dot{V}_k is given by the following equation

$$\dot{V}_k = -\|Z\|^2 - \frac{\|P_k Z\|^2}{\Upsilon_L^2} + 2Z^T P_k U, \quad (5.29)$$

and verifies

$$\dot{V}_k \leq -\|Z\|^2 + \Upsilon_L^2 \|U\|^2. \quad (5.30)$$

The Lyapunov function proposed for the global system (5.21) is

$$V = MV_k + k_1 \frac{y_1^2 + y_2^2}{2} + \eta y_2 + k_2 y_2 \xi, \quad (5.31)$$

where M, k_1, k_2 are positive constants to be chosen later in particular to ensure that V is positive definite function, see Proposition 5.3.6 below. Moreover, a straightforward computation yields the following:

Proposition 5.3.3. *The derivative of the Lyapunov function can be upper bounded as follows,*

$$\begin{aligned} \dot{V} \leq & -M(\xi^2 + \eta^2) - k_1 C_1 y_1 \sigma(y_1) - C_2 y_2 \sigma(y_2) + M \Upsilon_L^2 \left((\kappa_r C_1 \sigma(y_1))^2 + (C_2 \sigma(y_2))^2 \right) \\ & + k_1 y_2 (\sin \xi - \xi) + k_1 y_1 (\cos \xi - 1) - \mu \eta y_1 + \eta \sin \xi - k_2 y_2 \kappa_r C_1 \sigma(y_1) - k_2 \xi \mu y_1 + k_2 \xi \sin \xi. \end{aligned} \quad (5.32)$$

The rest of the argument is divided in two main steps. In the first step, the existence of appropriate constants M, k_1, k_2, C_1, C_2 is proven, such that V has a positive definite

quadratic form in all the variables. This means that there exists a bounded region Y_{k_2} (for k_2 typically large), in the (y_1, y_2) -plane:

$$Y_{k_2} = \{(y_1, y_2) \mid |y_1| \leq \frac{C}{k_2^2}, |y_2| \leq \frac{C}{k_2^{3/2}}\}, \quad (5.33)$$

such that outside this region, the derivative of V along trajectories of (5.21) fulfills the following inequality

$$\dot{V} \leq -\frac{M}{2}(\xi^2 + \eta^2) - k_1 \frac{C_1}{2} y_1 \sigma(y_1) - \frac{C_2}{2} y_2 \sigma(y_2). \quad (5.34)$$

In the second step, a bootstrap-type argument is applied to show the convergence of trajectories of (5.21) to zero, as t tends to infinity.

These two steps have been achieved in the following manner: the L_2 -gain of (S_k) , denoted by Y_L is calculated, then P_k is estimated for k_2 tending to infinity. Then ISS (input-to-state) type bounds are calculated for ξ and η and the derivative of the Lyapunov function is estimated outside Y_{k_2} , and the argument is concluded. The detailed calculations have been presented in the following subsections.

5.3.1 L_2 -gain Y_L

Let us study the system (S_k) , defined in the equation (5.24). We recall that, (S_k) can be presented in the following matrix form

$$\underbrace{\begin{pmatrix} \dot{\xi} \\ \dot{\eta} \end{pmatrix}}_Z = \underbrace{\begin{pmatrix} 0 & 1 \\ -k_1 & -k_2 \end{pmatrix}}_A \underbrace{\begin{pmatrix} \xi \\ \eta \end{pmatrix}}_Z + \underbrace{\begin{pmatrix} 1 & 0 \\ 0 & 1 \end{pmatrix}}_B \underbrace{\begin{pmatrix} v_1 \\ v_2 \end{pmatrix}}_U. \quad (5.35)$$

Lemma 5.3.4. *We will tune $k_2 \geq 20$ with $k_1 = \frac{3}{16}k_2^2$, then $1 < Y_L < 1.2$.*

The proof of Lemma 5.3.4 is given in Appendix.

5.3.2 Estimation of P_k for large k_2

In this section, we take $k_1 = ak_2^2$ with $a = \frac{3}{16}$ and k_2 tending to infinity. We will prove the following two results whose proofs are given in Appendix.

Lemma 5.3.5. *As k_2 tends to infinity, the positive definite matrix P_k defined in (5.28) admits the following asymptotic expansion*

$$P_k = \begin{pmatrix} p_1 k_2 & p_2 \\ p_2 & \frac{p_3}{k_2} \end{pmatrix}, \quad (5.36)$$

with $p_i = F_i(1 + O(\frac{1}{k_2^2}))$, $1 \leq i \leq 3$, where the F_i are positive constants (only depending on a) so that $F_1 F_3 - F_2^2 > 0$.

Proposition 5.3.6. *For k_2 large enough and $M = \beta k_2$, the function V defined in (5.31) is a positive quadratic form in (ξ, η, y_1, y_2) .*

5.3.3 ISS bounds for ξ and η

For a real-valued continuous and bounded function f defined on \mathbb{R}^+ , we set

$$|f|^*(t) := \sup_{s \geq t} |f(s)|,$$

and

$$\|f\|^* := \limsup_{s \rightarrow \infty} |f(s)|.$$

Lemma 5.3.7. *Consider the system (5.35). By tuning $k_1 = \frac{3}{16} k_2^2$, the ISS bounds of ξ and η satisfy the following inequalities for $t \geq 0$,*

$$\begin{cases} |\xi|^*(t) \leq \frac{4}{k_2} \left(\kappa_{\max} C_1 + \frac{4}{3k_2} C_2 \right) + \|e^{At} Z_0\|, \\ |\eta|^*(t) \leq \kappa_{\max} C_1 + \frac{16}{3k_2} C_2 + \|e^{At} Z_0\|, \end{cases} \quad (5.37)$$

where Z_0 is the initial condition.

As a consequence, we have, for $t \geq 0$ large enough,

$$\begin{cases} |\xi|^*(t) \leq \frac{8}{k_2} \left(\kappa_{\max} C_1 + \frac{4}{3k_2} C_2 \right), \\ |\eta|^*(t) \leq 2\kappa_{\max} C_1 + \frac{32}{3k_2} C_2. \end{cases} \quad (5.38)$$

The proof of the above lemma is given in Appendix.

From the argument of Lemma 5.3.7, other ISS bounds for ξ and η can simply be derived by considering the system (S_k) defined in (5.24) with the controls v_1 and v_2 given in (5.25).

Lemma 5.3.8. *Let (S_k) be the system defined in (5.24) with the controls v_1 and v_2 given in (5.25). Assume that*

$$\|y_1\|^* < \kappa_{max}, \quad \|y_2\|^* < 1.$$

Then the bounds (5.38) can be improved as follows: there exists $T > 0$ such that, for every $t > T$,

$$\begin{cases} |\xi|^*(t) \leq \frac{8}{k_2} \left(C_1 |y_1|^*(t) + \frac{4}{3k_2} C_2 |y_2|^*(t) \right), \\ |\eta|^*(t) \leq 2C_1 |y_1|^*(t) + \frac{32}{3k_2} C_2 |y_2|^*(t). \end{cases} \quad (5.39)$$

Proof. The argument is straightforward by replacing C_1 and C_2 , which were used to bound v_1 and v_2 in (36) by $\kappa_{max} C_1 |y_1|^*(t)$ and $C_2 |y_2|^*(t)$. \square

For the rest of the chapter, we choose $C_1, C_2 \ll 1$ so that the limsup of both ξ and η are very small. In the subsequent computations, we can assume with no loss of generality that $|\cos \xi - 1| \leq \frac{\xi^2}{2}$, $|\sin \xi| \leq |\xi|$ and $|\sin \xi - \xi| \leq \frac{|\xi|^3}{3}$.

Proposition 5.3.9. *The following inequality holds true*

$$\begin{aligned} \dot{V} \leq & -M(\xi^2 + \eta^2) - k_1 C_1 y_1 \sigma(y_1) - C_2 y_2 \sigma(y_2) + M Y_L^2 \left((\kappa_r C_1 \sigma(y_1))^2 + (C_2 \sigma(y_2))^2 \right) \\ & + \frac{k_1 |y_2| |\xi|^3}{3} + \frac{k_1 |y_1| \xi^2}{2} + \mu \eta y_1 + |\eta \xi| - k_2 y_2 \kappa_r C_1 \sigma(y_1) - k_2 \xi \mu y_1 + k_2 \xi^2. \end{aligned} \quad (5.40)$$

5.3.4 Estimation of \dot{V} for $y \notin Y_{k_2}$

In this subsection, we choose the several parameters so that \dot{V} verifies (5.34) outside the region Y_{k_2} , for k_2 large enough. The results are summarized in the next lemma.

Lemma 5.3.10. *For the choice of parameters defined in Theorem 5.3.2, there exists k_2 large enough and $T > 0$, such that, for every $t > T$, Eq. (5.34) is verified.*

The proof of Lemma 5.3.10 is given in Appendix.

In the rest of the chapter, the symbol C has been used to represent arbitrary constants, depending only on β .

Remark 5.3.11. *Notice that inside Y_{k_2} , the term $k_2 |y_1 \xi|$ cannot be controlled since we only have for that purpose the term $\beta k_2 \xi^2 + C y_1^2$.*

5.3.5 Final step

Note that outside Y_{k_2} , for t large enough, $\dot{V} \leq -\frac{C}{k_2^4}$. To see that, we proceed as before since either $|y_1| \geq \frac{C}{k_2^2}$ or $|y_2| \geq \frac{C}{k_2^{3/2}}$. As a consequence, every trajectory of (5.21) must reach Y_{k_2} in finite time. Therefore, along every trajectory of (5.21), the value of V is eventually smaller than V_{max} , the maximal value of V over the set

$$\|\xi\| \leq \frac{C}{k_2^3}, \quad \|\eta\| \leq \frac{C}{k_2^2}, \quad |y_1| \leq \frac{C}{k_2^2}, \quad |y_2| \leq \frac{C}{k_2^{3/2}}.$$

By using (41) and Lemma 5.3.7, we get

$$V_{max} \leq \frac{C}{k_2}.$$

We deduce by using again (41) that, along every trajectory of (5.21) and for t large enough

$$y_1^2 + y_2^2 \leq \frac{C}{k_2^3}.$$

We can then use the improved ISS bounds for ξ and η obtained in Lemma 5.3.8. In particular, one gets that, for t large enough,

$$|\xi|^*(t) \leq \frac{C}{k_2^{3+3/2}}, \quad |\eta|^*(t) \leq \frac{C}{k_2^{2+3/2}},$$

In turn, this new bound for ξ allows one to shrink the bounded region Y_{k_2} outside which \dot{V} verifies (5.34). Indeed, one has to satisfy either (39) or (40), which leads to either $|y_1| \geq \frac{C}{k_2^{2+3/2}}$ or $|y_2| \geq \frac{C}{k_2^3}$.

Continuing the procedure described before, we construct inductively four sequences of positives numbers $y_{1,n}$, $y_{2,n}$, ξ_n and η_n , $n \geq 0$, of upper bounds of $\|y_1\|^*$, $\|y_2\|^*$, $\|\xi\|^*$ and $\|\eta\|^*$ respectively, such that the following inequalities are verified

$$\xi_n \leq C \frac{y_{1,n} + y_{2,n}}{k_2^3}, \quad \eta_n \leq C \frac{y_{1,n} + y_{2,n}}{k_2^2},$$

which are obtained from (5.39), and

$$y_{1,n+1} \leq C \xi_n, \quad y_{2,n+1}^2 \leq C k_2^2 \xi_n y_{1,n},$$

which are, according to (39) and (40), the equations needed to define, at the $(n+1)$ -th step, the bounded region outside which \dot{V} verifies (5.34). It is simple to prove that, for all non negative integer n , we have

$$y_{1,n+1} + y_{2,n+1} \leq \frac{C}{\sqrt{k_2}} (y_{1,n} + y_{2,n}).$$

This immediately yields the convergence to zero of trajectories of (5.21).

Remark 5.3.12. *The bootstrap procedure we have used above is clearly an instance of a small gain theorem.*

□

5.4 Stabilization of the original system

We have stabilized System (5.21) in case there is no saturation on $\dot{\eta}$. We will now show that for every initial condition, the term inside the outer saturation in $\dot{\eta}$ becomes bounded by 1 for t sufficiently large (i.e. there exists $T > 0$ such that, for $t > T$, the thesis holds true). Thus the last two equations of (5.21) are given by (5.24). To show that, we need an ISS-type of result on the system

$$(S_k) \quad \begin{cases} \dot{\xi} = \eta + C_1 d_1, \\ \dot{\eta} = -D\sigma\left(\frac{k_1}{D}\xi + \frac{k_2}{D}\eta + \frac{C_2}{D}d_2\right), \end{cases} \quad (5.41)$$

where d_1 and d_2 are amplitude-bounded perturbations which amplitudes are bounded by constants eventually depending on κ_{max} . We first perform the linear change of variable defined by

$$X(t) = \frac{k_1}{D}\xi\left(\frac{k_2 t}{k_1}\right), \quad Y(t) = \frac{k_2}{D}\eta\left(\frac{k_2 t}{k_1}\right).$$

A direct computation shows that the dynamics of (X, Y) is given by

$$\begin{cases} \dot{X} = Y + \frac{k_2 C_1}{D} d_1, \\ \dot{Y} = -\frac{1}{a}\sigma\left(X + Y + \frac{C_2}{D} d_2\right). \end{cases} \quad (5.42)$$

Since both $\frac{k_2 C_1}{D}$ and $\frac{C_2}{D}$ are of the magnitude of $\frac{1}{k_2 D}$, these constants can be chosen arbitrarily small. Then, as a consequence of results presented in section 4.3 pages 71-72, one gets that there exists $C(a) > 0$ a positive constant only depending on a so that

$$\limsup_{t \rightarrow \infty} (|X(t)| + |Y(t)|) \leq \frac{C(a)}{k_2 D} (\|d_1\|_\infty + \|d_2\|_\infty). \quad (5.43)$$

Therefore, $|X(t) + Y(t) + \frac{C_2}{D} d_2(t)|$ becomes strictly less than one for t large enough if $\frac{1}{k_2 D}$ is small enough.

The following lemma provides bounding conditions on u_1 and u_2 that would guarantee that the differential equation given in (5.8) is defined for all times $t \geq 0$.

Lemma 5.4.1. *For $k_2 D$ large enough, the differential equation in κ given by (5.8) is defined for all times $t \geq 0$.*

Proof of Lemma 5.4.1 After multiplying (5.8) by κ , one can rewrite as follows,

$$\frac{d\kappa\dot{\kappa}}{(1+(d\kappa)^2)^{3/2}} = |\kappa|V_x \left[\text{sign}(\kappa)d\eta + \left(1 - \frac{d|\kappa|}{\sqrt{1+(d\kappa)^2}}\right) + (d\kappa_r \text{sign}(\kappa) - 1) \right]. \quad (5.44)$$

The right-hand side of the above inequality is majored by

$$|\kappa|V_x(d|\eta| + d\kappa_{\max} - 1 + \frac{1}{1+(d\kappa)^2}).$$

If we can ensure that

$$d\|\eta\|_\infty < 1 - d\kappa_{\max}, \quad (5.45)$$

then this will easily imply that κ does not blow up in finite time. Indeed, assuming that (5.45) holds, then there exists $K > 0$ (only depending on $d\|\eta\|_\infty$ and $d\kappa_{\max}$) such that the right-hand side of (5.44) becomes negative for $|\kappa| \geq K$. This readily yields that $|\kappa|$ becomes strictly less than K in finite time and therefore does not blow up in finite time.

We now show that (5.45) holds true with an appropriate choice of the constants k_1, k_2 . Without loss of generality we can assume that $\xi(0) = \eta(0) = 0$. In that case, one can replace the \limsup 's in the left-hand side of (5.43) by $\|X\|_\infty + \|Y\|_\infty$. Since $\frac{1}{k_2 D}$ can be chosen arbitrarily small, (5.45) follows.

Remark 5.4.2. *The proposed method appears to require global localization of the mobile robot and the desired trajectory at every sampling instant with respect to the world frame, which is usually very difficult to obtain in real applications. However, this does not restrict or limit the application of the presented controller in real life. For example, the position coordinates in (x, y) frame of reference can be obtained by a camera and the angle ψ (the direction of vehicle) by a gyroscope. The position of the target point can then be translated into (p, q) frame of reference given in Equation (5.4). From here, a finite time differentiator can be used to get \dot{p}, \dot{q} , and later on the angle θ . A simple exponential (even homogeneous finite time) observer can be used to get η as in [35].*

Remark 5.4.3. *Since the proof of the convergence is using a Lyapunov function which is strict outside Y_{k_2} , the results of Theorem 5.3.2 can easily be extended in case where we have only direct access to $(p_r(\cdot), q_r(\cdot))$. Note that the gradient of the Lyapunov function is linear in its argument and thus, if the states are obtained through observers of differentiators, this will require C_i , $i = 1, 2$ in (5.34) to be changed with $C_i + f_i(t)$, where $f_i(\cdot)$ is the observation or*

estimation error. There exist fixed time convergent differentiators such as [2], which ensure that the derivative converges in fixed finite time. On the other hand, if the estimation or convergence is asymptotic, it has been shown in [15, 35] that if f_1, f_2 tend to zero exponentially, then the controller will also converge and the proof will not change.

5.5 Simulations

The performance of the presented controller can be seen in the simulation results obtained using the following parameters:

$$d = 2 \text{ m}, \quad V_x = 5 \text{ m.s}^{-1}.$$

$d\kappa_{max}$ has been chosen much smaller than 1 in order to emphasize upon significant initial conditions (in particular, $\xi(0)$ close to π) so that the resultant illustrations highlight our claim. The initial conditions imposed upon the error are

$$e_p(0) = e_q(0) = 10 \text{ m}, \quad \xi(0) = 9\pi/10,$$

The parameters of the controller was taken as follow:

$$C_1 = 0.1172, \quad C_2 = 0.5, \quad k_1 = 7500, \quad k_2 = 200, \quad D = 50.$$

Figure 5.2 shows the reference trajectory, the target point and vehicle in a 2D co-ordinate plane. It can be seen that the system converges to the reference trajectory asymptotically. Once the vehicle converges, the target point and the vehicle follow the trajectory very closely. The convergence can also be seen in the error graph shown in figure 5.3, where the initial conditions are also visible.

Figures 5.4 and 5.5 show the control signals u and ρ respectively. It is clear from these figures that the controller does not attain extremely large values, and is bounded. This is an essential property in real systems, which does not result in impossible control signals when the initial error is very large.

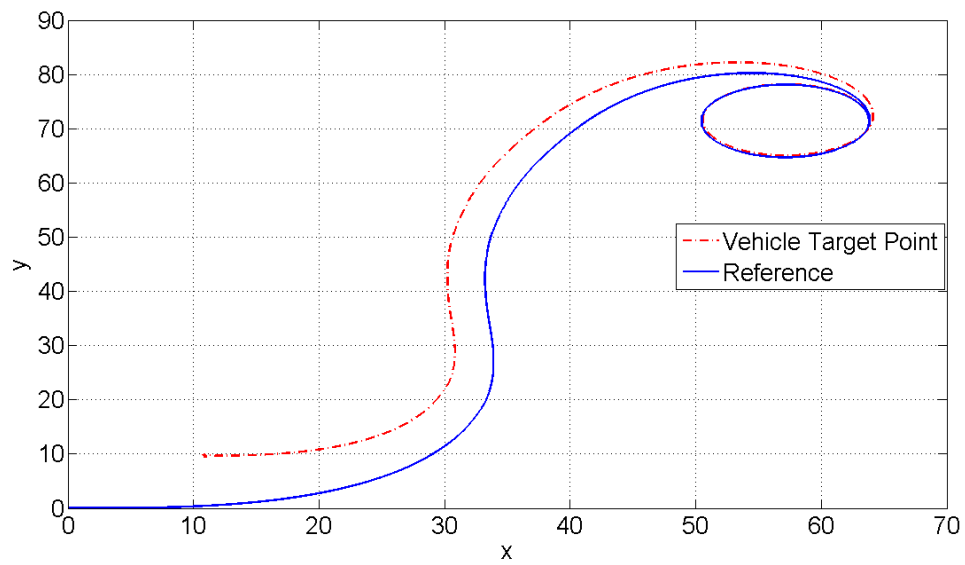


Figure 5.2. Reference trajectory, of the vehicle and its target point

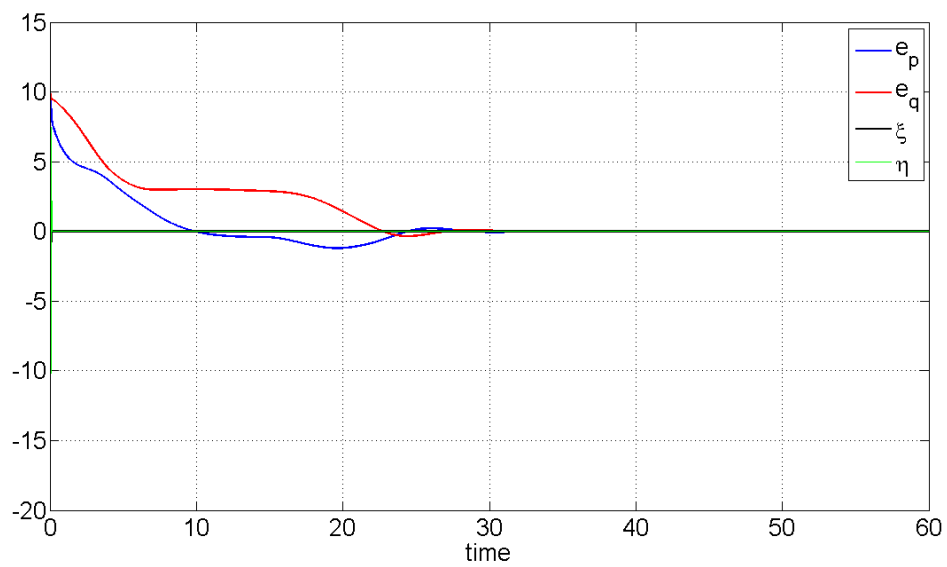
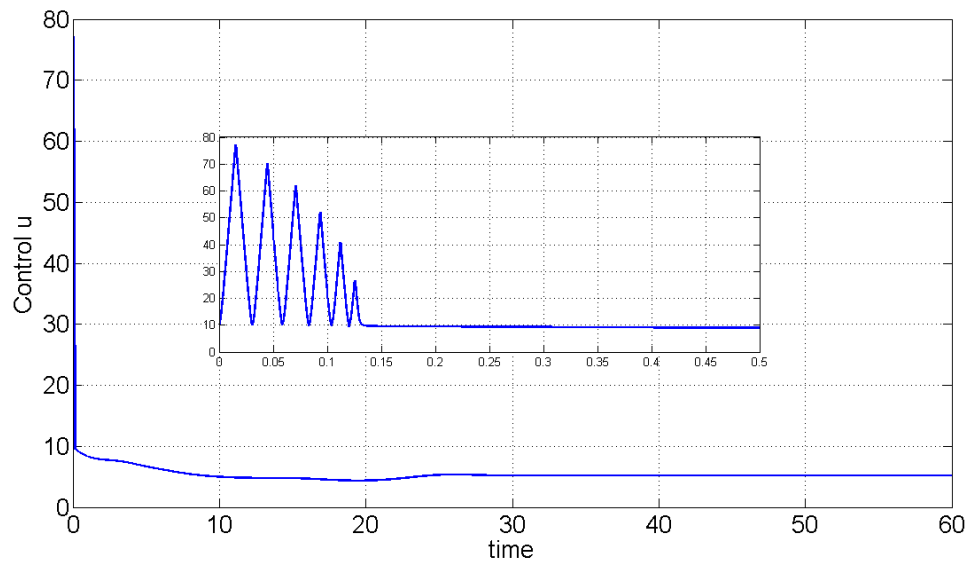
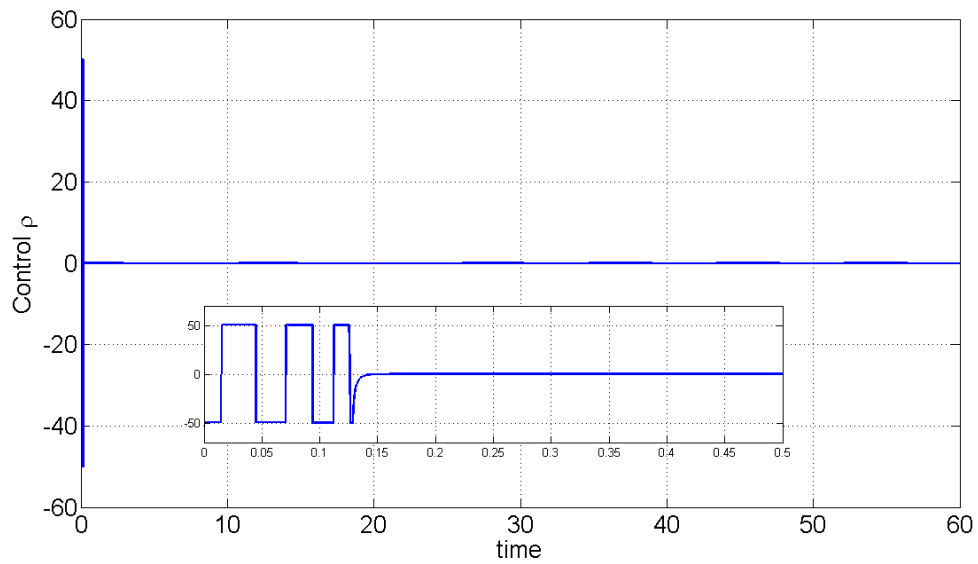


Figure 5.3. Errors e_p , e_q , ξ and η

**Figure 5.4.** *Control u* **Figure 5.5.** *Control ρ*

5.6 Summary

In this chapter, we have addressed the problem of path following using a target point rigidly attached to a car type vehicle, by controlling only the orientation of the vehicle by its angular acceleration. The main idea was to determine a control law using saturation which ensures global stabilization in two steps. The proposed Lyapunov function forces the errors to enter a neighborhood of the origin in finite time. The Lyapunov analysis also shows that by a bootstrap procedure, this neighborhood contracts asymptotically to zero. Simulation results illustrate the GAS performance of the controller.

Chapter 6

Tracking of a Underactuated Marine Vessel

The next problem related to underactuated systems, as introduced in Chapter 4, is the precise tracking of surface marine vessels. In this chapter, we consider the problem of tracking control of a 3-DOF vessel model (surge, sway and yaw [31]), working under two independent actuators capable of generating surge force and yaw moment only.

6.1 State-of-the-art and contribution

Precise tracking control of surface marine vessels (ships and boats) is often required in critical operations such as support around off-shore oil rigs [69]. It has been shown in [12, 20, 94] that under Brockett's necessary condition [12], stabilization of this system is impossible with continuous or discontinuous time-invariant state feedback. This can be seen in [34] where the authors developed a continuous time-invariant controller that achieved global exponential position tracking but the vessel orientation could not be controlled. In addition, it is shown in [76] that the underactuated ship can not be transformed into a driftless chained system; which means that the control techniques used for the similar problem of nonholonomic mobile robot control cannot be applied directly to the underactuated ship control. Accordingly, control of underactuated vessels in this configuration has been studied rigorously by contemporary researchers, examples of which are [70, 32, 5, 79, 14].

In [76], the author showed that under discontinuous time-varying feedback, the underactuated vessel is strongly accessible and small-time locally controllable at any equilibrium. A discontinuous time-invariant controller was proposed which showed exponential convergence of the vessel towards a desired equilibrium point, under certain hypotheses imposed on the initial conditions. In [69], a continuous periodic time-varying feedback controller was presented that locally exponentially stabilizes the system on the desired equilibrium point by using a global coordinate transformation to render the vessel's model homogenous. In [70], a combined integrator backstepping and averaging approach was used for tracking control, together with the continuous time-varying feedback controller for position and orientation control. This combined approach, later on used in [71], provides practical global exponential stability as the vessel converges to a neighborhood of the desired location or trajectory, the size of which can be chosen arbitrarily small. Jiang [43] used Lyapunov's direct method for global tracking under the assumption that the reference yaw velocity requires persistent excitation condition; therefore implying that a straight line trajectory could not be tracked. This drawback was overcome in [23] and [3]. Do et al. [23] proposed a Lyapunov based method and backstepping technique for stabilization and tracking of underactuated vessel. In this work, conditions were imposed on the trajectory to transform the tracking problem into dynamic positioning, circular path tracking, straight line tracking and parking.

6.1.1 Contribution

In this chapter, we address the global tracking control of underactuated vehicles, using saturated state feedback control. Our work addresses the particular case, that has not been treated in [23], i.e. the yaw angle of the tracked trajectory does not admit a limit at time goes to infinity. This research is therefore in the same direction as in [17], where the author achieved practical stability. Our algorithm provides asymptotic convergence to the tracked trajectory from any initial point. The advantage of using saturated controls is that the global asymptotic stability is ensured while the control inputs remain bounded, as real life actuators are all limited in output, see for instance [36]. The proposed controller has been proven to work with state measurements, as well as with observers in the case where all states may not be measured (cf. also [36]).

6.2 Problem Formulation

As derived in Chapter 4, the dynamics of the vessel, denoted by (S), are as follows,

$$(S) \begin{cases} \begin{pmatrix} \dot{x} \\ \dot{y} \end{pmatrix} &= R_{\psi} D_{\rho} \begin{pmatrix} u \\ v \end{pmatrix}, \\ \begin{pmatrix} \dot{u} \\ \dot{v} \end{pmatrix} &= -D \begin{pmatrix} u \\ v \end{pmatrix} - r A_1 \begin{pmatrix} u \\ v \end{pmatrix} + \tau_1 \begin{pmatrix} 1 \\ 0 \end{pmatrix}, \\ \dot{\psi} &= r, \\ \dot{r} &= \beta u v - r + \tau_2. \end{cases} \quad (6.1)$$

The goal of this work is tracking control of the presented underactuated marine vessel by controlling its position and orientation. The vessel is forced to follow a reference trajectory which is generated by a “virtual vessel”, as follows,

$$(S_{re}) \begin{cases} \begin{pmatrix} \dot{x}_{re} \\ \dot{y}_{re} \end{pmatrix} &= R_{\psi_{re}} D_{\rho} \begin{pmatrix} u_{re} \\ v_{re} \end{pmatrix}, \\ \begin{pmatrix} \dot{u}_{re} \\ \dot{v}_{re} \end{pmatrix} &= -D \begin{pmatrix} u_{re} \\ v_{re} \end{pmatrix} - r_{re} A_1 \begin{pmatrix} u_{re} \\ v_{re} \end{pmatrix} + \begin{pmatrix} 1 \\ 0 \end{pmatrix} \tau_{1,re}, \\ \dot{\psi}_{re} &= r_{re}, \\ \dot{r}_{re} &= \beta u_{re} v_{re} - r_{re} + \tau_{2,re}, \end{cases} \quad (6.2)$$

where all variables have similar meanings as in System (6.1). Tracking control is achieved by using saturated control inputs and under the assumption that the velocities are bounded [15, 49]. This assumption holds true physically as resistive drag forces increase as the velocity increases and therefore the latter cannot increase indefinitely if the control is bounded. These assumptions are also valid for the reference system and are formalized in the following manner:

Assumption 6.2.1. *There exist constraints on the control inputs such that*

$$|\bar{\tau}_1| \leq \bar{\tau}_{1,\max}, \quad |\bar{\tau}_2| \leq \bar{\tau}_{2,\max}, \quad (6.3)$$

where $\bar{\tau}_{1,\max}$ and $\bar{\tau}_{2,\max}$ are known positive constants. The forces $\tau_{1,re}$ and $\tau_{2,re}$ verify the same bounds as above and the reference angle ψ_{re} does not converge to a finite limit as t tends towards infinity.

The variable and time-scale change defined in the previous section requires the following new bounds to be defined for the new control inputs τ_1 and τ_2 , denoted by $\tau_{1,\max}$ and $\tau_{2,\max}$

respectively: $\tau_{1,max} = \frac{\bar{\tau}_{1,max}}{\rho d^2}$ and $\tau_{2,max} = \frac{\bar{\tau}_{2,max}}{d^2}$. We consider the following condition upon the saturation limits of the control inputs, to be used later on in the control design. We use here m_1 to denote $\min(a_1/2, b_1)$.

$$\mathbf{C1:} \quad \beta \frac{\tau_{1,max}^2}{a_1 m_1} < \tau_{2,max}. \quad (6.4)$$

Note that this condition is always satisfied by an appropriate choice of the parameter ρ . Our control objective is that (S) follows (S_{re}) . With respect to the frame of reference of the reference trajectory (S_{re}) , the error system is defined as

$$\begin{aligned} e_x &= \cos(\psi_{re})(x - x_{re}) + \sin(\psi_{re})(y - y_{re}), \\ e_y &= -\sin(\psi_{re})(x - x_{re}) + \cos(\psi_{re})(y - y_{re}), \\ e_u &= u - u_{re}, \quad e_v = v - v_{re}, \\ e_\psi &= \psi - \psi_{re}, \quad e_r = r - r_{re}. \end{aligned} \quad (6.5)$$

Defining new controllers w_1 and \tilde{w}_2 , as follows, $w_1 := \tau_1 - \tau_{1,re}$ and $\tilde{w}_2 := \tau_2 - \tau_{2,re}$, the dynamics of system (6.5) becomes

$$(S_e) \left\{ \begin{aligned} \begin{pmatrix} \dot{e}_x \\ \dot{e}_y \end{pmatrix} &= -r_{re} A_1 \begin{pmatrix} e_x \\ e_y \end{pmatrix} + D_\rho \begin{pmatrix} e_u \\ e_v \end{pmatrix} + \sin(e_\psi) A_1 D_\rho \begin{pmatrix} u_{re} \\ v_{re} \end{pmatrix} \\ &\quad + (\cos(e_\psi) - 1) D_\rho \begin{pmatrix} u_{re} \\ v_{re} \end{pmatrix} + (R_{e_\psi} - Id_2) \begin{pmatrix} e_u \\ e_v \end{pmatrix}, \\ \begin{pmatrix} \dot{e}_u \\ \dot{e}_v \end{pmatrix} &= -D \begin{pmatrix} e_u \\ e_v \end{pmatrix} - r_{re} A_1 \begin{pmatrix} e_u \\ e_v \end{pmatrix} - e_r A_1 \begin{pmatrix} u_{re} \\ v_{re} \end{pmatrix} + \begin{pmatrix} 1 \\ 0 \end{pmatrix} w_1 \\ &\quad + e_r \begin{pmatrix} -e_v \\ e_u \end{pmatrix}, \\ \dot{e}_\psi &= e_r, \\ \dot{e}_r &= \beta(uv - u_{re}v_{re}) - e_r + \tilde{w}_2. \end{aligned} \right.$$

The control objective is to force the error system (S_e) to 0, using w_1 and \tilde{w}_2 .

6.3 Controller design

We first develop the following intermediate result, concerning the bounds of u , v , r .

Lemma 6.3.1. *The variables u , v , r are bounded and satisfy*

$$\begin{aligned} \limsup_{t \rightarrow \infty} \|(u, v)\| &\leq \frac{\tau_{1,max}}{2\sqrt{a_1 m_1}}, \\ \limsup_{t \rightarrow \infty} |r| &\leq \tau_{2,max} + \beta \frac{\tau_{1,max}^2}{2a_1 m_1}. \end{aligned} \quad (6.6)$$

Proof. Let us consider

$$\begin{aligned} u\dot{u} + v\dot{v} &= u(-a_1u + rv + \tau_1) + v(-b_1v - ru) \\ &\leq -\frac{a_1}{2}u^2 - b_1v^2 + \frac{\tau_1^2}{2a_1} \leq -m_1(u^2 + v^2) + \frac{\tau_1^2}{2a_1}, \end{aligned}$$

then deriving the first inequality in (6.6). Similarly, consider the following equation, $r\dot{r} = -r^2 - r(\tau_2 + \beta uv) = -r(r + \tau_2 + \beta uv)$, from which we derive the second inequality in (6.6). \square

Remark 6.3.2. *As the reference trajectory system is similar to the vessel model, it can be shown that the limits defined in Lemma 6.3.1 are valid for u_{re} , v_{re} , r_{re} as well.*

We define a new control variable $w_2 := \beta(uv - u_{re}v_{ref}) + \bar{w}_2$. As the upper bounds of u , v , u_{re} and v_{ref} are known according to Lemma 6.3.1 and Remark 6.3.2, we obtain

$$\limsup_{t \rightarrow \infty} \beta |uv - u_{re}v_{ref}| \leq \beta \frac{\tau_{1,max}^2}{a_1 m_1}. \quad (6.7)$$

If $|w_2| \leq U_2$, for a positive constant U_2 , one must have $U_2 + \beta \frac{\tau_{1,max}^2}{a_1 m_1} \leq \tau_{2,max}$, which is guaranteed by Condition **C1**. With these preliminaries established, we will now proceed to fulfill the control objective by using the bounded controls w_1 and w_2 . Let $\sigma(\cdot)$ be the standard saturation function, i.e., $\sigma(t) = \frac{t}{\max(1, |t|)}$. The main result of this work is given next.

Theorem 6.3.3. *If Assumption 6.2.1 and Condition **C1** are fulfilled, then for an appropriate choice of constants U_1 , ρ_1 , ξ , M , U_2 , k_1 , k_2 , μ , the following controller ensures global asymptotic stability of the tracking error system (S_e) :*

$$\begin{aligned} w_1 &= -U_1 \sigma\left(\frac{\xi e_u}{U_1}\right) - \rho_1 \sigma\left(M(e_x + \frac{1}{\mu} e_u)\right), \\ w_2 &= -U_2 \sigma\left(\frac{k_1}{U_2} e_\psi + \frac{k_2 - 1}{U_2} e_r\right). \end{aligned} \quad (6.8)$$

Proof of Theorem 6.3.3.

We first consider the errors e_ψ and e_r and take $k_1, k_2 > 0$ large in the control input w_2 defined previously. The dynamics of e_ψ and e_r in (S_e) $\dot{e}_\psi = e_r$ and $\dot{e}_r = -e_r - U_2 \sigma\left(\frac{k_1}{U_2} e_\psi + \frac{k_2 - 1}{U_2} e_r\right)$.

Lemma 6.3.4. *If $U_2 > 0$ and $k_1 > k_2 - 1 > 0$, then after a sufficiently large time, the saturated control operates in its linear region and the errors e_ψ and e_r converge to zero exponentially.*

Proof. Let us consider the Lyapunov function V ,

$$V = \frac{\alpha}{2} e_r^2 + S \left(\frac{k_1}{U_2} e_\psi + \frac{k_2 - 1}{U_2} e_r \right), \quad (6.9)$$

where $S(\xi) := \int_0^\xi \sigma(s) ds$, and $\alpha = \frac{k_1 - k_2 + 1}{U_2^2} > 0$. Set $z := \frac{k_1}{U_2} e_\psi + \frac{k_2 - 1}{U_2} e_r$. Then, one has

$$\dot{V} = \alpha e_r \dot{e}_r + \sigma(z) \dot{z} = -\alpha e_r^2 - (k_2 - 1) \sigma^2(z). \quad (6.10)$$

Then $\dot{V} < 0$ for $(e_\psi, e_r) \neq (0, 0)$; and after a finite time we obtain $\left| \frac{k_1}{U_2} e_\psi + \frac{k_2 - 1}{U_2} e_r \right| \leq 1$. The dynamics of e_ψ and e_r becomes linear, i.e., $\dot{e}_\psi = e_r$ and $\dot{e}_r = -k_1 e_\psi - k_2 e_r$. As $k_1, k_2 > 0$, (e_ψ, e_r) converges exponentially to zero. \square

Lemma 6.3.4 shows that the errors e_ψ and e_r converge to zero under the control w_2 . We will now consider the errors e_u and e_v . We choose the constants μ and ξ such that $a_1 + \xi = \mu\rho$ and $b_1 = \mu c\rho$, implying that $\xi = b_1/c - a_1$ and $\mu > 0$.

Lemma 6.3.5. *Consider the dynamics of e_u and e_v given in Equation (6.6). If U_1 and ρ are chosen as $a_1 > U_1 + \rho$ and $U_1 > \frac{|a_1 - \frac{b_1}{c}|}{\min(a_1, \frac{b_1}{c})} \rho$, then the control $w_1 := -U_1 \sigma\left(\frac{\xi e_u}{U_1}\right) - \rho \sigma_1(\cdot)$, with $\sigma_1(\cdot)$ to be chosen later, ensures that e_u and e_v satisfy the following inequalities:*

$$\begin{aligned} \limsup_{t \rightarrow \infty} \|(e_u, e_v)\| &\leq \frac{\rho}{\sqrt{m_2 \tilde{a}}}, \\ \text{with } \tilde{a} &= \inf_{t > 0} \left(a_1 + \xi \frac{\sigma\left(\frac{\xi e_u}{U_1}\right)}{\frac{\xi e_u}{U_1}} \right) > 0, \quad m_2 := \min(\tilde{a}/2, b_1). \end{aligned} \quad (6.11)$$

Proof. Notice that $\tilde{a} > 0$ since it is trivially the case if $\xi \geq 0$, and otherwise, $\tilde{a} \geq a_1 + \xi = \frac{b_1}{c}$. Then, one has $e_u \dot{e}_u + e_v \dot{e}_v = -a_1 e_u^2 - b_1 e_v^2 + e_r(e_u v_{re} - e_v u_{re}) + e_u w_1$. By applying the control w_1 , we get $e_u \dot{e}_u + e_v \dot{e}_v \leq -a_1 e_u^2 - b_1 e_v^2 - U_1 e_u \sigma\left(\frac{\xi e_u}{U_1}\right) - \rho e_u \sigma_1(\cdot) + C_0 |e_r| \sqrt{e_u^2 + e_v^2}$, where $C_0 := \bar{u}_{max} + \bar{v}_{max}$. According to Lemma 6.3.4, e_r tends to zero, i.e., for large t , one has $e_u \dot{e}_u + e_v \dot{e}_v \leq -[a_1 + \xi s(t)] e_u^2 - b_1 e_v^2 - \rho e_u \sigma_1(\cdot)$. Then (6.11) results from the following inequality

$$e_u \dot{e}_u + e_v \dot{e}_v \leq -m_2(e_u^2 + e_v^2) + \frac{\rho^2 \sigma_1^2(\cdot)}{\tilde{a}}. \quad (6.12)$$

\square

Lemma 6.3.5 proves the convergence of e_u and e_v to a neighborhood of zero. Since $\tilde{a} \geq \min\left(a_1, \frac{b_1}{c}\right)$, one gets that $\limsup_{t \rightarrow \infty} \left| \frac{\xi e_u}{U_1} \right| < 1$, and the controller exits saturation in finite

time and enter its linear region of operation. We get $\sigma\left(\frac{\xi e_u}{U_1}\right) = \frac{\xi e_u}{U_1}$, and the dynamics of e_u and e_v become

$$\begin{aligned}\dot{e}_u &= -\mu\rho e_u + r_{re}e_v - \rho\sigma_1(.) + e_r v_{re} - e_r e_v, \\ \dot{e}_v &= -\mu c\rho e_v - r_{re}e_u - e_r u_{re} + e_r e_u.\end{aligned}$$

Define $W = (W_1, W_2)^T := (e_x, e_y)^T + (e_u, e_v)^T/\mu$. Then one has the following result.

Lemma 6.3.6. *Let W defined previously and the controller w_1 given in (6.8) with $\sigma_1(.) = \sigma(MW_1)$, where M is an arbitrary positive constant. Then W tends to a finite limit $\bar{W} = (0, \bar{W}_2)^T$.*

Proof. The dynamics of W can be expressed as

$$\begin{aligned}\dot{W} &= -r_{re}A_1W + \frac{r_{re}}{\mu}A_1\begin{pmatrix} e_u \\ e_v \end{pmatrix} + \sin(e_\psi)A_1D_\rho\begin{pmatrix} u_{re} \\ v_{re} \end{pmatrix} \\ &\quad + O\left(e_\psi^2, |e_\psi|\begin{pmatrix} e_u \\ e_v \end{pmatrix}\right) - r_{re}\frac{A_1}{\mu}\begin{pmatrix} e_u \\ e_v \end{pmatrix} \\ &\quad - \frac{\rho}{\mu}\sigma(MW_1)\begin{pmatrix} 1 \\ 0 \end{pmatrix} + O(|e_r|(1 + \|(e_u, e_v)\|)).\end{aligned}$$

In order to find the limsup of $\|W\|$, we calculate

$$\begin{aligned}W^T\dot{W} &= \sin(e_\psi)W^TA_1D_\rho\begin{pmatrix} u_{re} \\ v_{re} \end{pmatrix} - \frac{\rho}{\mu}W_1\sigma(MW_1) \\ &\quad + W^T\left[O\left(e_\psi^2, |e_\psi|\begin{pmatrix} e_u \\ e_v \end{pmatrix}\right) + O(|e_r|)\right], \\ &= O(\|W\| \cdot \|e_\psi, e_r\|) - \frac{\rho}{\mu}W_1\sigma(MW_1),\end{aligned}$$

which implies that $|W^T\dot{W}| + \frac{\rho}{\mu}W_1\sigma_1(MW_1) \leq \|W\|O(\|e_\psi, e_r\|)$. One deduces first that the time derivative of $\|W\|$ is integrable over \mathbb{R}_+ and thus W admits a limit as t tends to infinity. Therefore, the right-hand side of the previous inequality is integrable over \mathbb{R}_+ implying the same conclusion for $W_1\sigma(MW_1)$. As both W_1 and \dot{W}_1 are bounded, then according to Barbalat's Lemma, $W_1 \rightarrow 0$ as $t \rightarrow \infty$. Consequently W_2 tends towards a finite value \bar{W}_2 as t tends to infinity. \square

Lemma 6.3.6 permits us to further improve the result of Lemma 6.3.5, as follows.

Lemma 6.3.7. *If Lemmas 6.3.5 and 6.3.6 hold true, then e_u and e_v converge to zero asymptotically.*

Proof. From Lemma 6.3.5 and setting $G(e_u, e_v) := (e_u^2 + e_v^2)/2$, Equation (6.12) is rewritten as $\dot{G} + 2m_2 G \leq \frac{\rho^2 \sigma_1^2(MW_1)}{\tilde{a}}$. One concludes using Barbalat's Lemma. \square

So far, we have established that the errors e_ψ , e_r , e_u and e_v converge to zero. From Lemmas 6.3.6 and 6.3.7, we deduce that if $W_1 \rightarrow 0$ and $e_u \rightarrow 0$, then e_x will converge asymptotically to zero as well. We next address the convergence of the remaining error variable, e_y .

Lemma 6.3.8. *If Assumption 6.2.1 is satisfied, then $\tilde{W}_2 = 0$ and e_y converges asymptotically to zero.*

Proof. From Equation (6.13) in Lemma 6.3.6, the dynamics of W can be expressed as follows, $\dot{W} = -r_{re} A_1 W + O(|e_\psi|, |e_r|, W_1 \sigma(MW_1))$. We define the new variable \tilde{W} as follows, $\tilde{W} := R_{\psi_{re}} W$, and the dynamics of \tilde{W} is given by

$$\begin{aligned} \dot{\tilde{W}} &= \dot{\psi}_{re} A_1 R_{\psi_{re}} W - r_{re} R_{\psi_{re}} A_1 W + R_{\psi_{re}} O(|e_\psi|, |e_r|, W_1 \sigma(MW_1)) \\ &= O(|e_\psi|, |e_r|, W_1 \sigma(MW_1)). \end{aligned}$$

Since e_ψ and e_r converge exponentially to zero and $W_1 \sigma(MW_1)$ is integrable over \mathbb{R}_+ , then $\|\tilde{W}\|$ is also integrable over \mathbb{R}_+ , which means that \tilde{W} converges to a finite limit W^l . Then, one gets that $-W_2 \sin(\psi_{re})$ and $W_2 \cos(\psi_{re})$ tend to W_1^l and W_2^l respectively, as t tends to infinity. If $\tilde{W}_2 \neq 0$, then one easily shows that ψ_{re} converges to a finite limit by considering whether $(W_{re})_2 = 0$ or not. That contradicts Assumption 2 and W must converge asymptotically to as well as e_y . \square

It should be noted that the controller presented in Theorem 1 has been designed under the assumption that all state variables are known. In the next section, the study is extended to the case where only the position and orientation states of the vessel are available and the velocities need to be observed.

6.4 Tracking without velocity measurement

In practical cases, only position and orientation feedbacks are available for navigation. Therefore the only available states of the vessel are x , y , ψ along with the complete

coordinate state set of the virtual vessel to be followed. For such output feedback systems, the variables u, v, r need to be observed. In this section, we will show that the controller presented in Theorem 6.3.3 is applicable in this case and the use of observation instead of measurement does not affect the stability. We suppose that the velocities are obtained through an observer such as that presented by Fossen and Strand in [33], or a robust differentiator such as that presented in [16]. In both cases, observation errors converge exponentially to zero. It can be noted that, when we use a differentiator, the estimated values $(\hat{u}, \hat{v}, \hat{r})$ of (u, v, r) , can be determined according to the following equation $(\hat{u}, \hat{v})^T = D_\rho^{-1} R_{-\psi}(\hat{x}, \hat{y})^T$ and $\hat{r} = \hat{\psi}$, where $(\hat{x}, \hat{y}, \hat{\psi})$ are the estimated values of (x, y, ψ) respectively.

Let us follow the same steps used in the demonstration of stability of system (S_e) with velocity measurement. The observation error related to the velocity are define as below: $f_u = u - \hat{u}$, $f_v = v - \hat{v}$ and $f_r = r - \hat{r}$. As the references are common, the observation errors can be described in terms of trajectory pursuit errors as $f_u = e_u - \hat{e}_u$, $f_v = e_v - \hat{e}_v$, and $f_r = e_r - \hat{e}_r$, where, $\hat{e}_u = \hat{u} - u_{re}$, $\hat{e}_v = \hat{v} - v_{re}$ and $\hat{e}_r = \hat{r} - r_{re}$. We note that the variable x, y, ψ are measured and the related observation errors are null. The problem is transformed to demonstrate the stability of the error system (S_e) under control laws w_1 and \tilde{w}_2 , which are now based on the observed values.

As in the previous case, we define $w_2 := \beta(\hat{u}\hat{v} - u_{re}v_{re}) + \tilde{w}_2$. Then the result of this section can be stated as the following theorem.

Theorem 6.4.1. *If Assumption 6.2.1 and Condition C1 are fulfilled, then for an appropriate choice of constants U_1 , ρ , ξ , M , U_2 , k_1 , k_2 , μ , the following controller ensures global asymptotic stability of the tracking error system (S_e) :*

$$\begin{aligned} w_1 &= -U_1 \sigma \left(\frac{\xi \hat{e}_u}{U_1} \right) - \rho \sigma \left(M(e_x + \frac{1}{\mu} \hat{e}_u) \right), \\ w_2 &= -U_2 \sigma \left(\frac{k_1}{U_2} e_\psi + \frac{k_2 - 1}{U_2} \hat{e}_r \right), \end{aligned} \quad (6.13)$$

if in addition the observer errors f_u , f_v and f_r converge asymptotically to zero and are integrable over \mathbb{R}_+ (i.e., the integrals of their norms over \mathbb{R}_+ are finite).

Remark 6.4.2. *The choice of constants U_1 , ρ , ξ , M , U_2 , k_1 , k_2 , μ remain the same as in the case of Theorem 6.3.3, therefore their expressions and conditions will not be repeated in this section.*

Proof. The proof of Theorem 6.4.1 is largely based upon the proof of Theorem 6.3.3, and

is developed similarly. We first consider the dynamics of error variables e_ψ and e_r :

$$\dot{e}_\psi = e_r, \quad \dot{e}_r = -e_r - U_2 \sigma \left(\frac{k_1}{U_2} e_\psi + \frac{k_2 - 1}{U_2} e_r + f_1(t) \right) + f_2(t), \quad (6.14)$$

where $f_1(t) = -\frac{k_2 - 1}{U_2} f_r$ and $f_2(t) = \beta(uv - \hat{u}\hat{v})$.

Lemma 6.4.3. *If $f_1(t)$ and $f_2(t)$ converge to zero asymptotically, then for some large positive constants k_1 and k_2 , System (6.14) is globally asymptotically stable.*

Proof. Consider the Lyapunov function V defined in (6.9). If $z := \frac{k_1}{U_2} e_\psi + \frac{k_2 - 1}{U_2} e_r$, one gets

$$\begin{aligned} \dot{V} &= \alpha e_r \dot{e}_r + \sigma \left(\frac{k_1}{U_2} e_\psi + \frac{k_2 - 1}{U_2} e_r \right) \left[\frac{k_1}{U_2} \dot{e}_\psi + \frac{k_2 - 1}{U_2} \dot{e}_r \right], \\ &= \alpha e_r (-e_r - U_2 \sigma(z + f_1) + f_2) \\ &\quad + \sigma(z) \left[\frac{k_1}{U_2} e_r + \frac{k_2 - 1}{U_2} (-e_r - U_2 \sigma(z + f_1) + f_2) \right]. \end{aligned} \quad (6.15)$$

Using the inequality, $|ab| \leq \frac{a^2 + b^2}{2}$, and taking $\alpha U_2 = \frac{k_1 - k_2 + 1}{U_2} > 0$, we get

$$\begin{aligned} \dot{V} &\leq -\frac{\alpha}{2} e_r^2 - (k_2 - 1) \sigma(z) \sigma(z + f_1) \\ &\quad + \alpha U_2 e_r (\sigma(z) - \sigma(z + f_1)) + \frac{\alpha}{2} f_2^2 + \frac{k_2 - 1}{U_2} |f_2|. \end{aligned}$$

Using the inequalities $|\sigma(z) - \sigma(z + f_1)| \leq |f_1|$ and $\sigma(z) \sigma(z + f_1) \geq \sigma^2(z) - |f_1|$, one has

$$\begin{aligned} \dot{V} &\leq -\frac{\alpha}{2} e_r^2 - (k_2 - 1) \sigma^2(z) + (k_2 - 1) |f_1| \\ &\quad + \alpha U_2 |e_r| |f_1| + \frac{\alpha}{2} f_2^2 + \frac{k_2 - 1}{U_2} |f_2|. \end{aligned}$$

After a sufficiently large time interval T , it is assured that $|U_2 f_1| < \frac{1}{6} \forall t > T$, and

$$\dot{V} \leq -\frac{\alpha}{3} e_r^2 - (k_2 - 1) \sigma^2(z) + O(f_1^2, |f_2|, f_2^2). \quad (6.16)$$

From here, we obtain that $\limsup_{t \rightarrow \infty} |e_r| = \limsup_{t \rightarrow \infty} |\sigma(z)| = 0$. \square

Following the same steps as used in the previous section, we now demonstrate the convergence of the error variables (e_u, e_v, e_x, e_y) of System (S_e).

Lemma 6.4.4. *Consider the dynamics of e_u and e_v presented in Equation (6.6). Then, the control*

$$w_1 = -U_1 \sigma \left(\frac{\xi \hat{e}_u}{U_1} \right) - \rho_1 \sigma_1(.) \quad (6.17)$$

ensures that e_u and e_v are bounded and again verify the estimate (6.11).

Proof. The argument exactly follows the line of the argument of Lemma 6.3.5 with the controller w_1 written as $w_1 := -U_1\sigma\left(\frac{\xi e_u}{U_1} + f\right) - \rho_1\sigma_1(\cdot)$, where $f := -\frac{\xi}{U_1}f_u$ converges to zero asymptotically and is integrable over \mathbb{R}_+ , and by using the inequality $x\sigma(x+f) \geq x\sigma(x) - |x\sigma(f)|$. \square

Similarly, the proof of convergence of W_1 to zero and W_2 to a finite limit, presented in Lemma 6.3.8, holds true and one concludes by showing that the limit of W_2 is zero as well. \square

6.5 Simulations

The performance of the presented controller is illustrated by simulation. We apply the controller on an example of a monohull vessel, as considered in [23]. The length of this vessel is 32 m, and a mass of 118×10^3 kg. The parameters of the damping matrices as given as follow:

$$\begin{aligned} d_1 &= 215 \times 10^2 \text{ Kg s}^{-1}, & d_2 &= 97 \times 10^3 \text{ Kg s}^{-1}, \\ d_3 &= 802 \times 10^4 \text{ Kg m}^2 \text{ s}^{-1}, & m_1 &= 120 \times 10^3 \text{ Kg}, \\ m_2 &= 172.9 \times 10^3 \text{ Kg}, & m_3 &= 636 \times 10^5 \text{ Kg m}^2. \end{aligned} \quad (6.18)$$

Based on these physical parameters, we find the parameters of System (5.21) as

$$a = 0.179, \quad b = 0.561, \quad c = 0.694, \quad \beta = 0.126, \quad \kappa = 8.32 \times 10^{-4}. \quad (6.19)$$

Then, the parameters of the controller and the normalized system (S) are given by

$$\begin{aligned} a_1 &= 1.421, & b_1 &= 4.449, & d &= 0.126, \\ k_1 &= 10, & k_2 &= 10, & U_2 &= 0.1, \\ U_1 &= \frac{a_1}{2}, & \rho &= \frac{a_1}{4}, & M &= 0.1. \end{aligned}$$

The reference trajectory is generated by considering the surge force and the yaw moment as constants $\tau_{1,re} = 10$ and $\tau_{2,re} = 0.05$ with the initial values

$$\begin{aligned} &(x_{re}(0), y_{re}(0), \psi_{re}(0), u_{re}(0), v_{re}(0), r_{re}(0)) \\ &= (0 \text{ m}, 0 \text{ m}, 0 \text{ rad}, 0 \text{ ms}^{-1}, 0 \text{ ms}^{-1}, 0 \text{ rads}^{-1}). \end{aligned}$$

The initial conditions of the vessel are as follows:

$$\begin{aligned} &(x(0), y_{re}(0), \psi(0), u(0), v(0), r(0)) \\ &= \left(50 \text{ m}, -150 \text{ m}, \frac{\pi}{4} \text{ rad}, 50 \text{ ms}^{-1}, 0 \text{ ms}^{-1}, 0 \text{ rads}^{-1}\right). \end{aligned}$$

The reference trajectory and the vessel are shown in a 2D coordinate plane in Figure 6.1. The vessel converges to the reference trajectory asymptotically and similarly for the position errors graph in Figure 6.2. The orientation error and its derivative also converge to zero, as seen in Figure 6.4. The convergence of e_u and e_v is shown in Figure 6.3. Figures 6.5 and 6.6 show the control signals τ_1 and τ_2 respectively and the controllers are clearly bounded. This is an essential property in real systems, where the control signals are constrained.

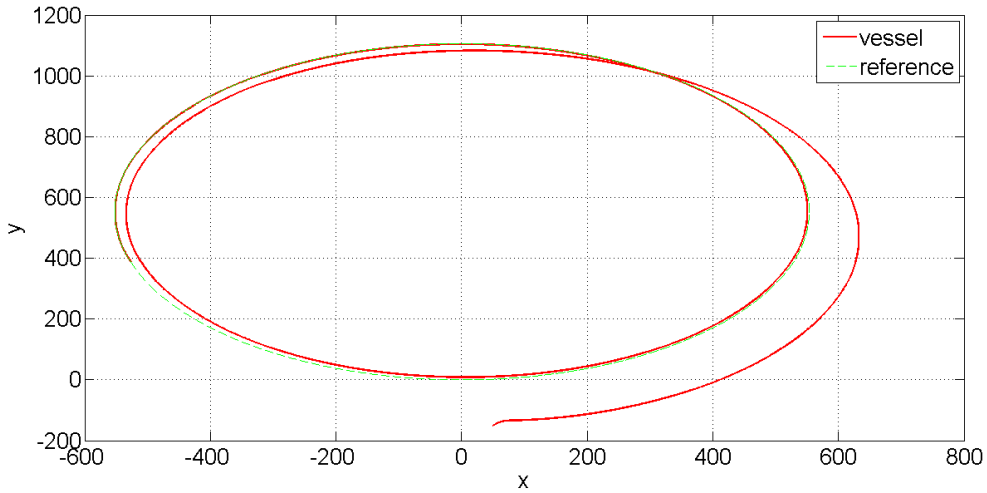
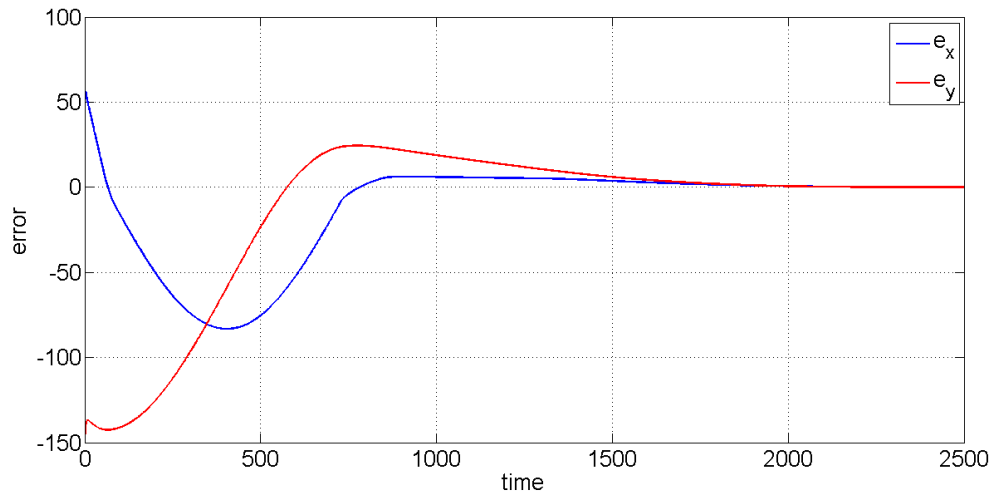
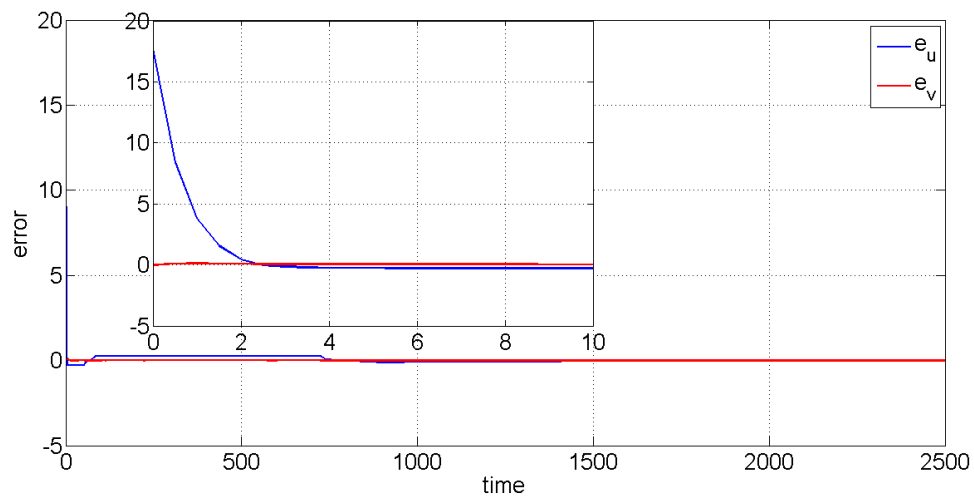


Figure 6.1. *Reference trajectory and the vessel*

6.6 Summary

In this chapter, we have addressed the problem of tracking of an underactuated surface vessel with only surge force and yaw moment. The proposed controller ensures global asymptotic tracking of the vessel, following a reference trajectory modeled by a virtual vessel. It is also shown that the stability of the system is not affected if the state measurements are replaced by observers. The using of saturated inputs is essential as in real life the actuators have limited output. Simulation results illustrate the performance of the controller.

**Figure 6.2.** Errors e_x and e_y **Figure 6.3.** Errors e_u and e_v

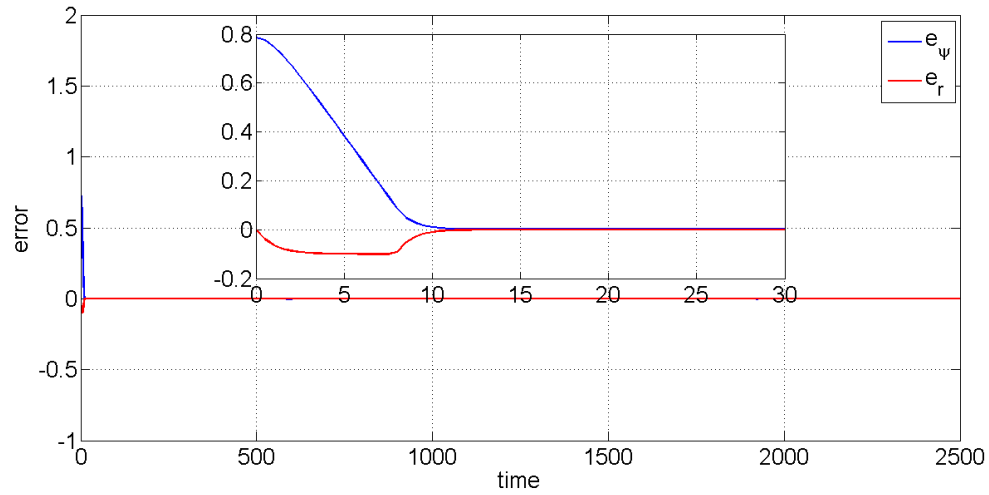


Figure 6.4. Errors e_ψ and e_r

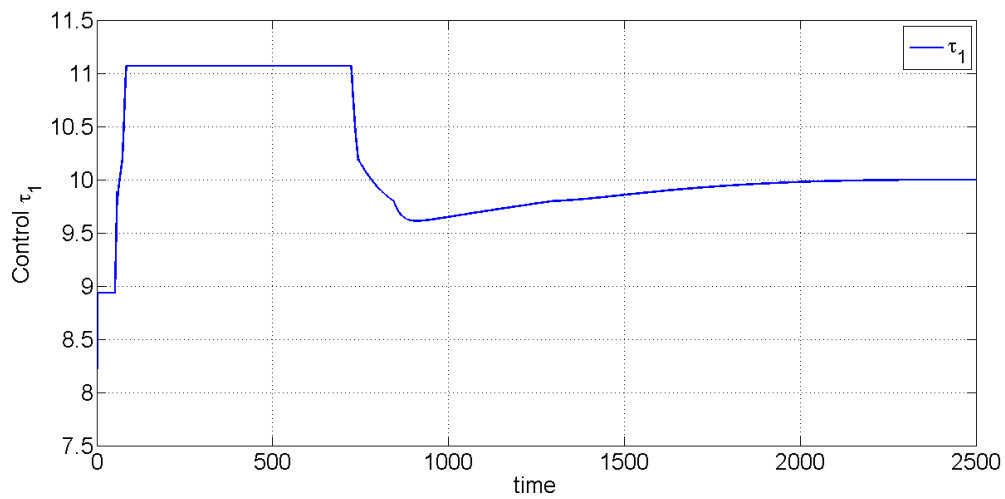
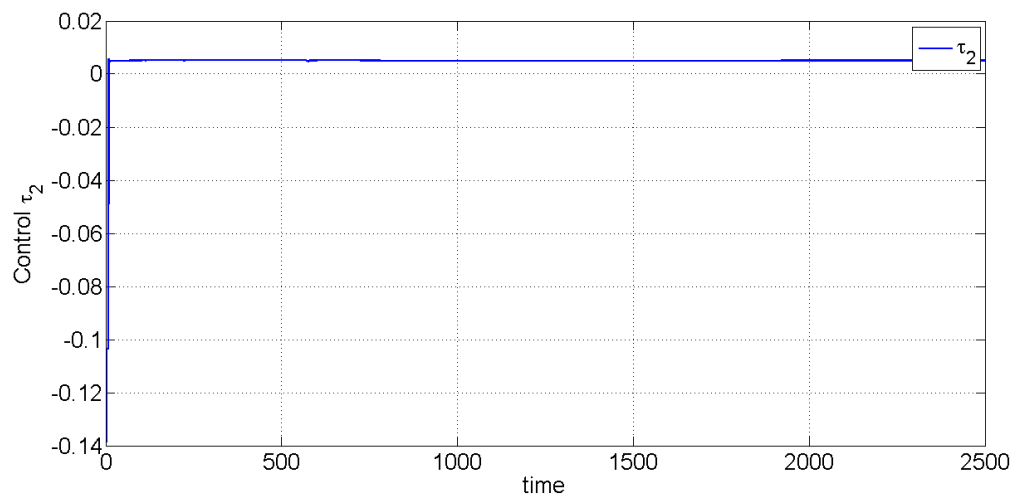


Figure 6.5. Control τ_1

**Figure 6.6.** *Control τ_2*

Conclusion and Perspectives

Overview

In this thesis, two nonlinear control problems were studied and contributions were presented for their solution. The first problem consisted of control of nonlinear uncertain systems. The second problem was related to control of underactuated systems. Accordingly, the report was divided in two parts

In the first part, higher order sliding mode controllers were studied as a means of controlling nonlinear systems with parametric uncertainty. After a detailed state-of-the-art study, the advantages and shortcomings of existing controllers were identified. Then, Lyapunov-based robust and adaptive arbitrary HOSM controllers were proposed for these systems. These controllers were designed using a class of controllers for finite-time stabilization of pure integrator chains. The main contributions in this regard are the existence of a Lyapunov function for control design for both the robust and adaptive controllers and the development of the first adaptive arbitrary HOSM controller. The performance of these controllers was demonstrated using a Hardware-in-Loop fuel cell emulation system. The control problem addressed in this example was the control of the air-feed system of the fuel cell in order to optimize the net power output. The results showed that both the robust and adaptive controllers achieved the control objective successfully, and their output performance was comparable to existing controllers in the contemporary literature.

Then, it was shown that the homogeneity degree of controllers can be manipulated in order to achieve different characteristics in them. A general form of the controllers was formulated, based on Hong's homogeneous finite-time controller [39] for the stabilization of pure integrator chains. It was observed that for a particular choice of homogeneity degree, Levant's arbitrary HOSM controller [55] became a particular case of this general controller.

Then, by switching the homogeneity degree, a bounded controller was developed with minimum amplitude of discontinuity after convergence. The switching of homogeneity degree also permitted to design a fixed-time controller.

In the next part, the focus was on the control problems of underactuated systems. The first problem was the path-following of a car type vehicle, using target-point, rigidly attached to the vehicle. This was achieved by first transforming the problem of path-following into that of trajectory tracking, by defining the path curvature as a dynamic virtual vehicle. Saturated control laws were then developed, which ensured global stabilization. The proposed Lyapunov function forced the errors to enter a neighborhood of the origin in finite time. The Lyapunov analysis also showed that by a bootstrap procedure, this neighborhood contracts asymptotically to zero. Simulation results illustrate the GAS performance of the controller.

The next problem concerned tracking of an underactuated surface marine vessel with only surge force and yaw moment. Again, the controller design was based on saturated inputs and definition of the trajectory using a virtual vessel model. The proposed controller ensured global asymptotic tracking and it was shown that the stability of the system was not affected if the state measurements are replaced by observers. Simulation results illustrate the performance of the controller.

Conclusion

This thesis required an in-depth comprehension of nonlinear systems and the problems associated with specific types of these systems. The scope required simultaneous study of many different domains in nonlinear control. The results of the developments presented in the thesis were satisfactory and the significance of the contributions was established in accordance with the contemporary research work.

Future Research

There are many remained directions in which the research can be explored and improved. These include:

Generalization of the adaptation techniques for the higher order multi-input-multi-output systems.

Development of Lyapunov Based Adaptive HOSM controllers, ensuring real sliding mode, in which the output converges to a predetermined neighborhood.

Development of HOSM controllers that do not require many differentiators, such as supertwisting for second order sliding mode.

Development of adaptive observers in the same direction as adaptive controllers.

Application of bounded control to more complex underactuated systems, such as 3DOF Helicopters and submarine robots.

Inclusion of external constraints and disturbance in the study of underactuated systems, such as wind and waves in the case of ships and wind and road characteristics in the case of cars.

Bibliography

- [1] A.P. Aguiar and J.P. Hespanha. Trajectory-tracking and path-following of underactuated autonomous vehicles with parametric modeling uncertainty. *IEEE Transactions on Automatic Control*, 52(8):1362–1378, 2007. [cited at p. 79]
- [2] M.T. Angulo, J.A. Moreno, and L. Fridman. An exact and uniformly convergent arbitrary order differentiator. In *50th IEEE Conference on Decision and Control and European Control Conference (CDC-ECC)*, 2011. [cited at p. 94]
- [3] A. Behal, D.M. Dawson, W.E. Dixon, and Y. Fang. Tracking and regulation control of an underactuated surface vessel with nonintegrable dynamics. *IEEE Transactions on Automatic Control*, 47(3):495–500, 2002. [cited at p. 100]
- [4] S. Bennett. *A history of Control Engineering 1939-1955*. IEE Control Engineering Series, 1993. [cited at p. 1]
- [5] S.P. Berge, K. Ohtsu, and T.I. Fossen. Nonlinear control of ships minimizing the position tracking errors. *Modeling, Identification and Control*, 20(3):177–187, 1999. [cited at p. 5, 99]
- [6] M. Bertozzi and A. Broggi. Gold: a parallel realtime stereo vision system for generic obstacle and lane detection. *IEEE Transactions on Image Processing*, 7(1):62–81, 1998. [cited at p. 72, 80]
- [7] S.P. Bhat and D.S. Bernstein. Finite-time stability of continuous autonomous systems. *SIAM Journal of Control and Optimization*, 38(3):751 – 766, 2000. [cited at p. 4, 27, 29, 49, 50]

- [8] S.P. Bhat and D.S. Bernstein. Geometric homogeneity with applications to finite-time stability. *Mathematics of Control, Signals and Systems*, 17(2):101–127, 2005. [cited at p. 21, 33, 50, 51]
- [9] A.M Bloch and S Drakunov. Stabilization and tracking in the nonholonomic integrator via sliding modes. *Systems and Control Letters*, 29(2):91–99, October 1996. [cited at p. 3, 79]
- [10] A.M. Bloch, M. Reyhanoglu, and N.H. McClamroch. Control and stabilization of non-holonomic dynamic systems. *IEEE Transactions on Automatic Control*, 37(11):1746–1757, 1992. [cited at p. 3]
- [11] Vincent Bregeault. *Quelques contributions à la théorie de la commande par modes glissants*. PhD thesis, Ecole Centrale de Nantes. [cited at p. v, 18]
- [12] R.W. Brockett. Asymptotic stability and feedback stabilization. In *Differential Geometric Control Theory*, pages 181–191. Birkhauser, Boston, 1983. [cited at p. 99]
- [13] A. Broggi, M. Bertozzi, A. Fascioli, C.G. Lo Bianco, and A. Piazzzi. The argo autonomous vehicle’s vision and control systems. *International Journal of Intelligent Control and Systems*, 3(4):409–441, 1999. [cited at p. 4, 72, 80]
- [14] F. Bullo. Stabilization of relative equilibria for underactuated systems on Riemannian manifolds. *Automatica*, 36(12):1819–1834, 2000. [cited at p. 5, 99]
- [15] Y. Chitour. On the l^p -stabilization of the double integrator subject to input saturation. *ESAIM: Control, Optimisation and Calculus of Variations*, 6:291–331, 2001. [cited at p. vii, 5, 28, 71, 72, 94, 101]
- [16] Y. Chitour. On Time-Varying High-Gain Observers for Numerical Differentiation. *IEEE Transactions on Automatic Control*, 47(9):1565–1569, 2002. [cited at p. 107]
- [17] D. Chwa. Global Tracking Control of Underactuated Ships With Input and Velocity Constraints Using Dynamic Surface Control Method. *IEEE Transactions on Control Systems Technology*, 19(6):1357–1370, 2011. [cited at p. 74, 100]
- [18] L. Consolini, A. Piazzzi, and M. Tosques. Motion planning for steering car-like vehicles. In *European Control Conference*, Porto, Portugal, 2001. [cited at p. 5, 79]

- [19] L. Consolini, A. Piazzzi, and M. Tosques. A dynamic inversion based controller for path following of car-like vehicles. In *IFAC world congress*, 2002. [cited at p. 80]
- [20] J.M. Coron and L. Rosier. A relation between continuous time-varying and discontinuous feedback stabilization. *Journal of Mathematical Systems, Estimation and Control*, 4(1):67–84, 1994. [cited at p. 99]
- [21] M. Defoort, T. Floquet, A. Kokosy, and W. Perruquetti. A novel higher order sliding mode control scheme. *Systems and Control Letters*, 58(2):102 – 108, 2009. [cited at p. 19]
- [22] F. Dinuzzo and A. Fererra. Higher Order Sliding Mode Controllers with Optimal Reaching. *IEEE Transactions on Automatic Control*, 54(9):2126–2136, 2009. [cited at p. 16, 19]
- [23] K.D. Do, Z.P. Jiang, and J. Pan. Universal controllers for stabilization and tracking of underactuated ships. *Systems and Control Letters*, 47(4):299 – 317, 2002. [cited at p. 5, 100, 109]
- [24] K.D. Do, Z.P. Jiang, and J. Pan. A global output-feedback controller for simultaneous tracking and stabilization of unicycle-type mobile robots. *IEEE Transactions on Robotics and Automation*, 20(3):589–594, 2004. [cited at p. 79]
- [25] K.D. Do, Z.P. Jiang, and J. Pan. Simultaneous tracking and stabilization of mobile robots: an adaptive approach. *IEEE Transactions on Automatic Control*, 49(7):1147–1152, 2004. [cited at p. 79]
- [26] M. Egerstedt, X. Hu, and A. Stotsky. Control of mobile platforms using a virtual vehicle approach. *IEEE Transactions on Automatic Control*, 46(11):1777–1782, 2001. [cited at p. 79]
- [27] S.V. Emel’yanov, S.K. Korovin, and A. Levant. High-order sliding modes in control systems. *Computational Mathematics and Modeling*, 7(3):294–318, 1996. [cited at p. 3, 4, 11, 15]
- [28] I. Fantoni, R. Lozano, and M.W. Spong. Energy based control of the pendubot. *IEEE Transactions on Automatic Control*, 45(4):725–729, 2000. [cited at p. 67]
- [29] A.F. Filippov. *Differential Equations with Discontinuous Right-Hand Side*. Kluwer, Dordrecht, The Netherlands, 1988. [cited at p. 17]

- [30] M. Fliess, J. Levine, P. Martin, and P. Rouchon. A lie-backlund approach to equivalence and flatness of nonlinear systems. *IEEE Transactions on Automatic Control*, 44(5):922–937, 1999. [cited at p. 79]
- [31] T.I. Fossen. *Guidance and control of ocean vehicles*. Wiley, New York, 1994. [cited at p. 74, 99]
- [32] T.I. Fossen, J.M. Godhavn, S.P. Berge, and K.P. Lindegaard. Nonlinear control of underactuated ships with forward speed compensation. In *the IFAC NOLCOS'98*, 1998. [cited at p. 5, 99]
- [33] T.U. Fossen and J.P. Strand. Passive nonlinear observer design for ships using lyapunov methods: full-scale experiments with a supply vessel. *Automatica*, 35(1):3 – 16, 1999. [cited at p. 107]
- [34] J.M. Godhavn. Nonlinear tracking of underactuated surface vessels. In *the 35th IEEE Conference on Decision and Control*, 1996. [cited at p. 99]
- [35] A. Gruszka, M. Malisoff, and F. Mazenc. Tracking control and robustness analysis for pvtol aircraft under bounded feedbacks. *International Journal of Robust and Nonlinear Control*, 22(17):1899–1920, 2012. [cited at p. 93, 94]
- [36] A. Gruszka, M. Malisoff, and F. Mazenc. Bounded tracking controllers and robustness analysis for uavs. *IEEE Transactions on Automatic Control*, 58(1):180–187, 2013. [cited at p. 67, 100]
- [37] Ahmad Hably. *Approches bornées pour la commande des drones*. PhD thesis, INP Grenoble, 2007. [cited at p. 69]
- [38] M. Harmouche, S. Laghrouche, and Y. Chitour. Robust and adaptive higher order sliding mode controllers. In *IEEE 51st Annual Conference on Decision and Control (CDC)*, 2012. [cited at p. 54]
- [39] Y. Hong. Finite-time stabilization and stabilizability of a class of controllable systems. *Systems and Control Letters*, 46(4):231–236, 2002. [cited at p. 4, 6, 20, 21, 30, 31, 47, 49, 50, 54, 115]
- [40] X. Huang, W. Lin, and B. Yang. Global finite-time stabilization of a class of uncertain nonlinear systems. *Automatica*, 41(5):881–888, 2005. [cited at p. 30]

- [41] Y.J. Huang, T.C. Kuo, and S.H. Chang. Adaptive sliding-mode control for nonlinear systems with uncertain parameters. *IEEE Transactions on Automatic Control*, 38(2):534–539, 2008. [cited at p. 22]
- [42] A. Isidori. *Nonlinear control systems: An introduction (3rd ed.)*. Springer, Berlin, 1995. [cited at p. 1, 16]
- [43] Z.P. Jiang. Global tracking control of underactuated ships by lyapunov’s direct method. *Automatica*, 38(2):301–309, 2002. [cited at p. 100]
- [44] Z.P. Jiang, E. Lefeber, and H. Nijmeijer. Saturated stabilization and tracking of a non-holonomic mobile robot. *Systems & Control Letters*, 42(5):327–332, 2001. [cited at p. 5, 79]
- [45] Z.P. Jiang and H. Nijmeijer. Tracking control of mobile robots: A case study in backstepping. *Automatica*, 33:1393–1399, 1997. [cited at p. 79]
- [46] Hassan K. Khalil. *Nonlinear Systems*. Prentice Hall, New Jersey, USA, third edition, 2002. [cited at p. 1, 48, 70]
- [47] J. Kochalummoottil, Y.B. Shtessel, J.A. Moreno, and L. Fridman. Adaptive twist sliding mode control: A lyapunov design. In *50th IEEE Conference on Decision and Control and European Control Conference (CDC-ECC)*, 2011. [cited at p. vi, 23]
- [48] C. Kunusch, P.F. Puleston, M.A. Mayosky, and L. Fridman. Experimental results applying second order sliding mode control to a {PEM} fuel cell based system. *Control Engineering Practice*, 21(5):719 – 726, 2013. [cited at p. 34, 36]
- [49] S. Laghrouche, Y. Chitour, M. Harmouche, and F.S. Ahmed. Path following for a target point attached to a unicycle type vehicle. *Acta. Applicandae Mathematicae*, 2012. [cited at p. 28, 81, 101]
- [50] S. Laghrouche, M. Harmouche, and Y. Chitour. Target-point based path following controller for car-type vehicle using bounded feedback. In *IEEE 51st Annual Conference on Decision and Control (CDC)*, 2012. [cited at p. 28]
- [51] S. Laghrouche, F. Plestan, and A. Glumineau. Higher order sliding mode control based on integral sliding mode. *Automatica*, 43(3):531–537, 2007. [cited at p. 19]
- [52] J.P. Laumond, editor. *Robot motion planning and control*. Springer, 1998. [cited at p. 3]

- [53] T.C Lee, K.T Song, C.H Lee, and C.C Teng. Tracking control of unicycle-modeled mobile robots using a saturation feedback controller. *IEEE Transactions on Control Systems Technology*, 8(2):305–318, 2001. [cited at p. 80, 81]
- [54] A. Levant. Sliding order and sliding accuracy in sliding mode control. *International Journal of Control*, 58(6):1247–1263, 1993. [cited at p. v, 17, 18, 19, 32]
- [55] A. Levant. Universal Single-Input-Single-Output (SISO) Sliding-Mode Controllers With Finite-Time Convergence. *IEEE Transactions on Automatic Control*, 46(9):1447 – 1451, 2001. [cited at p. 4, 19, 21, 25, 47, 49, 55, 56, 61, 64, 115]
- [56] A. Levant. Higher-order sliding modes, differentiation and output-feedback control. *International Journal of Control*, 76(9/10):924 – 941, 2003. [cited at p. 21]
- [57] A. Levant. Homogeneity approach to high-order sliding mode design. *Automatica*, 41(5):823 – 830, 2005. [cited at p. 21, 54]
- [58] D. Liberzon, A.S. Morse, and E.D. Sontag. Output-input stability and minimum-phase nonlinear systems. *IEEE Transactions on Automatic Control*, 47(3):422 – 436, 2002. [cited at p. 16]
- [59] L. Ljung and T. Soderstrom. *Theory and Practice of Recursive Identification*. The MIT Press, Cambridge, MA. USA, 1983. [cited at p. 81]
- [60] C.G. Lo Bianco, A. Piazzzi, and M. Romano. Smooth motion generation for unicycle mobile robots via dynamic path inversion. *IEEE Transactions on Robotics*, 20(5):884–891, 2004. [cited at p. 79]
- [61] C. Low and D. Wang. Robust path following of car-like wmr in the presence of skidding effects. In *ICM '05. IEEE International Conference on Mechatronics*, 2005. [cited at p. 79]
- [62] A. Martynyuk and Y. A. Martynyuk. *Uncertain Dynamical Systems, Stability and Motion Control*. CRC Press, 2012. [cited at p. 2]
- [63] I. Matraji, S. Laghrouche, S. Jemei, and M. Wack. Robust control of the {PEM} fuel cell air-feed system via sub-optimal second order sliding mode. *Applied Energy*, 104(0):945 – 957, 2013. [cited at p. 34, 35, 36, 38]

- [64] A. Megretski. L2 BIBO output feedback stabilization with saturated control. In *13th IFAC World Congress*, 1996. [cited at p. 69]
- [65] P. Morin and C. Samson. Trajectory tracking for non-holonomic vehicles: overview and case study. In *Fourth International Workshop on Robot Motion and Control*, 2004. [cited at p. 80]
- [66] R.M. Murray and S.S. Sastry. Nonholonomic motion planning: steering using sinusoids. *IEEE Transactions on Automatic Control*, 38(5):700–716, 1993. [cited at p. 3]
- [67] R. Ortega, M.W. Spong, F. Gomez-Estern, and G. Blankenstein. Stabilization of a class of underactuated mechanical systems via interconnection and damping assignment. *IEEE Transactions on Automatic Control*, 47(8):1218–1233, 2002. [cited at p. 67]
- [68] W. Pasillas-Lepine. Hybrid modelling and limit cycle analysis for a class of anti-lock brake algorithms. In *International Symposium on Advanced Vehicle Control*, 2004. [cited at p. 80]
- [69] K.Y. Pettersen and O. Egeland. Exponential stabilization of an underactuated surface vessel. In *the 35th IEEE Conference on Decision and Control*, 1996. [cited at p. 5, 99, 100]
- [70] K.Y. Pettersen and H. Nijmeijer. Global practical stabilization and tracking for an underactuated ship : a combined averaging and backstepping approach . *Modeling, Identification and Control*, 20(4):189–199, 1999. [cited at p. 5, 99, 100]
- [71] K.Y. Pettersen and H. Nijmeijer. Underactuated ship tracking control: Theory and experiments. *International Journal of Control*, 74(14):1435–1446, 2001. [cited at p. 100]
- [72] A. Piazzzi, C.G. Lo Bianco, M. Bertozzi, A. Fascioli, and A. Broggi. Quintic g2-splines for the iterative steering of vision-based autonomous vehicles. *IEEE Transactions on Intelligent Transportations Systems*, 3(2):27–36, 2002. [cited at p. 4, 72, 80]
- [73] F. Plestan, Y. Shtessel, V. Brégeault, and A. Poznyak. New methodologies for adaptive sliding mode control. *International Journal of Control*, 83(9):1907 – 1919, 2010. [cited at p. v, 6, 22, 23, 28]
- [74] A. Polyakov. Nonlinear feedback design for fixed-time stabilization of linear control systems. *IEEE Transactions on Automatic Control*, 57(8):2106 –2110, 2012. [cited at p. 49, 50]

- [75] J. Pukrushpan, A. Stefanopoulou, and H. Peng. *Control of Fuel Cell Power Systems: Principles, Modeling and Analysis and Feedback Design*. Springer, 2004. [cited at p. 36]
- [76] M. Reyhanoglu. Control and stabilization of an underactuated surface vessel. In *the 35th IEEE Conference on Decision and Control*, 1996. [cited at p. 5, 99, 100]
- [77] L. Rosier. Homogeneous lyapunov function for homogeneous continuous vector field. *Systems and Control Letters*, 19(6):467 – 473, 1992. [cited at p. 51]
- [78] P. Rouchon, M. Fliess, J. Levine, and P. Martin. Flatness and motion planning: the car with n trailers. In *Proceedings of the European Control Conference, ECC'93*, 1993. [cited at p. 79]
- [79] C. Samson. Control of Chained Systems Application on Path Following and Time-Varying Point-Stabilization of Mobile Robots. *IEEE Transactions on Automatic Control*, 40(1):64–77, 1995. [cited at p. 5, 79, 99]
- [80] C. Samson and K. Ait-Abderrahim. Feedback control of a nonholonomic wheeled cart in cartesian space. In *Proc. International conference on robotics and automation*, 1991. [cited at p. 5, 79]
- [81] Y. Shtessel, M. Taleb, and F. Plestan. A novel adaptive gain supertwisting sliding mode controller: methodology and application. *Automatica*, 48(5):759–769, 2011. [cited at p. vi, 6, 23]
- [82] B. Siciliano and K.P. Valavanis. *Control problems in robotics and automation*. Springer, 1998. [cited at p. 2, 3]
- [83] J.J. Slotine. Sliding controller design for non-linear systems. *International Journal of Control*, 40(2):421 – 434, 1984. [cited at p. 3, 11]
- [84] H.J. Sussman, E.D. Sontag, and Y. Yang. A general result on the stabilization of linear systems using bounded controls. *Automatic Control, IEEE Transactions on*, 39(12):2411–2425, 1994. [cited at p. 67]
- [85] H.J. Sussman and Y. Yang. On the stability of multiple integrators by means of bounded feedback controls. *30 IEEE Conference on Decision and Control*, 1991. [cited at p. 67, 68]

- [86] M. Taleb, A. Levant, and F. Plestan. Pneumatic actuator control: Solution based on adaptive twisting and experimentation. *Control Engineering Practice*, 21(5):727 – 736, 2013. [cited at p. 6]
- [87] D.G. Taylor, P.V. Kokotovic, R. Marino, and I. Kanellakopoulos. Adaptive regulation of nonlinear systems with unmodelled dynamics. *IEEE Transactions on Automatic Control*, 34(4):405–412, 1989. [cited at p. 2]
- [88] A.R. Teel. Global stabilization and restricted tracking for multiple integrators with bounded controls. *Systems and Control Letters*, 40(3):165–171, 1995. [cited at p. 67, 68]
- [89] V.I. Utkin. *Sliding Mode Control and Optimization*. Springer, Verlag, Berlin, 1992. [cited at p. 2, 3, 11, 13, 15]
- [90] V.I. Utkin, J. Guldner, and J. Shi. *Sliding mode in control in electromechanical systems*. Taylor and Francis, London, 1999. [cited at p. 11]
- [91] M. Vidyasagar. *Nonlinear Systems Analysis*. Society for Industrial and Applied Mathematic, 2002. [cited at p. 1]
- [92] K.Y. Wichlund, O.J. Sørдалen, and O. Egeland. Control of vehicles with second-order nonholonomic constraints: Underactuated vehicles. In *Third European Control Conference ECC95*, 1995. [cited at p. 3]
- [93] K.D. Young, V.I. Utkin, and U. Ozguner. A control engineer’s guide to sliding mode control. *IEEE Transactions on Control System Technology*, 7(3):328–342, 1999. [cited at p. 3, 11]
- [94] J. Zabczyk. Some comments on stabilizability. *Journal of Applied Mathematics and Optimization*, 19(1):1–9, 1989. [cited at p. 99]

Appendices

Appendices

A Proof of technical lemmas

A.A Proof of Lemma 5.3.4

The transfer function related to System (5.35) is defined by

$$G(s) = (sI_2 - A)^{-1}, \quad (20)$$

and the L_2 -gain is defined by

$$\Upsilon_L = \sup_{\omega \in R} \bar{\sigma}(G(j\omega)). \quad (21)$$

where $\bar{\sigma}$ is the largest singular value of $G(j\omega)$. Since

$$S(\omega) := G(j\omega)G^*(j\omega) = \omega^2 I_2 + j\omega(A - A^T) + A^T A.$$

We define Υ_L^2 as the inverse of the smallest eigenvalue of $S(\omega)$:

$$S = \begin{bmatrix} k_1^2 + \omega^2 & k_1 k_2 + j\omega(1 + k_1) \\ k_1 k_2 - j\omega(1 + k_1) & 1 + k_2^2 + \omega^2 \end{bmatrix}. \quad (22)$$

The minimum eigenvalue is equal to

$$\lambda_{min}(\omega) = \frac{1 + k_1^2 + k_2^2 + 2\omega^2 - \sqrt{(1 + k_1^2 + k_2^2 + 2\omega^2)^2 - 4(\omega^2 k_2^2 + (\omega^2 - k_1)^2)}}{2}. \quad (23)$$

The minimum of λ_{min} with respect to ω is equal to

$$\lambda_{min} = \frac{1 + k_1^2 + k_2^2}{2} - \sqrt{\frac{(1 - k_1^2)^2 + k_2^2(k_2^2 + 2 + 2k_1^2)}{4}}. \quad (24)$$

We deduce that

$$\Upsilon_L^2 = \frac{1}{2} + \frac{1+k_2^2}{2k_1^2} + \frac{1}{2} \sqrt{1 + \left(\frac{2k_2}{k_1}\right)^2 + \left(\frac{2(1+k_2^2)}{k_1^2}\right)^2} > 1. \quad (25)$$

If we tune $k_1 = \frac{3}{16}k_2^2$ and $k_2 \geq 20$, then $0.93 < \lambda_{min} < 1$, and $1 < \Upsilon_L < 1.2$.

A.B Proof of Lemma 5.3.5

By using the Taylor expansion of equation (25), we have the following asymptotic expansion of Υ_L^2 ,

$$\Upsilon_L^2 = 1 + \frac{3}{2a^2k_2^2} + \frac{1}{2a^2k_2^4} + O\left(\frac{1}{k_2^6}\right), \quad (26)$$

Then, the Riccati equation proposed in (5.28) takes the following form

$$\left(\frac{P_k}{\Upsilon_L} + \Upsilon_L A\right)^T \left(\frac{P_k}{\Upsilon_L} + \Upsilon_L A\right) = S, \text{ where } S = -I + \Upsilon_L^2 A^T A. \quad (27)$$

As $\det(S) > 0$, S is clearly positive definite:

$$S = \begin{bmatrix} -1 + \Upsilon_L^2 a^2 k_2^4 & \Upsilon_L^2 a k_2^3 \\ \Upsilon_L^2 a k_2^3 & -1 + \Upsilon_L^2 (1 + k_2^2) \end{bmatrix},$$

and we get:

$$\det(S) = \Upsilon_L^2 k_2^2 (a^2 k_2^2 (\Upsilon_L^2 - 1) - 1) - (\Upsilon_L^2 - 1),$$

and we deduce from (25) the following Taylor expansion for $\det(S)$,

$$\det(S) = \frac{1}{2} \Upsilon_L^2 k_2^2 \left(1 + \frac{1}{k_2^2} + O\left(\frac{1}{k_2^4}\right)\right).$$

Then, the Riccati equation (27), takes the form:

$$X^T X = S,$$

where $X = \frac{P_k}{\Upsilon_L} + \Upsilon_L A$, and the solution is:

$$X = \frac{P_k}{\Upsilon_L} + \Upsilon_L A = R_\phi \sqrt{S}, \quad (28)$$

where R_ϕ is a rotation of angle ϕ and \sqrt{S} is the unique symmetric positive definite matrix whose square is equal to S . We first estimate \sqrt{S} and then ϕ .

We clearly have

$$S = b b^T + \gamma e_2 e_2^T,$$

where $b = \begin{pmatrix} \alpha \\ \beta \end{pmatrix}$, $e_2 = \begin{pmatrix} 0 \\ 1 \end{pmatrix}$ and

$$\alpha = \sqrt{(\Upsilon_L a k_2^2)^2 - 1}, \quad \beta = \frac{\Upsilon_L^2 a k_2^3}{\alpha}, \quad \gamma = \frac{\det(S)}{\alpha^2}.$$

The asymptotic expansions of the above quantities are

$$\begin{pmatrix} \alpha \\ \beta \end{pmatrix} = \Upsilon_L k_2 \begin{pmatrix} a k_2 \left(1 - \frac{1}{2\Upsilon_L^2 a^2 k_2^4} + O\left(\frac{1}{k_2^8}\right)\right) \\ 1 + \frac{1}{2\Upsilon_L^2 a^2 k_2^4} + O\left(\frac{1}{k_2^8}\right) \end{pmatrix}, \quad \gamma = \frac{1}{2a^2 k_2^2} \left(1 + \frac{1}{k_2^2} + O\left(\frac{1}{k_2^4}\right)\right).$$

We also need the asymptotic expansions of the eigenvalues of S . Since

$$S = \begin{bmatrix} \alpha^2 & \alpha\beta \\ \alpha\beta & \beta^2 + \gamma \end{bmatrix},$$

then,

$$\lambda_{1,2} = \frac{\alpha^2 + \beta^2 + \gamma \pm \sqrt{(\alpha^2 + \beta^2 + \gamma)^2 - 4\alpha^2\gamma}}{2}$$

We immediately deduce the following asymptotic expansions for the eigenvalues of S ,

$$\lambda_1 = \alpha^2 + \beta^2 + O\left(\frac{1}{k_2^4}\right), \quad \lambda_2 = \gamma \left(1 + O\left(\frac{1}{k_2^2}\right)\right). \quad (29)$$

We use \bar{b} to denote the unit vector $b/\|b\|$ and define the angle ϕ_b so that $R_{\phi_b} e_1 = \bar{b}$, where $e_1 = \begin{pmatrix} 1 \\ 0 \end{pmatrix}$.

We have

$$\|b\| = \Upsilon_L a k_2^2 \left(1 + \frac{1}{2a^2 k_2^2} + O\left(\frac{1}{k_2^4}\right)\right), \quad \bar{b} = \begin{pmatrix} 1 - \frac{1}{2a^2 k_2^2} + O\left(\frac{1}{k_2^4}\right) \\ \frac{1}{a k_2} \left(1 + \frac{1}{2a^2 k_2^2} + O\left(\frac{1}{k_2^4}\right)\right) \end{pmatrix},$$

and

$$R_{\phi_b} = l_2 Id_2 + l_1 A_0,$$

where $A_0 = \begin{pmatrix} 0 & -1 \\ 1 & 0 \end{pmatrix}$ and

$$l_1 = \frac{1}{a k_2} \left(1 - \frac{3}{2a^2 k_2^2} + O\left(\frac{1}{k_2^4}\right)\right), \quad l_2 = \left(1 - \frac{1}{2a^2 k_2^2} + O\left(\frac{1}{k_2^4}\right)\right).$$

We then get that $R_{-\phi_b}e_2 = l_2e_2 - l_1e_1$. We can therefore write

$$R_{-\phi_b}SR_{\phi_b} = \|b\|^2e_1e_1^T + \gamma R_{-\phi_b}e_2e_2^TR_{\phi_b},$$

and deduce that

$$R_{-\phi_b}SR_{\phi_b} = (\|b\|^2 + \gamma l_1^2)e_1e_1^T + \gamma l_2^2e_2e_2^T - \gamma l_1l_2(e_1e_2^T + e_2e_1^T). \quad (30)$$

Finally, we seek a formula of the type

$$R_{-\phi_b}\sqrt{S}R_{\phi_b} = s_1e_1e_1^T + s_2e_2e_2^T - s_3(e_1e_2^T + e_2e_1^T), \quad (31)$$

where the s_i 's are positive. A simple identification leads to the equations

$$s_1^2 + s_3^2 = \|b\|^2 + \gamma l_1^2, \quad s_2^2 + s_3^2 = \gamma l_2^2, \quad s_3 = \frac{\gamma l_1 l_2}{Tr(\sqrt{S})}.$$

We deduce at once from the asymptotic expansions of the eigenvalues of S obtained in (29) that

$$s_1 = \|b\|(1 + O(\frac{1}{k_2^8})), \quad s_2 = \sqrt{\gamma}(1 + O(\frac{1}{k_2^2})), \quad s_3 = O(\frac{1}{k_2^5}). \quad (32)$$

From the expression $\Upsilon_L(A - A^T) = R_\phi\sqrt{S} - \sqrt{S}R_{-\phi}$, we obtain

$$\Upsilon_L(1 + ak_2^2) \begin{bmatrix} 0 & 1 \\ -1 & 0 \end{bmatrix} = -Tr(\sqrt{S})\sin(\phi) \begin{bmatrix} 0 & 1 \\ -1 & 0 \end{bmatrix},$$

and we deduce that $\Upsilon_L(1 + ak_2^2) = -Tr(\sqrt{S})\sin(\phi)$, i.e.,

$$\sin(\phi) = -\left(1 - \frac{C_0^2}{2k_2^2} + O(\frac{1}{k_2^3})\right),$$

where $C_0 = \frac{\sqrt{1-2a}}{a}$. It implies that

$$R_\phi = \frac{C_0}{k_2}(1 + O(\frac{1}{k_2}))Id_2 - \left(1 - \frac{C_0^2}{2k_2^2} + O(\frac{1}{k_2^3})\right)A_0.$$

We now collect the result of the equation (28) and (32) to get,

$$\frac{P_k}{\Upsilon_L} = -\Upsilon_L A + R_\phi R_{\phi_b} \left[s_1e_1e_1^T + s_2e_2e_2^T + O(\frac{1}{k_2^5}) \right] R_{-\phi_b}.$$

After a straightforward computation of the expansion of Υ_L , R_ϕ , R_{ϕ_b} , s_1 and s_2 in the previous equation, we arrive at (5.36).

A.C Proof of Proposition 5.3.6

The proof is developed using Young inequality, $|\eta\xi| \leq \frac{\epsilon\eta^2}{2} + \frac{\xi^2}{2\epsilon}$, where ϵ is an arbitrary positive constant.

First of all, according to Lemma 5.3.5, for large k_2 , the quadratic form $V_k(\xi, \eta)$ satisfies the following inequality

$$V_k(\xi, \eta) \geq F_1 k_2 \xi^2 + 2F_2 \xi \eta + F_3 \frac{\eta^2}{k_2} - \frac{C}{k_2} (\xi^2 + \frac{\eta^2}{k_2^2}),$$

for some positive universal constant $C > 0$. Then, by setting $X := \sqrt{k_2 F_1} \eta$ and $Y := \frac{\eta}{\sqrt{k_2 F_3}}$, we obtain

$$V_k(\xi, \eta) \geq (1 - \frac{C}{k_2^2}) X^2 + 2 \frac{F_2}{\sqrt{F_1 F_3}} XY + (1 - \frac{C}{k_2^2}) Y^2.$$

Since $\frac{F_2^2}{F_1 F_3} < 1$, the above inequality ensures, for k_2 large enough, the existence of $l > 0$ only dependent of a such that

$$V_k(\xi, \eta) \geq l \left(k_2 \xi^2 + \frac{\eta^2}{k_2} \right).$$

The previous inequality with $M = \beta k_2$ and $k_1 = a k_2^2$ computed in (5.29) implies

$$V(y_1, y_2, \xi, \eta) \geq l \beta k_2^2 \xi^2 + l \beta \eta^2 + \frac{a k_2^2}{2} (y_1^2 + y_2^2) - |\eta y_2| - |k_2 y_2 \xi|.$$

By using Young's inequality, we get

$$\begin{aligned} |\eta y_2| &\leq l \beta \frac{\eta^2}{2} + \frac{1}{l \beta} \frac{y_2^2}{2}, \\ |k_2 y_2 \xi| &\leq l \beta \frac{k_2^2 \xi^2}{2} + \frac{1}{l \beta} \frac{y_2^2}{2}. \end{aligned}$$

Which implies,

$$V \geq \left(\frac{a k_2^2}{2} + \frac{1}{l \beta} \right) y_2^2 + \frac{l \beta k_2^2}{2} \xi^2 + \frac{l \beta}{2} \eta^2 + \frac{a k_2^2}{2} y_1^2.$$

then for large enough k_2 , V is a positive quadratic form in (ξ, η, y_1, y_2) .

A.D Proof of Lemma 5.3.7

The solution of the equation (5.26) is

$$Z(t) = \int_0^t e^{A(t-s)} U(s) ds + e^{At} Z_0, \quad (33)$$

where Z_0 is the initial value of Z for $t = 0$. We start by diagonalization of the matrix A , whose eigenvalues are equal to

$$\begin{aligned}\lambda_+ &= -\frac{k_2}{2} + \frac{1}{2}\sqrt{k_2^2 - 4k_1}, \\ \lambda_- &= -\frac{k_2}{2} - \frac{1}{2}\sqrt{k_2^2 - 4k_1},\end{aligned}\tag{34}$$

with corresponding eigenvectors $V_+ = \begin{pmatrix} 1 \\ \lambda_+ \end{pmatrix}$ and $V_- = \begin{pmatrix} 1 \\ \lambda_- \end{pmatrix}$. From here, we obtain $A = PDP^{-1}$, where

$$D = \begin{pmatrix} \lambda_+ & 0 \\ 0 & \lambda_- \end{pmatrix}; P = \begin{pmatrix} V_+ & V_- \end{pmatrix} = \begin{pmatrix} 1 & 1 \\ \lambda_+ & \lambda_- \end{pmatrix};\tag{35}$$

We get

$$e^{A(t-s)}U(s) = \frac{1}{\lambda_- - \lambda_+} \begin{pmatrix} (\lambda_- v_1 - v_2)e^{\lambda_+(t-s)} + (\lambda_+ v_1 + v_2)e^{\lambda_-(t-s)} \\ \lambda_+(\lambda_- v_1 - v_2)e^{\lambda_+(t-s)} + \lambda_-(\lambda_+ v_1 + v_2)e^{\lambda_-(t-s)} \end{pmatrix}\tag{36}$$

The control variables v_1 and v_2 are bounded respectively by $\kappa_{max}C_1$ and C_2 and we obtain that the components of the vector $\int_0^t e^{A(t-s)}U(s)ds$ are bounded componentwise by

$$\begin{pmatrix} \frac{1}{|\lambda_+|} \left(\kappa_{max}C_1 + \frac{C_2}{|\lambda_-|} \right) \\ \kappa_{max}C_1 + \frac{C_2}{|\lambda_+|} + \frac{C_2}{|\lambda_-|} \end{pmatrix}.\tag{37}$$

By taking $k_1 = \frac{3}{16}k_2^2$, we get $\lambda_+ = -\frac{k_2}{4}$ and $\lambda_- = -\frac{3k_2}{4}$. We can bound the components of the vector defined in (5.9) by

$$\begin{pmatrix} \frac{4}{k_2} \left(\kappa_{max}C_1 + \frac{4}{3k_2}C_2 \right) \\ \kappa_{max}C_1 + \frac{16}{3k_2}C_2 \end{pmatrix}.\tag{38}$$

Equation (5.37) can be deduced directly from Equations (33) and (38). Moreover, since A is Hurwitz, we arrive to (5.38).

A.E Proof of Lemma 5.3.10

The terms $|\eta\xi|$ and $k_2\xi^2$ are clearly dominated by $\frac{M}{4}(\xi^2 + \eta^2)$.

In (5.40), one has $M(Y_L \kappa_r C_1 \sigma(y_1))^2 \leq CM(C_1 \sigma(y_1))^2$, which is dominated by $\frac{k_1 C_1}{4} y_1 \sigma(y_1)$ if $C\beta C_1 \leq \frac{ak_2}{4}$. The latter clearly holds true for k_2 large enough.

We have $M(Y_L C_2 \sigma(y_2))^2 \leq CM(C_2 \sigma(y_2))^2$, which is dominated by $C_2 y_2 \sigma(y_2)/4$ if $AMC_2^2 \leq C_2/4$. The latter is true according to the choice of C_2 in (5.23).

We now turn to the control of the term $k_2 C_1 |y_2 \kappa_r \sigma(y_1)|$ by $\frac{k_1 C_1}{4} y_1 \sigma(y_1) + \frac{C_2}{4} y_2 \sigma(y_2)$. If $|y_2| \geq 1$, the second term is in control if $\frac{C_2}{4} \geq Ck_2 C_1$ which holds true. Assume now that $|y_2| \leq 1$. In the case where $|y_1| \geq 1$, the first term is in control if $\frac{k_1 C_1}{4} \geq Ck_2 C_1$ which obviously holds true. It remains the case where $|y_1| \leq 1$. It is immediate to check that the quadratic form $\frac{k_1 C_1}{4} y_1^2 + \frac{C_2}{4} y_2^2 - Ck_2 C_1 y_1 y_2$ is definite positive.

We next consider the term $k_1 |y_2| |\xi|^3$. To control it, we first bound $|\xi|^2$ by $\frac{C}{k_2^6}$ for t large enough. In case $|y_2| \geq 1$, then the term is immediately dominated by $\frac{C_2}{4} |y_2|$. Otherwise, one has, for k_2 large enough,

$$k_1 |y_2| |\xi|^3 \leq C \frac{|y_2|}{k_2} \frac{|\xi|}{k_2^4} \leq C \left(\frac{y_2^2}{k_2^2} + \frac{\xi^2}{k_2^4} \right),$$

the last two terms being controlled by $\frac{C_2}{4} |y_2|^2 + \frac{M}{4} \xi^2$.

Using again the estimate $|\xi|$ by $\frac{C}{k_2^3}$ for t large enough, the control of $k_1 |y_1| |\xi|^2$ reduces to that of $k_2 |y_1 \xi|$. It therefore remain to control the latter. This is where we need the hypothesis that $y \notin Y_{k_2}$. Assume first that one wants to get the inequality

$$k_2 |y_1 \xi| \leq \frac{k_1 C_1}{4} y_1 \sigma(y_1). \quad (39)$$

This holds true if $|y_1| \geq \frac{C}{k_2^2}$. On the other hand, if one wants to get the inequality

$$k_2 |y_1 \xi| \leq \frac{C_2}{4} y_2 \sigma(y_2), \quad (40)$$

it holds if $|y_2| \geq \frac{C}{k_2^{3/2}}$. In any case, outside Y_{k_2} , one of the two inequalities (39) or (40) must hold true and Lemma 5.3.10 is established.

Finally, with the choice of $M = \beta k_2$ together with (5.36), it is immediate to verify that V is positive definite. Moreover, we get

$$a_1 k_2 \xi^2 + \frac{a_2}{k_2} \eta^2 + a_3 k_2^2 (y_1^2 + y_2^2) \leq V \leq d_1 k_2 \xi^2 + \frac{d_2}{k_2} \eta^2 + d_3 k_2^2 (y_1^2 + y_2^2), \quad (41)$$

for some positive constants $a_i, d_i, 1 \leq i \leq 3$.

Résumé :

Les systèmes non-linéaires sont si diverses que des outils communs de contrôle sont difficiles à développer. La théorie du contrôle non-linéaire nécessite une analyse mathématique rigoureuse pour motiver ses conclusions. Cette thèse aborde deux branches distinctes et bien importantes de la théorie du contrôle non-linéaire: le contrôle des systèmes non-linéaires incertains et le contrôle des systèmes sous-actionnés.

Dans la première partie, une classe de contrôleurs par mode glissant d'ordre supérieur (MGOS) robuste, basée sur la synthèse de Lyapunov, est développée pour le contrôle des systèmes non-linéaires incertains. Cette classe de contrôleurs est basée sur une classe de régulateurs qui stabilisent une pure chaîne d'intégrateurs en temps fini, et nécessite la connaissance a priori des bornes sur les incertitudes du système. Puis, afin d'éliminer la dépendance liée à la connaissance de ces bornes, un contrôleur par MGOS adaptatif est développé. Dans un deuxième temps, un contrôleur par MGOS homogène universel est développé où il est montré que le degré d'homogénéité peut être manipulé pour obtenir des avantages supplémentaires, tels que la bornitude de la commande, la garantie d'une amplitude minimale de la discontinuité de la commande et la convergence en temps fixe. Les performances des contrôleurs proposés ont été démontrées par des simulations et à travers des résultats expérimentaux sur un système pile à combustible.

Dans la deuxième partie de la thèse, deux problèmes de commande de systèmes sous-actionnés sont étudiés. Le premier problème concerne le suivi de chemin global d'un robot mobile avec un point de visée. Le deuxième problème concerne la poursuite de trajectoire globale d'un bateau. Ces deux problèmes sont de nature distincte, cependant, ils sont soumis à des contraintes physiques similaires liées à la bornitude de la commande. Ainsi, les contrôleurs proposés sont basés sur l'utilisation de commandes saturées. Des simulations ont été effectuées pour démontrer les performances de ces contrôleurs.

Mots clés : Fonction de Lyapunov, mode glissant d'ordre supérieur, commande robuste, commande adaptative, système sous-actionné, saturation, suivi de chemin, poursuite de trajectoire, point de visée.

Abstract:

Nonlinear systems are so diverse that generalized tools for control are difficult to develop. Nonlinear control theory requires rigorous mathematical analysis to justify its conclusions. This thesis addresses two distinct, yet important branches of nonlinear control theory: control of uncertain nonlinear systems and control of under-actuated systems.

In the first part, a class of Lyapunov-based robust arbitrary higher order sliding mode (HOSM) controllers is developed for the control of uncertain nonlinear systems. This class of controllers is based on a class of controllers for finite-time stabilization of pure integrator chain, and requires the limits of the system uncertainty to be known a-priori. Then, in order to eliminate the dependence on the knowledge of these limits, an adaptive arbitrary HOSM controller is developed. Using this new class, a universal homogeneous arbitrary HOSM controller is developed and it is shown that the homogeneity degree can be manipulated to obtain additional advantages in the proposed controllers, such as bounded control, minimum amplitude of discontinuous control and fixed time convergence. The performance of the controllers has been demonstrated through simulations and experiments on a fuel cell system.

In the next part, the control of two under-actuated systems is studied. The first control problem is the global path following of car-type robotic vehicle, using target-point. The second problem is the precise tracking of surface marine vessels. Both these problems are distinct in nature; however, they are subjected to similar physical constraints. The solutions proposed for these control problems use saturated controls, taking into account the physical bounds on the control inputs. Simulations have been performed to demonstrate the performance of these controllers.

Keywords: Lyapunov method, higher order sliding mode control, robust control, adaptive control, under-actuated system, saturation, path following, trajectory tracking, target point.

